

TAUP 2465 - 97
DESY 97 - 213
October 1997

EVERYTHING ABOUT REGGEONS

Part I : REGGEONS IN “SOFT” INTERACTION.

E u g e n e L e v i n

*School of Physics and Astronomy, Tel Aviv University
Ramat Aviv, 69978, ISRAEL*

and

*DESY Theory, Notkrstr. 85, D - 22607, Hamburg, GERMANY
leving@ccsg.tau.ac.il; levin@mail.desy.de;*

Academic Training Program
DESY, September 16 - 18, 1997

Abstract: This is the first part of my lectures on the Pomeron structure which I am going to read during this academic year at the Tel Aviv university. The main goal of these lectures is to remind young theorists as well as young experimentalists of what are the Reggeons that have re-appeared in the high energy phenomenology to describe the HERA and the Tevatron data. Here, I show how and why the Reggeons appeared in the theory, what theoretical problems they have solved and what they have failed to solve. I describe in details what we know about Reggeons and what we do not. The major part of these lectures is devoted to the Pomeron structure, to the answer to the questions: what is the so called Pomeron; why it is so different from other Reggeons and why we have to introduce it. In short, I hope that this lectures will be the shortest way to learn everything about Reggeons from the beginning to the current understanding. I concentrate on the problem of Reggeons in this lectures while the Reggeon interactions or the shadowing corrections I plan to discuss in the second part of my lectures. I include here only a short lecture with an outline of the main properties of the shadowing corrections to discuss a correct (from the point of the Reggeon approach) strategy of the experimental investigation of the Pomeron structure.

I dedicate these lectures to the memory of Prof. Vladimir Gribov (1930 - 1997) who was my teacher and one of the most outstanding physicists in this century. I grew up as a physicist under his strong influence and for the rest of my life I will look at physics with his eyes. Being a father of Regge approach to high energy asymptotic, he certainly stood behind my shoulders, when I was preparing these lectures. I hope that I will be able to share with you all our hopes, ideas, results and disappointments that we discussed, solved and accepted under his leadership in seventies in our Leningrad Nuclear Physics Institute.

In the next page I put the obituary of the Russian Academy of Science. This document gives a good description of the best Gribov's results which will be really with us in these lectures. You need to know a bit about our life in the Soviet Union to understand this document and to try to answer such questions like why he had to teach at the night school, why he was not elected as a full member of the Academy of Science or why the fact that he was the leader and the head of the theoretical physics department at the Leningrad Nuclear Physics Institute during his best twenty years was not mentioned in the document. This is a good illustration that you need to know a little bit to understand. I hope, that my lectures will give you this "a little bit" for the Reggeon approach.

The eminent Russian theorist Corresponding Member of Russian Academy of Sciences Vladimir Naumovich Gribov passed away on August 13, 1997, in Budapest, after short and grave illness. V.N.Gribov was born on March 25, 1930 in Leningrad. Having graduated Leningrad University in 1952 he was forced to work as a teacher at the night school for working people. In 1954, he joined the Ioffe Physico-Technical Institute in Leningrad, and before long became the leading member of the Theory Division and one of unquestionable leaders in Soviet and the world theoretical high energy physics. Many a theorists in Russia and FSU are his pupil.

Gribov's theory of threshold multiparticle reactions, the Gribov - Froissar expansion, Gribov's factorization, the Gribov - Pomeranchuk shrinkage of the diffraction

cone, Gribov - McDowell symmetry, Gribov - Volkov conspiracy, Gribov - Morrison selection rules, Glauber - Gribov theory of diffraction scattering on nuclei, Gribov - Pomeranchuk - Ter-Martirosian reggeon unitarity, Gribov's reggeon calculus, Abramovski - Gribov - Kancheli (AGK) cutting rules, Gribov - Ioffe- Pomeranchuk growth of spatial scales in strong interactions, Gribov's extended vector dominance, Gribov - Pontecorvo analysis of neutrino oscillations, Gribov's theorem for Bremsstrahlung at high energies, Gribov - Lipatov evolution equations, Gribov - Lipatov reciprocity, Gribov's vacuum copies, Frolov - Gorshkov - Gribov - Lipatov theory of Regge processes in gauge theories are jewels in the crown of modern theoretical physics.

Gribov was the foreign member of the American Academy of Arts and Sciences in Boston. His distinctions include the L.D.Landau medal of the Academy of Sciences of USSR, of which he was the first ever recipient, J.J.Sakurai prize of the American Physical Society, Alexander von Humboldt prize and the Badge of Honor. Since 1980 he has been a member of the

L.D.Landau Institute for Theoretical Physics (Moscow) and the last decade also a Professor at the R.Etvoesh University in Budapest.

Exceptionally warm and cheerful personality, who generously shared his ideas and fantastic erudition with his students and colleagues, indefatigable discussion leader V.Gribov was universaly revered in his country and elsewhere. His family, friends, colleagues and the whole of high energy physics community shall miss him dearly.

Several words about these lectures: goals, structure and style.

Let me start saying several words about my personal activity in the Reggeon approach. I started to be involved in the Pomeron problem in early 70's not because I felt that this was an interesting problem for me but rather because everybody around worked on this problem.

It was a heroic time in our department when we worked as one team under the leadership of Prof. Gribov. He was for us, young guys, not only a dominant leader but a respected teacher. I took his words seriously: "Genya, it seems to me that you are a smart guy. I am sure, you will be able to do something more reasonable than this quark stuff." So I decided to try and, frankly speaking, there was another reason behind my decision. I felt that I could not develop my calculation skill, doing the additive quark model. However, I must admit, very soon I took a deep interest in the Pomeron problem, so deep that I decided to present here all my ups and downs in the attempts to attack this problem.

I hope, that these lectures show the development of the main ideas in their historical perspective from the first enthusiastic attempts to find a simple solution to understanding of the complexity and difficulty of the problem. In other words, these are lectures of a man who wanted to understand everything in high energy interactions, who did his best but who is still at the beginning, but who has not lost his temper and considers the Pomeron structure as a beautiful and difficult problem, which deserves his time and efforts to be solved.

Based on this emotional background, I will try to give a selected information on the problem, to give not only a panorama of ideas and problems but to teach you to perform all calculations within the Reggeon approach. I tried to collect here the full information that you need to start doing calculations. It is interesting to notice that that the particular contents of my lectures will cover the most important of Gribov results which we can find in the obituary of the Russian Academy of Science attached to these lectures. However, you will find more than that. If you will not find something, do not think that I forgot to mention it. It means that I do think that you do not need this information. The criteria of my selection is very simple. I discuss only those topics which you, in my opinion, should take with you in future. As an example, everybody has heard that the Regge pole approach is closely related to the analytical properties of the scattering amplitude in angular moment representation. You will not find a single word about this here because, I think, it was only the historical way of how Regge poles were introduced. But, in fact, it can be done without directly mentioning the angular moment representation. I hope, that you will understand an idea, that my attempt to give you a full knowledge will certainly not be the standard way.

In this particular part I restrict myself to the consideration of Reggeons (Regge poles) in "soft" interaction while discussions of the shadowing corrections, the high energy asymptotic in perturbative QCD, the so called BFKL Pomeron and the shadowing corrections at short distances (high parton density QCD) will be given later in the following parts of these lectures and will be published elsewhere. However, to give you some feeling on what kind

of experiment will be useful from the point of view of the Reggeon approach I will outline some of the main properties of the shadowing corrections in the “soft” processes in the last lecture. I would like also to mention that I am going to read at the Tel Aviv university this year the complete course of lectures: “Everything about Reggeons” and it will consist of four parts:

1. Reggeons in the “soft” interaction;
2. Shadowing corrections and Pomeron interactions in “soft” processes;
3. The QCD Pomeron;
4. The high parton density QCD.

The “soft” processes at high energy were, are and will be the area of the Regge phenomenology which has been useful for 25 years. Unfortunately, we, theorists, could not suggest something better. This is the fact which itself gives enough motivation to learn what is the Reggeon approach. The second motivation for you is, of course, new data from HERA which can be absorbed and can be discussed only with some knowledge about Regge phenomenology. What you need to know is what is Regge phenomenology, where can we apply it and what is the real outcome for the future theory.

Let me make some remarks on the style of the presentation. It is not a text book or paper. It is a lecture. It means that it is a living creature which we together can change and make it better and better. I will be very thankful for any questions and suggestions. I am writing these lectures after reading them at DESY. I got a lot of good questions which I answer here.

Concluding my introductory remarks I would like to mention Gribov’s words: “Physics first”. Have a good journey.

Contents

1 Instead of introduction	9
1.1 Our strategy.	9
1.2 Unitarity and main definitions.	9
1.3 General solution to the elastic unitarity.	13
1.4 Inelastic channels in unitarity.	16
1.5 Unitarity at high energies.	18
1.6 Unitarity constraint in impact parameter (b).	19
1.7 A general solution to the unitarity constraint.	20
2 The great theorems.	20
2.1 Optical Theorem.	21
2.2 The Froissart boundary.	21
2.3 The Pomeranchuk Theorem.	24
2.4 An instructive model: the “ black disc ” approach.	25
3 The first puzzle and Reggeons.	28
3.1 The first puzzle.	28
3.2 Reggeons - solutions to the first puzzle.	32
4 The main properties of the Reggeon exchange.	32
4.1 Analyticity.	33
4.2 s - channel unitarity	33
4.3 Resonances.	33
4.4 Trajectories.	34
4.5 Definite phase.	35
4.6 The Reggeon exchange in b	35
4.7 Shrinkage of the diffraction peak.	36

5 Analyticity + Reggeons.	36
5.1 Duality and Veneziano model.	36
5.2 Quark structure of the Reggeons.	38
6 The second and the third puzzles: the Pomeron?!	41
6.1 Why we need the new Reggeon - the Pomeron?	41
6.2 Donnachie - Landshoff Pomeron.	42
7 The Pomeron structure in the parton model.	43
7.1 The Pomeron in the Veneziano model (Duality approach).	43
7.2 The topological structure of the Pomeron in duality approach.	43
7.3 The general origin of $\ln^n s$ contributions.	45
7.4 Random walk in b	47
7.5 Feynman gas approach to multiparticle production.	49
7.5.1 Rapidity distribution.	49
7.5.2 Multiplicity distribution.	50
7.5.3 Feynman gas.	50
8 Space - time picture of interaction in the parton model.	52
8.1 Collision in space - time representation.	52
8.2 Probabilistic interpretation.	54
8.3 “Wee” partons and hadronization.	56
8.4 Diffraction Dissociation.	58
9 Different processes in the Reggeon Approach.	58
9.1 Mueller technique.	58
9.2 Total cross section.	59
9.3 Elastic cross section.	61
9.4 Single diffraction dissociation	62
9.5 Non-diagonal contributions.	64
9.6 Double diffraction dissociation.	66
9.7 Factorization for diffractive processes.	66
9.8 Central Diffraction.	67
9.9 Inclusive cross section.	67
9.10 Two particle rapidity correlation.	68

10 Why the Donnachie - Landshoff Pomeron is not the right one.	69
11 Pomeron in photon - proton interaction.	74
11.1 Total cross section.	74
11.2 Diffractive dissociation	78
11.3 Exclusive (with restricted number of hadrons) final state.	78
11.4 Inclusive diffraction	82
12 Shadowing Corrections (a brief outline).	83
12.1 Why Pomeron is not enough?	83
12.2 Space - time picture of the shadowing corrections.	84
12.3 The AGK cutting rules.	85
12.4 The Eikonal model.	89
12.5 Large Rapidity Gap processes and their survival probability.	91
12.6 σ_{tot} , σ_{el} and slope B	95
12.7 Inclusive production.	97
12.7.1 Cross section.	97
12.7.2 Correlations.	99
13 The Pomeron from HERA and Tevatron experiments.	100
13.1 Reggeon approach strategy for measuring the Pomeron structure.	100
13.2 The Pomeron before HERA and Tevatron.	103
13.3 Pomeron at the Tevatron.	105
13.4 Pomeron at HERA.	106
14 Instead of conclusions.	109
14.1 My picture for the high energy interaction.	109
14.2 Apology and Acknowledgements.	110
15 References.	111

1 Instead of introduction

1.1 Our strategy.

My first remark is that in the 70's finding the asymptotic behaviour of the scattering amplitude at high energies was a highly priority job. During the last five years I have traveled a lot around the globe and I have found that it is very difficult to explain to young physicist why it was so. However, 25 years ago the common believe was that the analytical property of the scattering amplitude together with its asymptotic behaviour would give us the complete and selfconsistent theory of the strong interaction. The formula of our hope was very simple:

$$\begin{array}{c} \text{Analyticity} \\ \text{Unitarity} \quad + \quad \text{Asymptotic} \quad = \quad \text{Theory of Everything.} \\ \text{Crossing} \end{array}$$

Roughly speaking we needed the asymptotic behaviour at high energy to specify how many subtractions were necessary in dispersion relations to calculate the scattering amplitude.

Now the situation is quite different: we have good microscopic theory (QCD) although we have a lot of problems in QCD which have to be solved. High energy asymptotic behaviour is only one of many. I think it is time to ask yourselves why we spend our time and brain trying to find the high energy asymptotic behaviour in QCD. My lectures will be an answer to this question, but I would like to start by recalling you the main theorems for the high energy behaviour of the scattering amplitude which follow directly from the general properties of analyticity and crossing symmetry and should be fulfilled in any microscopic theory including QCD. Certainly, I have to start by reminding you what is analyticity and unitarity for the scattering amplitude and how we can use these general properties in our theoretical analysis of the experimental data.

1.2 Unitarity and main definitions.

Let us start with the case where we have only **elastic scattering**. The wave function of the initial state (before collision) is a plane wave moving say along the z-direction, namely:

$$\Psi^i = e^{ikz} = e^{i\vec{k}\cdot\vec{r}}$$

The wave function of the final state (after collision) is more complicated and has two terms: the plane wave and an outgoing spherical wave. The scattering amplitude is the amplitude of this spherical wave.

$$\Psi^f = e^{i\vec{k}\cdot\vec{r}} + \frac{f(\theta, k)}{r} e^{ikr},$$

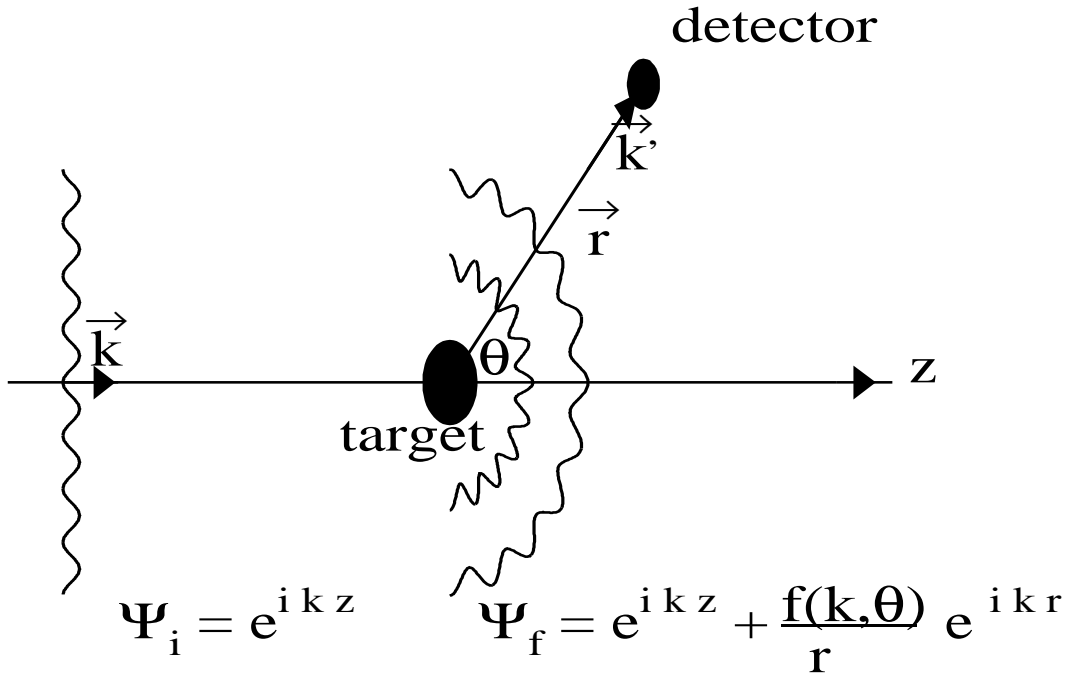


Figure 1: The elastic scattering.

where $r = \sqrt{x^2 + y^2 + z^2}$, $\vec{k} \cdot \vec{r} = k r \cos\theta$ and k is the value of the momentum. The scattering amplitude in this form is very useful since the cross section is equal to

$$d\sigma = \frac{v |\Psi_f|^2 dS}{v} , \quad (1)$$

where v is the velocity of the incoming particle and dS is the element of the sphere $dS = 2\pi r^2 \sin\theta d\theta$. Finally,

$$\frac{d\sigma}{dS} = 2\pi |f(k, \theta)|^2 . \quad (2)$$

Assumption: The incoming wave is restricted by some aperture (L)

$$r \gg L \gg a$$

where a is the typical size of the forces (potential) of interaction. Then one can neglect the incoming wave as $r \rightarrow \infty$.

To derive the unitarity constraint we have to consider a more general case of scattering, namely, the incoming wave is a package of plane waves coming from different angles not directed only along z-direction.

It means that

$$\Psi^i = \int d\Omega_n F(\vec{n}) e^{ikr\vec{n}\cdot\vec{n}'} \quad (3)$$

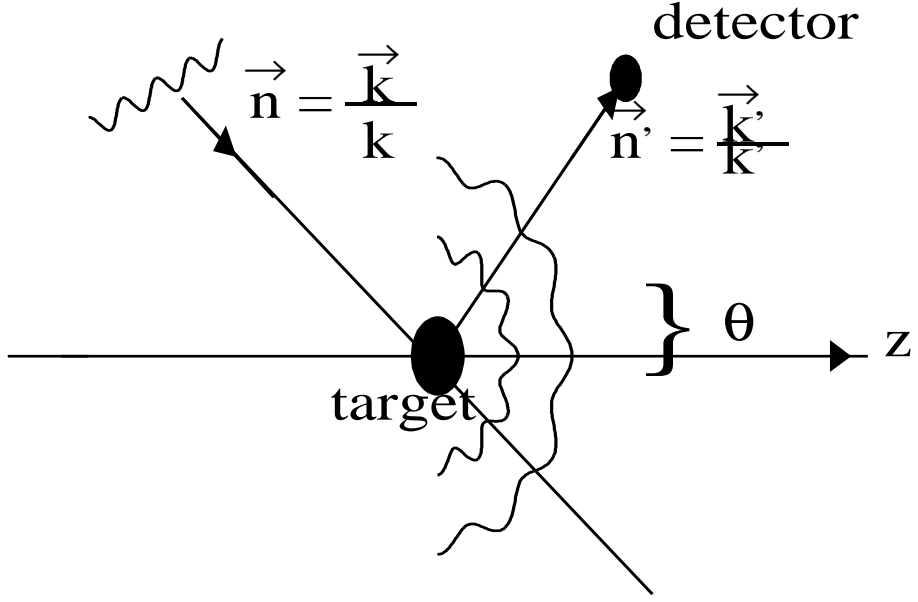


Figure 2: *The elastic scattering (general case).*

where we introduce two unit vectors $\vec{n} = \frac{\vec{k}}{k}$ and $\vec{n}' = \frac{\vec{k}'}{k'}$ (see Fig.2). $F(\vec{n})$ is an arbitrary function.

After scattering we have

$$\Psi^f = \int d\Omega_n F(\vec{n}) e^{ikr\vec{n}\cdot\vec{n}'} + \frac{e^{ikr}}{r} \int d\Omega_n F(\vec{n}) f(k, \vec{n}, \vec{n}') . \quad (4)$$

The first term can be explicitly calculated. Indeed, in vicinity of $z = \cos\theta = -1$ we have

$$\begin{aligned}
 \int d\Omega_n F(\vec{n}) e^{ikr\vec{n}\cdot\vec{n}'} &= 2\pi \int_{-1}^{-1+iz_0} dz F(z) e^{ikrz} = \\
 &2\pi F(-\vec{n}) \frac{1}{ikr} \{ e^{-krz_0} - e^{ikr} \} \rightarrow \frac{2\pi i}{kr} e^{-ikr} .
 \end{aligned}$$

Finally,

$$\int d\Omega_n F(\vec{n}) e^{ikr\vec{n}\cdot\vec{n}'} = 2\pi i \{ F(-\vec{n}) \frac{e^{-ikr}}{kr} - F(\vec{n}) \frac{e^{ikr}}{kr} \}$$

The resulting wave function for the final state is equal

$$\Psi^f = \frac{2\pi i}{k} \left\{ F(-\vec{n}) \frac{e^{-ikr}}{r} - F(\vec{n}) \frac{e^{ikr}}{r} \right\} + \frac{e^{ikr}}{r} \int f(k, \vec{n}, \vec{n}') F(\vec{n}) d\Omega_n ,$$

while the initial wave function is

$$\Psi^i = \frac{2\pi i}{k} \left\{ F(-\vec{n}) \frac{e^{-ikr}}{r} - F(\vec{n}) \frac{e^{ikr}}{r} \right\} .$$

The conservation of probability means that (V is the volume):

$$\int |\Psi^i|^2 dV = \int |\Psi^f|^2 dV . \quad (5)$$

Taking into account that

$$\int \frac{e^{-2ikr}}{r^2} r^2 dr d\Omega = 0$$

we obtain (see Fig. 3):

$$\text{Im } f(\vec{n}, \vec{n}', k) = \frac{k}{4\pi} \int f(\vec{n}, \vec{n}', k) f^*(\vec{n}', \vec{n}', k) d\Omega_{n'} \quad (6)$$

or

$$\text{Im } f(k, \theta) = \frac{k}{4\pi} \int f(k, \theta_1) f^*(k, \theta_2) d\Omega_1 , \quad (7)$$

where $\cos\theta = \cos\theta_1 \cos\theta_2 - \sin\theta_1 \sin\theta_2 \cos\phi$. Now, let us introduce the partial waves,

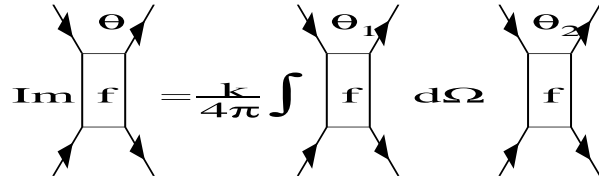


Figure 3: The s - channel unitarity.

namely, let us expand the elastic amplitude in terms of Legendre polynomials:

$$f(k, \theta) = \sum_{l=0}^{\infty} f_l(k) P_l(\cos\theta) (2l+1) . \quad (8)$$

Using two properties of Legendre polynomials, namely,

1.

$$\int_{-1}^1 dz P_l(z) P_{l'}(z) = 0 \quad (\text{if } l \neq l') = \frac{2}{2l+1} \quad (\text{if } l = l') ;$$

2.

$$P_l(\cos\theta) = P_l(\cos\theta_1) P_l(\cos\theta_2) + 2 \sum_{m=1}^l \frac{(l-m)!}{(l+m)!} P_l^m(\cos\theta_1) P_l^m(\cos\theta_2) \cos m\phi ;$$

one can easily get that the unitarity constraint looks very simple for the partial amplitude:

$$\text{Im} f_l(k) = k |f_l(k)|^2 \quad (9)$$

- What is k ?

$$\text{Im } A = \int \text{d}\Phi_2 \left(\begin{array}{c} \text{Diagram 1: } \text{Im } A_1 \text{ (left)} \\ \text{Diagram 2: } \text{Im } A_2 \text{ (right)} \end{array} \right)$$

Figure 4: The s - channel unitarity (relativistic normalization).

We define $s = (p_1 + p_2)^2$ and the unitarity constraint can be written as (see Fig.4):

$$\text{Im} A = \int A_1 A_2^* \frac{d^3 p''_1}{2 p''_{10}} \frac{d^3 p''_2}{2 p''_{20}} \delta^{(4)}(p_1 - p_2 - p''_1 - p''_2) \frac{(2\pi)^4}{(2\pi)^6} ;$$

In c.m.f. $\sqrt{s} = 2\sqrt{m^2 + k^2}$ or

$$k = \frac{\sqrt{s - 4m^2}}{2}$$

and

$$d^3 p''_1 = p''_1^2 d\Omega \frac{1}{2} p''_1 d p''_{10}^2$$

Therefore, the unitarity condition can be rewritten in the form for $f = \frac{A}{\sqrt{s}}$ in the usual way. The physical meaning of k in the unitarity constraint is, that k is equal to the phase space of two colliding particles.

1.3 General solution to the elastic unitarity.

It is easy to see that the elastic unitarity has a general solution, namely,

$$f_l = \frac{1}{g_l(k^2) - ik} , \quad (10)$$

where $g_l(k^2)$ is real, but otherwise arbitrary function.

Two applications of elastic unitarity:

1. The scattering length approximation and the deuteron structure.

Let us assume that

$$ka \ll 1$$

where a is the size of the target or more generally, let us assume that we consider our scattering at such small values of k that

$$g_{l=0}(k^2) = \frac{1}{a} + k^2 r_0 + \dots$$

and $r_0 k \ll 1$. At such energies

$$f_0(k) = \frac{a}{1 - ika} ,$$

where $k = \frac{1}{2}\sqrt{s - 4m^2}$. One can see that f_0 could have a pole at $1 - ika = 0$!?. However, first we have to define how we continue k into the complex plane. I want to stress that our analytical continuation is defined by our first formula (definition of the scattering amplitude) and from the condition that the bound state should have a wave function which decreases at large distance. Actually, $\sqrt{s - 4m^2}$ at $s < 4m^2$ could be $\pm\kappa = \pm\sqrt{4m^2 - s}$. Therefore the wave function for $s < 4m^2$ has the form:

$$\Psi \rightarrow f(\kappa, \theta) \frac{e^{\pm\kappa r}}{r}$$

As I have mentioned we have to choose $\int |\Psi|^2 dv < \infty$ and this condition tells us that

$$-ik \rightarrow \kappa .$$

Therefore at $s < 4m^2$ our scattering amplitude has the form

$$f_0(s) = \frac{a}{1 + a\sqrt{4m^2 - s}} . \quad (11)$$

One can see that at $a < 0$ we have a pole:

$$1 + a\sqrt{4m^2 - s} = 0 ;$$

$$s = 4m^2 - \frac{1}{a^2} = m_D^2 .$$

Introducing the binding energy (ϵ_D) $m_D = 2m + \epsilon_D$ we calculate $a = \frac{1}{\sqrt{m_D|\epsilon_D|}}$. For small values of the binding energy the value of a is big and therefore we can use our approximation. Such a situation, for example, occurs in proton - neutron scattering where the scattering length is large and negative. This is the reason for the deuteron state in this reaction. It is

interesting to calculate the wave function of the deuteron by just using the definition (for $l = 0$)

$$\Psi_D(t, r) = \int dE e^{-iEt} f_0(k) \frac{e^{-\kappa r}}{r} .$$

One can check that taking this integral one finds the deuteron wave function which can be found in any text book on quantum mechanics.

2. The Breit - Wigner resonance.

Let us assume that $g_l(s = M^2) = 0$ at some value of M which is not particularly close to $s = 4m^2$. In this case $k = k_M = \frac{1}{2}\sqrt{M^2 - 4m^2}$ and

$$g_l(s) = g'_l(M^2 - s) + g''_l(M^2 - s)^2 + ..$$

The partial amplitude at $s \rightarrow M^2$ reduces to

$$f_l = \frac{1}{g'_l(M^2 - s) - ik_m} = \frac{\gamma}{M^2 - s - ik_M\gamma} . \quad (12)$$

I hope that everybody recognizes the Breit - Wigner formula. If we introduce a new notation: $\Gamma = k_M \gamma$ then

$$f_l = \frac{\Gamma}{k_M(M^2 - s - i\Gamma)} . \quad (13)$$

This formula can be obtained in a little bit different form. For $s \rightarrow M$ $s - M^2 = (\sqrt{s} - M)(\sqrt{s} + M) \approx 2M(E - M)$, Eq. (13) can be rewritten as

$$f_l = \frac{\tilde{\Gamma}}{k_M(E - M - i\tilde{\Gamma})} \quad (14)$$

It is very instructive to check that this formula as well as Eq. (13) satisfies the unitarity constraint.

Substituting this Breit - Wigner form for the general formula we obtain

the following wave function

$$\begin{aligned} \Psi &= \int dE \frac{e^{-iEt}\tilde{\Gamma}}{k_M(E - M - i\tilde{\Gamma})} \frac{e^{ikr}}{r}, = \\ &= e^{-iMt} e^{-\tilde{\Gamma}t} \frac{\tilde{\Gamma}}{k_M} \frac{e^{ik_M r}}{r} . \end{aligned}$$

Therefore the physical meaning of $\tilde{\Gamma}$ is that $\tau = \frac{1}{\tilde{\Gamma}}$ is the lifetime of the resonance.

The contribution of the resonance to the total cross section at $s = M^2$ (maximum) is equal to

$$\sigma_l = \frac{4\pi^2(2l+1)}{k_M^2} = \sigma_l^{max} .$$

1.4 Inelastic channels in unitarity.

As discussed for the elastic scattering we have

$$\Psi_{el}^i(t < t_{interaction}) = e^{ikz}$$

and

$$\Psi_{el}^f(t > t_{interaction}) = e^{ikz} + \frac{f(k, \theta)}{r} e^{ikr}$$

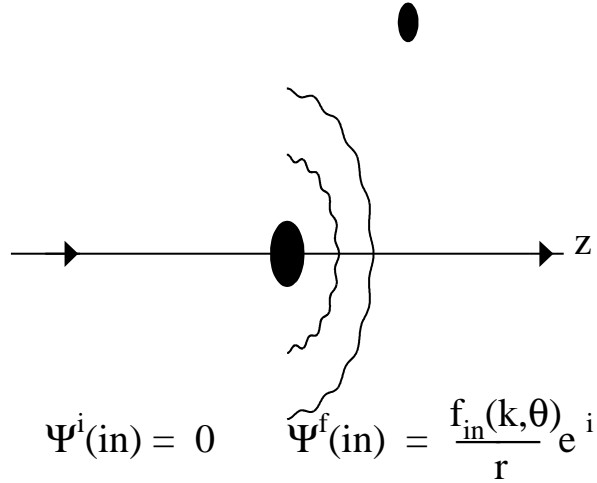
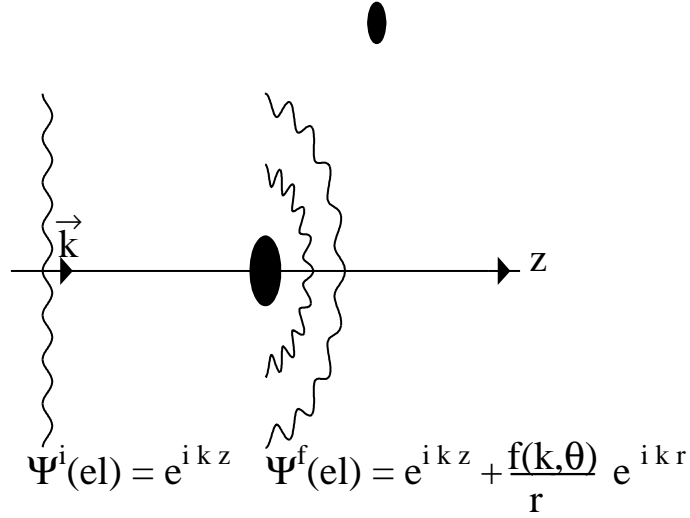


Figure 5: *Elastic and inelastic scattering.*

For inelastic (production) processes we have a totally different situation:

$$\Psi_{in}^i(t < t_{interaction}) = 0$$

after the collision there is a wave function, namely, a spherical outgoing wave:

$$\Psi_{in}^i(t > t_{interaction}) = \frac{f_{in}(k, \theta)}{r} e^{ikr}.$$

It is obvious that we have to add the inelastic channel to the r.h.s. of the unitarity constraint which reads

$$Im f_l^{el} = k |f_l^{el}|^2 + \Phi_i f_{l;i}^{in} f_{l;i}^{*in} \quad (15)$$

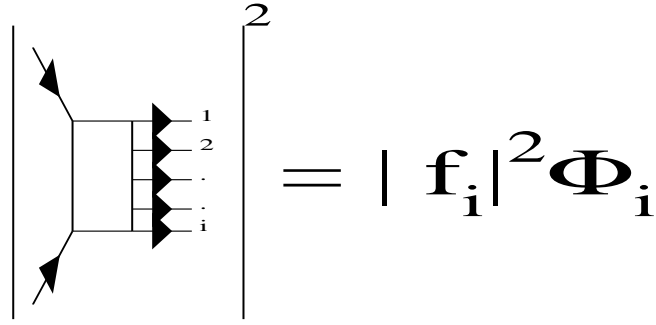


Figure 6: *The inelastic contribution to the unitarity constraint.*

For the Breit - Wigner resonance the full unitarity constraint of Eq. (15) has a simple graphical form (see Fig.7).

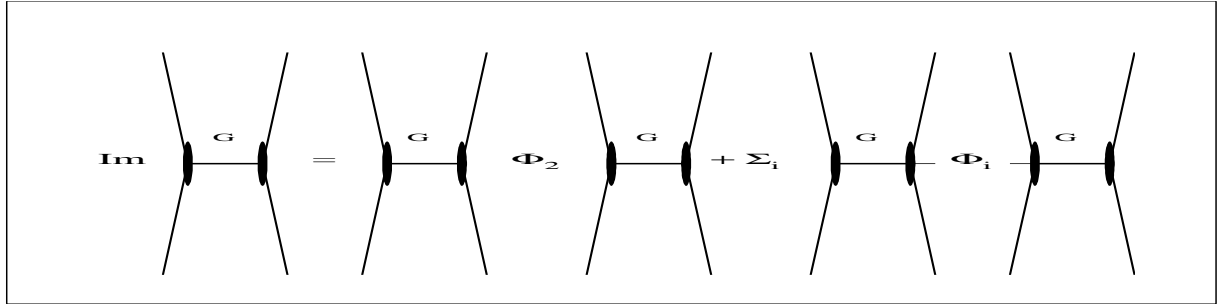


Figure 7: *The unitarity constraint for Breit - Wigner resonances.*

Introducing the notation $g_i g_i = \gamma_i$ and using the Breit - Wigner form

$$G = \frac{1}{k_M (s - M^2 - i \Gamma_{tot})}$$

we can rewrite the unitarity constraint in the form:

$$\Gamma_{tot} = k_M \gamma_{el} + \sum \gamma_i \Phi_i = \Gamma_{el} + \sum \Gamma_i. \quad (16)$$

1.5 Unitarity at high energies.

- Elastic scattering.

High energy means that

$$ka \gg 1$$

where a is the typical size of the interaction. It is very useful to introduce the impact

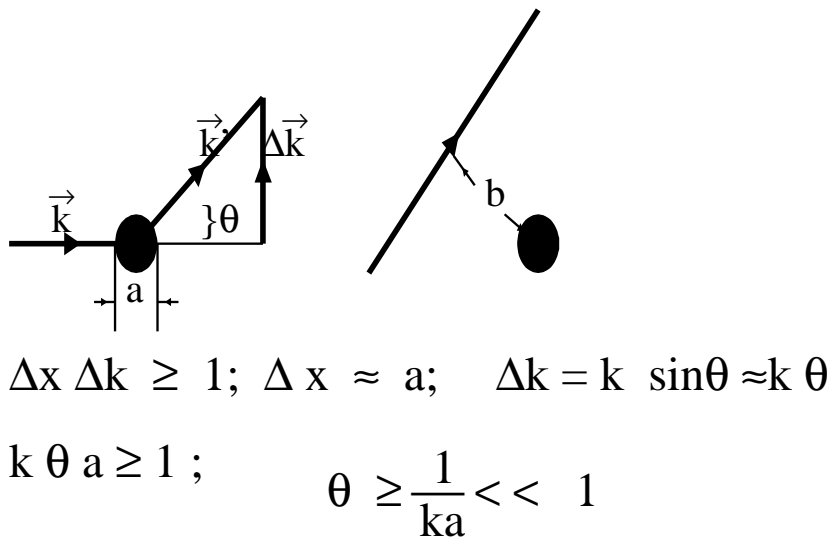


Figure 8: Useful kinematic variables and relations for high energy scattering.

parameter b (very often we denote it as b_t) by $l = kb$. The meaning of b is quite clear from the classical formula for the angular moment l and from Fig.8. The new variable b will be of the order of a ($b \approx a$) while l itself will be very large at high energy. Following this expectation, we rewrite the scattering amplitude in the form:

$$f = \sum_{l=0}^{\infty} f_l(k)(2l+1)P_l(\cos\theta) = \quad (17)$$

$$= \sum_{l=0}^{\infty} f_l(k)(2l+1)J_0(l\theta) \rightarrow 2 \int l dl f_l J_0(l\theta) .$$

Here we made use of the following property of P_l :

$$P_l(\cos \frac{\theta l}{l}) \rightarrow J_0(\theta l) ,$$

for $\theta l \approx 1$. Then

$$\theta l = kb\theta \approx \frac{kb}{ka} = \frac{b}{a} .$$

Now let us introduce a new notation:

$$1. t = (p_1 - p'_1)^2 = (p_{10} - p'_{10})^2 - p_1^2(1 - \cos^2\theta) \rightarrow -k^2\theta^2 \text{ at high energy};$$

$$2. -t = q_{\perp}^2 ;$$

$$3. A = \frac{f}{k} , \text{ this is a new definition for the scattering amplitude}$$

$$4. \text{ Instead of the partial amplitude } f_l(k) \text{ we introduce } a(b, k) = 2f_l k ;$$

$$5. \int d^2b = \int b db d\phi = \int 2\pi b db .$$

In the new notation the scattering amplitude can be written in the form:

$$A(s, t) = \frac{1}{2\pi} \int a(b, s) d^2b e^{i\vec{b} \cdot \vec{q}_{\perp}} , \quad (18)$$

where $\vec{q}_{\perp} = \vec{p}_1 - \vec{p}'_1$.

1.6 Unitarity constraint in impact parameter (b).

The **elastic unitarity** for the new amplitude looks as follows:

$$2 \operatorname{Im} a_{el}(s, b) = |a_{el}(s, b)|^2 . \quad (19)$$

The generalization of Eq. (19) for the case of inelastic interactions is obvious and it leads to

$$2 \operatorname{Im} a_{el}(s, b) = |a_{el}(s, b)|^2 + G_{in}(s, b) , \quad (20)$$

where G_{in} is the sum of all inelastic channels. This equation is our master equation which we will use frequently during these lectures. Let us discuss once more the normalization of our amplitude.

The scattering amplitude in b -space is defined as

$$a_{el}(s, b) = \frac{1}{2\pi} \int d^2q e^{-i\vec{q}_{\perp} \cdot \vec{b}} A(s, t) \quad (21)$$

where $t = -q_\perp^2$. The inverse transform for $A(s, t)$ is

$$A(s, t) = \frac{1}{2\pi} \int a_{el}(s, b) d^2b e^{i\vec{q}_\perp \cdot \vec{b}}. \quad (22)$$

In this representation

$$\sigma_{tot} = 2 \int d^2b \text{Im} a_{el}(s, b); \quad (23)$$

$$\sigma_{el} = \int d^2b |a_{el}(s, b)|^2. \quad (24)$$

1.7 A general solution to the unitarity constraint.

Our master equation (see Eq. (20)) has the general solution

$$G_{in}(s, b) = 1 - e^{-\Omega(s, b)}; \quad (25)$$

$$a_{el} = i \{ 1 - e^{-\frac{\Omega(s, b)}{2} + i\chi(s, b)} \};$$

where opacity Ω and phase $\chi = 2\delta(s, b)$ are real arbitrary functions.

The algebraic operations, which help to check that Eq. (25) gives the solution, are:

$$\text{Im} a_{el} = 1 - e^{-\frac{\Omega}{2}} \cos \chi;$$

$$|a_{el}|^2 = (1 - e^{-\frac{\Omega}{2} + i\chi}) \cdot (1 - e^{-\frac{\Omega}{2} - i\chi}) = 1 - 2e^{-\frac{\Omega}{2}} \cos \chi + e^{-\Omega}.$$

The opacity Ω has a clear physical meaning, namely $e^{-\Omega}$ is the probability to have no inelastic interactions with the target.

One can check that Eq. (20) in the limit, when Ω is small and the inelastic processes can be neglected, describes the well known solution for the elastic scattering: phase analysis. For high energies the most reasonable assumption just opposite, namely, the real part of the elastic amplitude to be very small. It means that $\chi \rightarrow 0$ and the general solution is of the form:

$$G_{in}(s, b) = 1 - e^{-\Omega(s, b)}; \quad (26)$$

$$a_{el} = i \{ 1 - e^{-\frac{\Omega(s, b)}{2}} \}.$$

We will use this solution at the end of our lectures. At the moment, I do not want to discuss the theoretical reason why the real part should be small at high energy. I prefer to claim that this is a general feature of all experimental data at high energy.

2 The great theorems.

Now, I would like to show you how one can prove the great theorems just from the unitarity and analyticity. Unfortunately, I have no time to prove all three theorems but I hope that you will do it yourselves following my comments.

2.1 Optical Theorem.

The optical theorem gives us the relationship between the behaviour of the imaginary part of the scattering amplitude at zero scattering angle and the total cross section that can be measured experimentally. It follows directly from Eq. (20), after integration over b . Indeed,

$$4\pi Im A(s, t = 0) = \int 2Im a_{el}(s, b) d^2b = \int d^2b \{ |a_{el}(s, b)|^2 + G_{in}(s, b) \} = \sigma^{el} + \sigma^{in} = \sigma_{tot} . \quad (27)$$

2.2 The Froissart boundary.

We call the Froissart boundary the following limit of the energy growth of the total cross section:

$$\sigma_{tot} \leq C \ln^2 s \quad (28)$$

where s is the total c.m. energy squared of our elastic reaction: $a(p_a) + b(p_b) \rightarrow a + b$, namely $s = (p_a + p_b)^2$. The coefficient C has been calculated but we do not need to know its exact value. What is really important is the fact that $C \propto \frac{1}{k_t^2}$, where k_t is the minimum transverse momentum for the reaction under study. Since the minimum mass in the hadron spectrum is the pion mass the Froissart theorem predicts that $C \propto \frac{1}{m_\pi^2}$. The exact calculation gives $C = 60mb$.

I think, it is very instructive to discuss a proof of the Froissart theorem. As we have mentioned the total cross section can be expressed through the opacity Ω due to the unitarity constraint. Indeed,

$$\sigma_{tot} = 2 \int d^2b \{ 1 - e^{-\frac{\Omega(s, b)}{2}} \} . \quad (29)$$

For small Ω Eq. (29) gives

$$\sigma_{tot} \rightarrow \int d^2b \Omega(s, b) .$$

It turns out that we know the b - behaviour of Ω at large b . Let us consider first the simple example : the exchange of a vector particle (see Fig.9).

Introducing Sudakov variables we can expand each vector in the following form:

$$q = \alpha_q p'_1 + \beta_q p'_2 + q_t$$

$$\text{where } p_1'^2 = p_2'^2 = 0$$

and

$$p_1 = p'_1 + \beta p'_2 ;$$

$$p_2 = \alpha_2 p'_1 + p'_2 ;$$

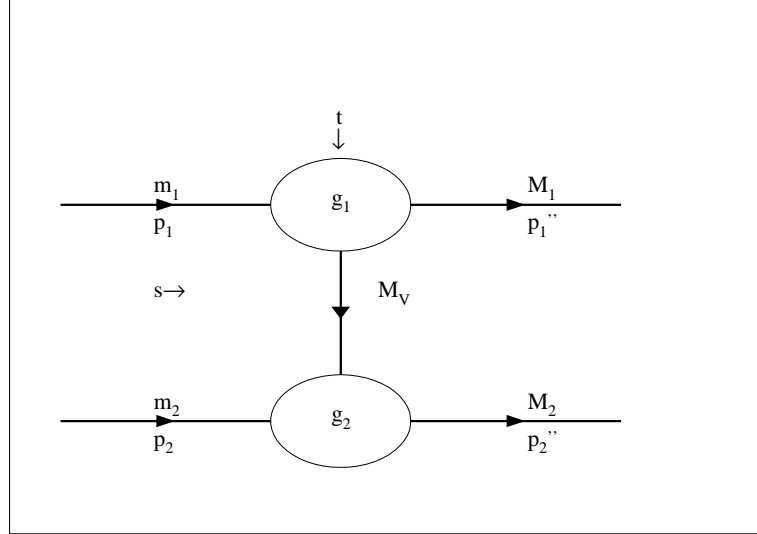


Figure 9: *Exchange of particle with mass M_V .*

It is easy to find that

$$\beta_1 = \frac{m_1^2}{s} ; \quad \alpha_1 = \frac{m_2^2}{s}$$

since

$$p_1^2 = m_1^2 = 2\beta_1 p'_1 \cdot p'_2 = \beta_1 s$$

From the equations

$$p_1'^2 = M_1^2 ; \quad p_2'^2 = M_2^2$$

we can find the values of α_q and β_q :

$$p_1'^2 = (p_q - q)^2 = ((1 - \alpha_q)p'_1 + (\beta_1 - \beta_q)p'_2)^2 = (1 - \alpha_q)(\beta_1 - \beta_q)s - q_t^2 = M_1^2$$

Therefore

$$\alpha_q = \frac{M_2^2 - m_2^2}{s} ; \quad \beta_q = \frac{m_1^2 - M_1^2}{s} \quad (30)$$

The above equations lead to

$$|q^2| = |\alpha_q \beta_q s - q_t^2| = \frac{(M_2^2 - m_2^2)(M_1^2 - m_1^2)}{s} + q_t^2 \rightarrow |_{s \rightarrow \infty} q_t^2 \quad (31)$$

Now, we are ready to write the expression for the diagram of Fig.9:

$$A(s, t) = g_1 g_2 \frac{(p_1 + p'_1)_\mu (p_2 + p'_2)_\mu}{q_t^2 + m_V^2} = g_1 g_2 \frac{4s}{q_t^2 + m_V^2} \quad (32)$$

where m_V is the mass of the vector meson.

Now, we are able to calculate the amplitude as a function of b :

$$\begin{aligned} a_{el}(s, b) &= g_1 g_2 4s \int \frac{J_0(bq_t) q_t dq_t}{q_t^2 + m_V^2} = \\ &= g_1 g_2 4s K_0(bm_V) \rightarrow |_{b \rightarrow \infty} g_1 g_2 4s \frac{e^{-m_V b}}{\sqrt{m_V b}} \end{aligned} \quad (33)$$

This calculation can be used in more general form based on the dispersion relation for the amplitude $A(s, t)$

$$A(s, t) = \frac{1}{\pi} \int_{4\mu^2}^{\infty} \frac{Im_t A(s, t')}{t' - t} dt,$$

where μ is the mass of the lightest hadron (pion). Using $t = -q_t^2$ we calculate $a_{el}(s, b)$

$$a_{el}(s, b) = \frac{1}{\pi} \int_{4\mu^2}^{\infty} dt' \int q_t dq_t J_0(bq_t) \frac{Im_t A(s, t')}{t' + q_t^2} dt \rightarrow |_{b \ll \mu} e^{-2\mu b} \quad (34)$$

Assumption: $a_{el}(s, b) < s^N e^{-2\mu b}$ at large values of b .

As we have discussed if $a_{el}(s, b) \ll 1$ opacity $\Omega = a_{el}$. Using the above assumption we can estimate the value of b_0 such that $\Omega \ll 1$ for $b > b_0$. For b_0 we have

$$s^N e^{-2\mu b_0} = 1$$

with the solution for b_0

$$b_0 = \frac{N}{2\mu} \ln s. \quad (35)$$

Eq.(29) can be integrated over b by dividing the integral into two parts $b > b_0$ and $b < b_0$. Neglecting the second part of the integral where Ω is very small yields

$$\begin{aligned} \sigma_{tot} &= 4\pi \int_0^{b_0} b db [1 - e^{-\frac{\Omega(s,b)}{2}}] + 4\pi \int_{b_0}^{\infty} b db [1 - e^{-\frac{\Omega(s,b)}{2}}] < \\ &< 4\pi \int_0^{b_0} b db = 2\pi b_0^2 = \frac{2\pi N^2}{4\mu^2} \ln^2 s. \end{aligned}$$

This is the Froissart boundary. Actually, the value of N can be calculated but it is not important. Indeed, inserting all numbers we have for the Froissart bound

$$\sigma_{tot} < N^2 30 mb \ln^2 s.$$

Because of the large coefficient in front of $\ln^2 s$ this bound has no practical application. What is really important for understanding of the high energy behaviour of the total cross section is the logic of derivation and the way how the unitarity constraint has been used.

2.3 The Pomeranchuk Theorem.

The Pomeranchuk theorem is the manifestation of the **crossing symmetry**, which can be formulated in the following form: one analytic function of two variables s and t describes the scattering amplitude of two different reactions $a + b \rightarrow a + b$ at $s > 0$ and $t < 0$ as well as $\bar{a} + b \rightarrow \bar{a} + b$ at $s < 0$ ($u = (p_{\bar{a}} + p_b)^2 > 0$) and $t < 0$.

The Pomeranchuk theorem says that the total cross sections of the above two reactions should be equal to each other at high energy if the real part of the amplitude is smaller than imaginary part.

To prove the Pomeranchuk theorem we need to use the dispersion relation for the elastic amplitude at $t = 0$.

$$A(s, t = 0) = \frac{1}{\pi} \left\{ \int \frac{Im_s A(s', t = 0)}{s' - s} + \int \frac{Im_u A(u', t = 0)}{u' - u} \right\}.$$

Using the optical theorem we have:

$$Im_s A(s, t = 0) = \frac{s}{4\pi} \sigma_{tot}(a + b);$$

$$Im_u A(s, t = 0) = \frac{u}{4\pi} \sigma_{tot}(\bar{a} + b).$$

Recalling that at large s $u \rightarrow -s$ we have

$$A(s, t = 0) = \frac{1}{4\pi^2} \int s' ds' \left\{ \frac{\sigma_{tot}(a + b)}{s' - s} + \frac{\sigma_{tot}(\bar{a} + b)}{s' + s} \right\}.$$

Since σ_{tot} can rise as $\ln^2 s$ we have to make one subtraction in the dispersion relation. Finally, we obtain

$$A(s, t = 0) = \frac{s}{4\pi^2} \int s' ds' \left\{ \frac{\sigma_{tot}(a + b)}{s'(s' - s)} - \frac{\sigma_{tot}(\bar{a} + b)}{s'(s' + s)} \right\}. \quad (36)$$

To illustrate the final step in our proof let us assume that at high s' $\sigma_{tot}(a + b) \rightarrow \sigma_0(a + b) \ln^\gamma s$ and $\sigma_{tot}(\bar{a} + b) \rightarrow \sigma_0(\bar{a} + b) \ln^\gamma s$. Substituting these expressions into Eq. (36), we obtain

$$ReA(s, t = 0) \rightarrow \frac{\sigma_0(a + b) - \sigma_0(\bar{a} + b)}{\gamma + 1} \ln^{\gamma+1} s \gg ImA(s, t = 0).$$

This is in contradiction with the unitarity constraint which has no solution if ReA increases with energy and is bigger than ImA . Therefore, the only way out of this contradiction is to assume that

$$\sigma_{tot}(a + b) = \sigma_{tot}(\bar{a} + b) \text{ at } s \rightarrow \infty. \quad (37)$$

2.4 An instructive model: the “black disc” approach.

Let us assume that

$$\Omega = \infty \text{ at } b < R(s) ;$$

$$\Omega = 0 \text{ at } b > R(s) .$$

The radius R can be a function of energy and it can rise as $R \approx \ln s$ due to the Froissart theorem.

As you may guess from the assumptions, this “black” disc model is just a rough realization of what we expect in the Froissart limit at ultra high energies.

It is easy to see that the general solution of the unitarity constraints simplifies to

$$a(s, b)_{el} = i\Theta(R - b) ;$$

$$G_{in}(s, b) = \Theta(R - b) ;$$

which leads to

$$\sigma_{in} = \int d^2b G_{in} = \pi R^2 ;$$

$$\sigma_{el} = \int d^2b |a_{el}|^2 = \pi R^2 ;$$

$$\sigma_{tot} = \sigma_{el} + \sigma_{in} = 2\pi R^2 ;$$

$$A(s, t) = \frac{i}{2\pi} \int d^2b \Theta(R - b) e^{i\vec{q} \cdot \vec{b}} = i \int_0^R b db J_0(bq_t) = i \frac{R}{q_t} J_1(q_t R) ;$$

$$\frac{d\sigma}{dt} = \pi |A|^2 = \pi \frac{J_1^2(R\sqrt{|t|})}{|t|} .$$

EXPERIMENT: The experimentalists used to present their data on t - dependence in the exponential form, namely

$$Ra = \frac{\frac{d\sigma}{dt}}{\frac{d\sigma}{dt}|_{t=0}} = e^{-B|t|}$$

Comparing this parameterization of the experimental data with the behaviour of the “black disc” model at small t , namely, $\frac{d\sigma}{dt} = \frac{\pi R^2}{4} (1 - \frac{R^2}{2} |t|)$, leads to $B = R^2/2$.

From experiment we have for proton - proton collision $B = 12 GeV^{-2}$ and, therefore, $R = 5 GeV^{-1} = 1 fm$. The t - distribution for this radius in the “black disc” model is given in Fig.10. The value of the total cross section which corresponds to this value of the radius is $80 mb$ while the experimental one is one half of this value, $\sigma_{tot}(exp) = 40 mb$. In Figs. 11 and 12 $b, \sigma_{el}, \sigma_{tot}$ and $\frac{d\sigma}{dt}$ are given as function of energy. One can see that experimentally $\sigma_{el}/\sigma_{tot} \approx 0.1 - 0.15$ while the “black disc” model predicts 0.5. Experimentally, one finds a diffractive structure in the t distribution but the ratio of the cross sections in the second and the first maximum is about 10^{-2} in the model and much smaller ($\approx 10^{-4}$) experimentally.

Conclusions: In spite of the fact that the “black disc” model predicts all qualitative features of the experimental data the quantitative comparison with the experimental data shows that the story is much more complicated than this simple model. Nevertheless, it is useful to have this model in front of your eyes in all further attempts to discuss the asymptotic behaviour at high energies. Nevertheless the “black” disc model produces all qualitative features of the experimental high energy cross sections, furthermore the errors in the numerical evaluation is only 200 - 300 %. This model certainly is not good but it is not so bad as it could be. Therefore, in spite of the fact that the Froissart limit will be never reached, the physics of ultra high energies is not too far away from the experimental data. Let us remember this for future and move on to understand number of puzzling problems.

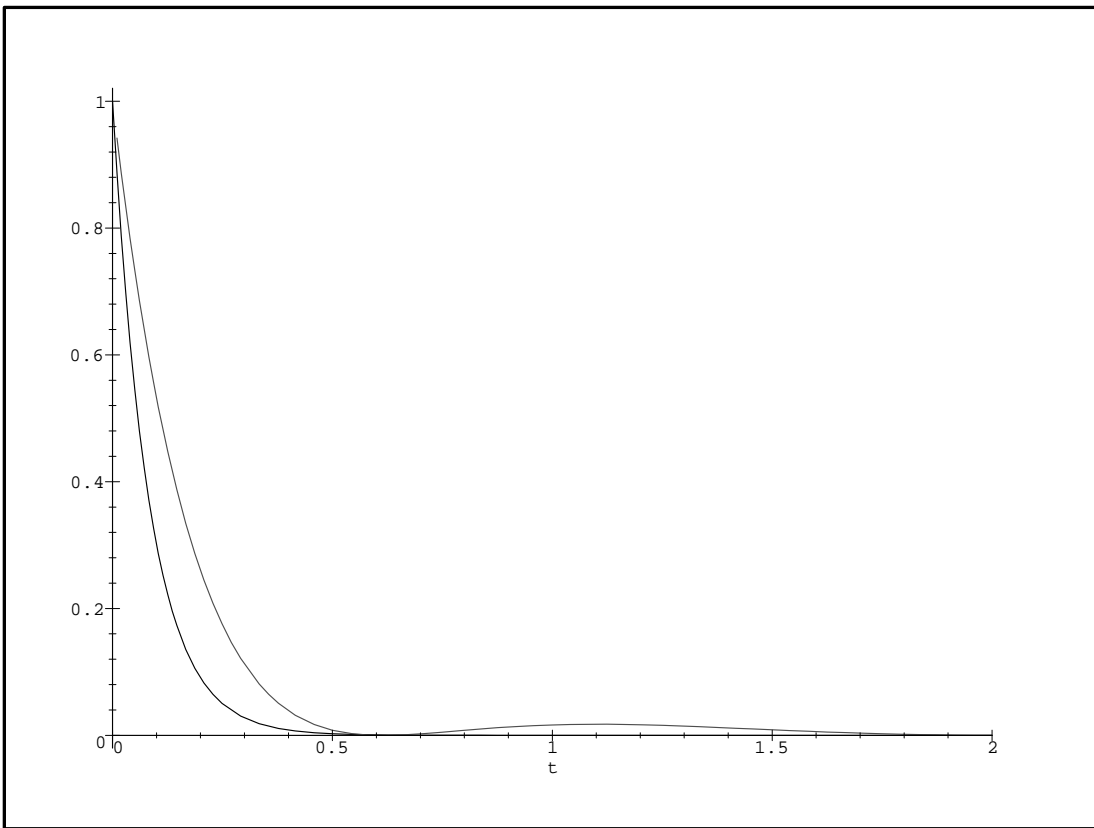


Figure 10: The t - dependence of the ratio Ra for the “black” disc model (dashed line) and for the exponential parameterization (solid line).

3 The first puzzle and Reggeons.

3.1 The first puzzle.

The first puzzle can be formulated as a question: *What happens in t - channel exchange of resonances for which the spin is bigger than 1 ?* On the one hand such resonances have been observed experimentally, on the other hand the exchange of the resonances with spin j leads to the scattering amplitudes to be proportional to s^j where s is the energy of two colliding hadrons. Such a behaviour contradicts the Froissart bound. It means that we have to find the theoretical solution to this problem.

We have considered the exchange of vector particle and saw that it gives the amplitude which grows as s . Actually, using this example, it is easy to show that the exchange of the resonance with spin j gives the scattering amplitude equals

$$A^{res}(s, t = -q_t^2) = g_1 g_2 \frac{(4s)^j}{q_t^2 + m_R^2} . \quad (38)$$

Indeed, the amplitude of the resonance in t -channel (for the reaction with energy \sqrt{t}) is equal to

$$A^{res}(s, t) = (2j + 1)g_1(t)g_2(t) \frac{P_j(z)}{t - M_R^2 - i\Gamma} , \quad (39)$$

As we know g_i has an additional kinematic factor k^j where k is momentum of particles in c.m.f. where \sqrt{t} is energy. z is cosine of the scattering angle in the same frame. To find the high energy asymptotic we need to continue this expression in the scattering kinematic region where $t < 0$ and $z \rightarrow \frac{s}{2k^2} \gg 1$. It is easy to do, if we notice that $P_j(z) \rightarrow z^j$ at $z \gg 1$ and all non analytical factors (of k^j - type) cancels in Eq. (39). recalling that $t \rightarrow -q_t^2$ at high energy we obtain Eq. (38), neglecting the width of the resonance in the first approximation. In b Eq. (39) looks as follows:

$$A \propto s^j \exp(-m_R b)$$

at large values of b and s .

Of course, the exchange of one resonance gives the real amplitude and, therefore, does not contribute to the cross section. To calculate the imaginary part of the scattering amplitude we can use the unitarity constraint, namely

$$ImA(s, t = 0) = \int d^2q \delta(p'^2 - M_1^2) \delta(p'^2 - M_2^2) |A^{res}(s, q^2)|^2 . \quad (40)$$

Recalling that the phase space $d^4q = \frac{|s|}{2} d\alpha_q \beta_q d^2q_t$ and values of β_q and α_q given in Eq.(30), we can take all integrals in Eq. (40). It is clear that at high energy

$$ImA(s, t = 0) \propto s^{2j-1}$$

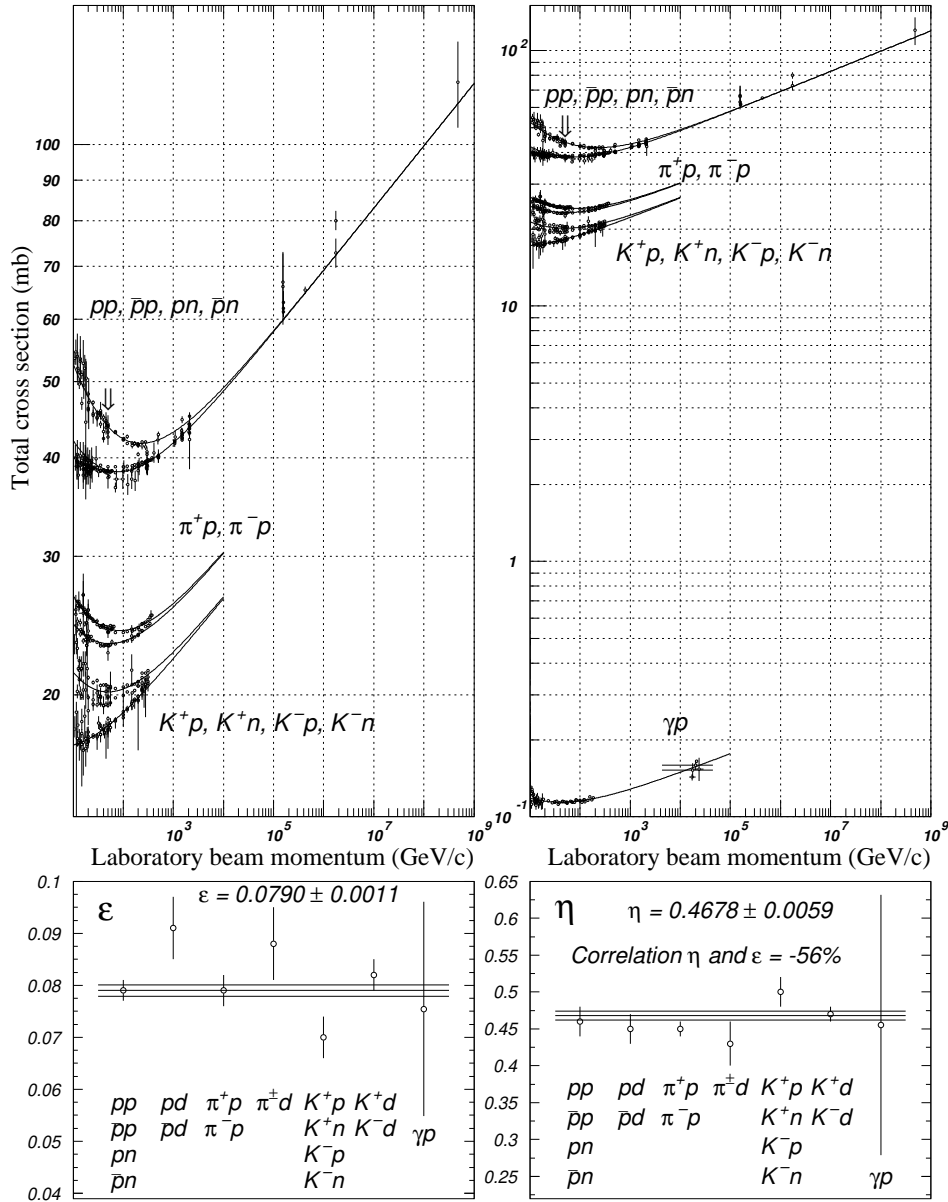


Figure 36.17: Summary of hadronic and γp total cross sections (top), and fit results to exponents for cross sections. (Courtesy of the COMPAS Group, IHEP, Protvino, Russia, 1996.)

Figure 11-a: *The experimental data on the total cross section (Particle Data Group 1996)*

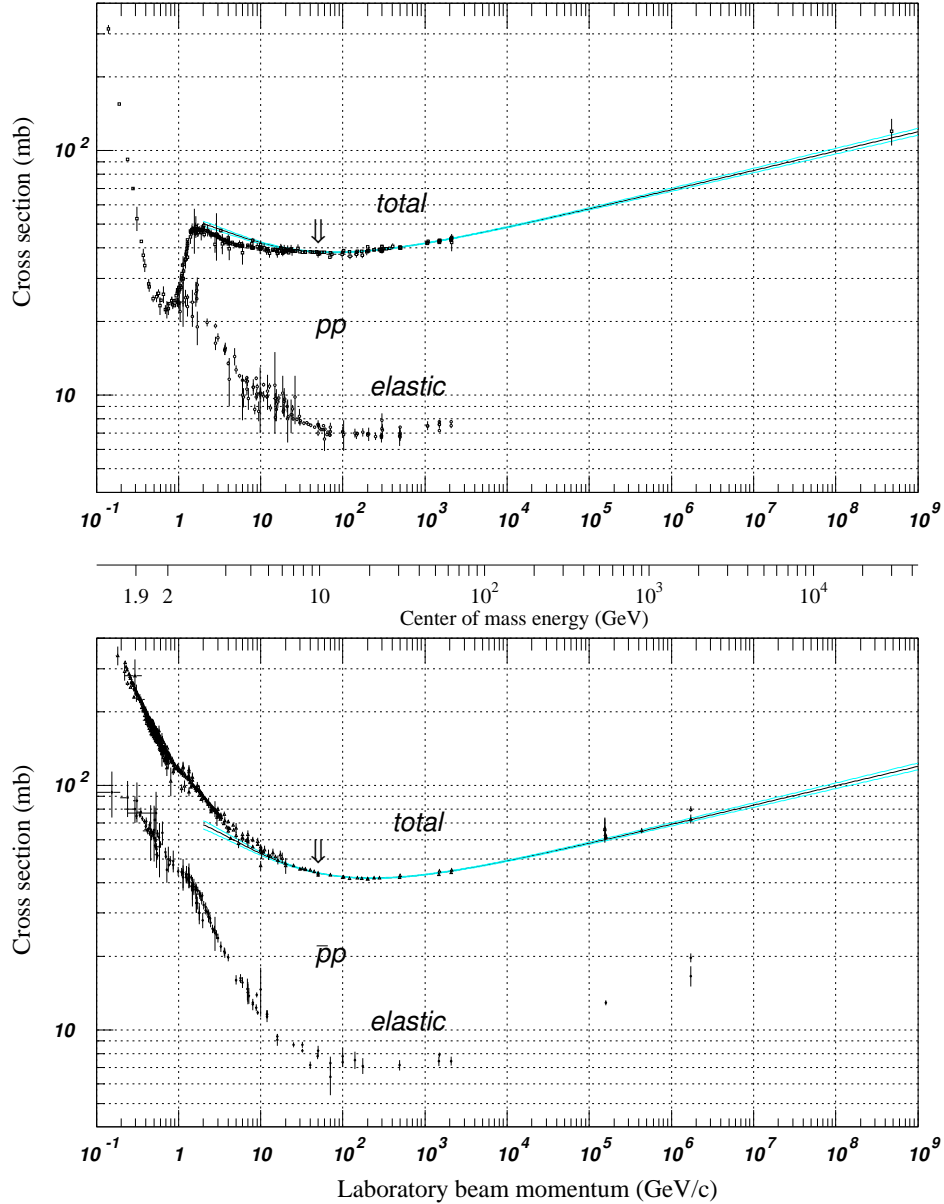


Figure 36.18: Total and elastic cross sections for pp and $\bar{p}p$ collisions as a function of laboratory beam momentum and total center-of-mass energy. Computer-readable data files may be found at <http://pdg.lbl.gov/xsect/contents.html> (Courtesy of the COMPAS Group, IHEP, Protvino, Russia, 1996.)

Figure 11-b: *The experimental data on total and elastic cross sections (Particle Data Group 1996).*

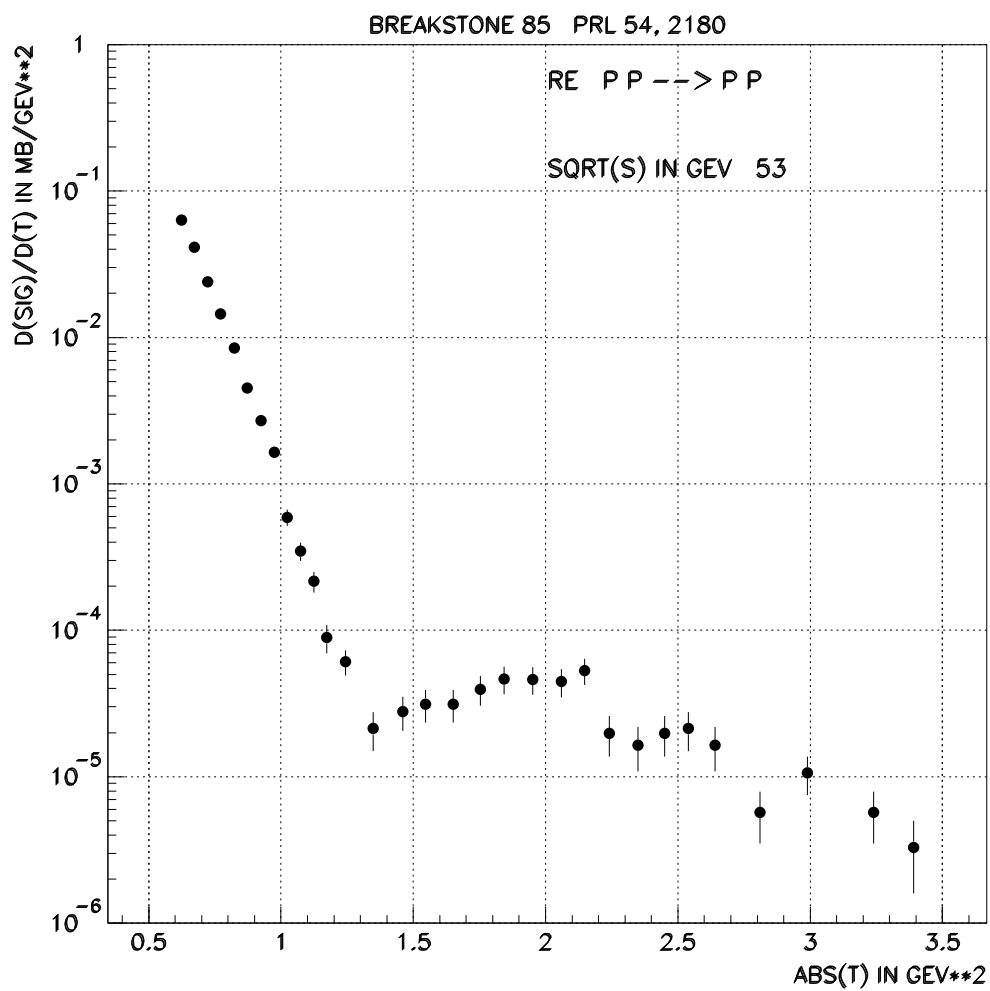


Figure 12: Differential elastic cross section.

which means that the total cross section due to exchange of two particles with spin j_1 and j_2

$$\sigma_{tot} \propto s^{j_1 + j_2 - 2}. \quad (41)$$

This formula is very instructive when we will discuss the contribution of different exchange at high energies. From Eq. (41) it is seen that the exchange of the resonance with spin bigger than 1 lead to the definite violation of the Froissart theorem.

3.2 Reggeons - solutions to the first puzzle.

The solution to the first puzzle has been found. It turns out that the exchange of all resonances can be described as an exchange of the new object - Reggeon and its contribution to the scattering amplitude is given by the simple function:

$$A_R(s, t) = g_1(m_1, M_1, t) g_2(m_2, M_2, t) \cdot \frac{s^{\alpha(t)} \pm (-s)^{\alpha(t)}}{\sin \pi \alpha(t)} \quad (42)$$

$\alpha(t)$ is a function of the momentum transfer which we call the Reggeon trajectory.

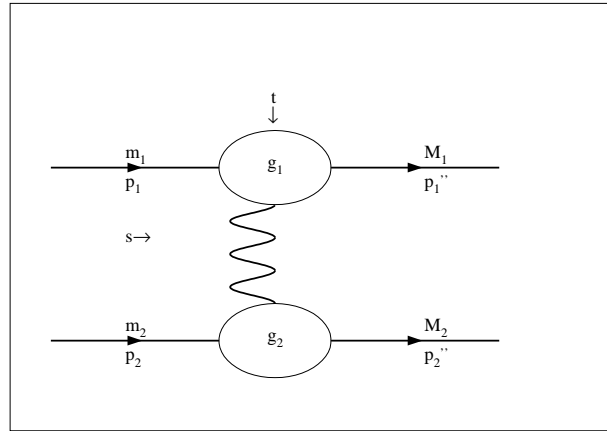


Figure 13: *The Reggeon exchange.*

The name of the new object as well as the form of the amplitude came from the analysis of the properties of the scattering amplitude in t channel using angular momentum representation. However, today it is not important the whole history of the approach. We need to understand and take for the future studies only the main properties of the above function which plays the crucial role in the theory and phenomenology of the high energy interaction.

4 The main properties of the Reggeon exchange.

4.1 Analyticity.

It is obvious that the Reggeon exchange is the analytic function in s , which has the imaginary part equals to

$$\pm g_1 g_2 s^{\alpha(t)}$$

in the s - channel and the imaginary part

$$g_1 g_2 s^{\alpha(t)}$$

in the u - channel (for $\bar{a} + b \rightarrow \bar{a} + b$ reaction). For different signs in Eq. (42) the function has different properties with respect to crossing symmetry. For plus (positive signature) the function is symmetric while for minus (negative signature) it is antisymmetric.

4.2 s - channel unitarity

To satisfy the s - channel unitarity we have to assume that trajectory $\alpha(t) \leq 1$ in the scattering kinematic region ($t < 0$). This is why the exchange of the Reggeons can solve our first puzzle.

4.3 Resonances.

Let us consider the same function but in the resonance kinematic region at $t > 4m_\pi^2$. Here $\alpha(t)$ is a complex function. If $t \rightarrow t_0$ $\alpha(t_0) = j = 2k$ where $k = 1, 2, 3, \dots$ the Reggeon exchange has a form for the positive signature:

$$A_R(s, t) \xrightarrow{t \rightarrow t_0} g_1 g_2 \cdot \frac{s^{2k}}{\alpha'(t_0)(t - t_0) - iIm\alpha(t_0)} \quad (43)$$

Since in this kinematic region the amplitude A_R describes the reaction $\bar{a} + a \rightarrow \bar{b} + b$

$$s = p^2 \sin\theta$$

where $p = \frac{\sqrt{t_0}}{2}$, the amplitude has a form

$$A_R = g_1 g_2 \cdot \frac{s^j}{\alpha'(t_0)(t - t_0) - iIm\alpha(t_0)} = \frac{g_1 g_2}{\alpha'(t_0)} \cdot \frac{p^{2j} \sin^j \theta}{t - t_0 - i\Gamma} \quad (44)$$

where the resonance width $\Gamma = \frac{Im\alpha(t_0)}{\alpha'(t_0)}$.

Therefore the Reggeon gives the Breit - Wigner amplitude of the resonance contribution at $t > 4m_\pi^2$. It is easy to show that the Reggeon exchange with the negative signature describes the contribution of a resonances with odd spin $j = 2k + 1$.

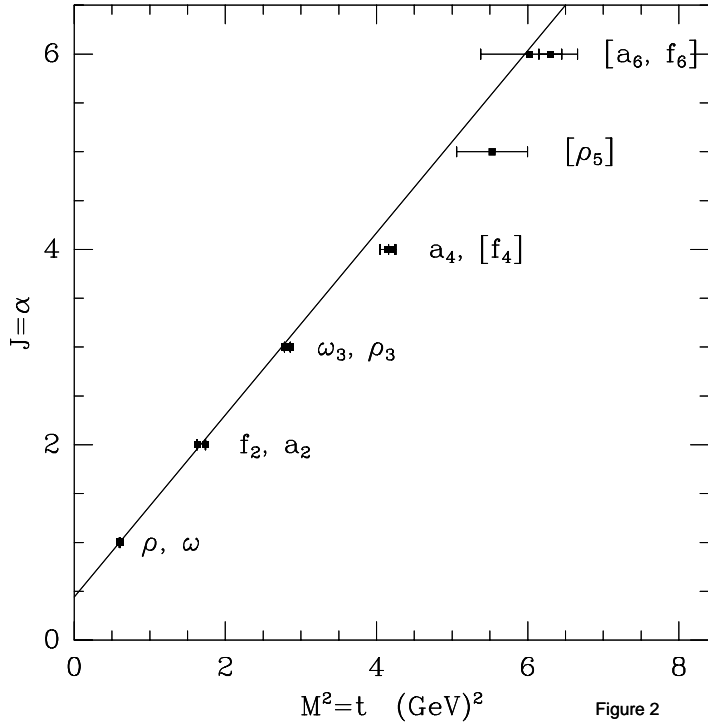


Figure 2

Figure 14: *The experimental ρ , f and a trajectories* .

4.4 Trajectories.

We can rephrase the previous observation in different words saying that the Reggeon describes the family of resonances that lies on the same trajectory $\alpha(t)$. It gives us a new approach to the classification of the resonances, which is quite different from usual SU_3 classification. Fig.14 shows the bosonic resonances classified according the Reggeon trajectories. The surprising experimental fact is that all trajectories are the straight lines

$$\alpha(t) = \alpha(0) + \alpha' t \quad (45)$$

with the same value of the slope $\alpha' \simeq 1 \text{ GeV}^{-2}$.

We would like to draw your attention to the fact that this simple linear form comes from two experimental facts: 1) the width of resonances are much smaller than their mass ($\Gamma_i \ll M_{R_i}$) and 2) the slope of the trajectories which is responsible for the shrinkage of the diffraction peak turns out to be the same from the experiments in the scattering kinematic region.

The SU_3 means in terms of trajectories that

$$\alpha_\rho(0) = \alpha_\omega(0) = \alpha_\phi(0)$$

in addition to the same value of the slope. The simple estimates show that the value of the intercept $\alpha(0) \simeq 0.5$ and therefore the exchange of the Reggeons give the cross section falling down as function of the energy without any violation of the Froissart theorem.

4.5 Definite phase.

The Reggeon amplitude of Eq. (42) can be rewritten in the form:

$$A_R = g_1 g_2 \eta_{\pm} s^{\alpha(t)} \quad (46)$$

where η is the signature factor

$$\begin{aligned} \eta_+ &= \operatorname{ctg} \frac{\pi \alpha(t)}{2} + i \\ \eta_- &= \operatorname{tg} \frac{\pi \alpha(t)}{2} - i \end{aligned}$$

It means that the exchange of the Reggeon brings very definite phase of the scattering amplitude. This fact is very important especially for the description of the interaction with a polarized target.

Factorization.

The amplitude of Eq. (42) has a simple factorized form in which all dependences on the particular properties of colliding hadrons are concentrated in the vertex functions g_1 and g_2 . To make it clear let us rewrite this factorization property in an explicit way:

$$A_R = g_1(m_1, M_1, q_t^2) g_2(m_2, M_2, q_t^2) \cdot \eta_{\pm} \cdot s^{\alpha(q_t^2)} \quad (47)$$

For example this form of the Reggeon exchange means that if we try to describe the electron deep inelastic scattering with the target through the Reggeon exchange, only the vertex function should depend on the value of the virtuality of photon (Q^2) while the energy dependence does not depends on Q^2 .

4.6 The Reggeon exchange in b .

It is easy to show that the Reggeon exchange has the following form in b :

$$a_R(s, b) = g_1(0) g_2(0) s^{\alpha(0)} \cdot \frac{1}{4\pi(R_1^2 + R_2^2 + \alpha' \ln s)} \cdot e^{-\frac{b^2}{4(R_1^2 + R_2^2 + \alpha' \ln s)}} \quad (48)$$

if we assume the simple exponential parameterization for the vertices:

$$\begin{aligned} g_1(q_t^2) &= g_1(0) e^{-R_1^2 q_t^2} ; \\ g_2(q_t^2) &= g_2(0) e^{-R_2^2 q_t^2} . \end{aligned}$$

To do this we need to take a simple integral (see eq.(21)), namely

$$a_R(s, b) = g_1(0) g_2(0) s^{\alpha(0)} \frac{1}{2} \int dq_t^2 J_0(q_t b) e^{-[R_1^2 + R_2^2 + \alpha' \ln s] q_t^2} ,$$

which gives Eq. (48). From Eq. (48) one can see that the Reggeon exchange leads to the radius of interaction, which is proportional to $\sqrt{R_1^2 + R_2^2 + \alpha' \ln s} \rightarrow \sqrt{\alpha' \ln s}$ at high energy. Recalling that in the “black disc” (Froissart) limit we have the radius of interaction which increases proportional to $\ln s$ only. Therefore, we see that the Reggeon exchange gives a picture which is quite different from the “black disk” one.

4.7 Shrinkage of the diffraction peak.

Using the linear trajectory for the Reggeons it is easy to see that the elastic cross section due to the exchange of the Reggeon can be written in the form:

$$\frac{d\sigma_{el}}{dt} = g_1^2(q_t^2) \cdot g_2^2(q_t^2) \cdot s^{2(\alpha(0)-1)} \cdot e^{-2\alpha'(0) \ln s q_t^2} \quad (49)$$

The last exponent reflects the phenomena which is known as the shrinkage of the diffraction peak. Indeed, at very high energy the elastic cross section is concentrated at values of $q_t^2 < \frac{1}{\alpha' \ln s}$. It means that the diffraction peak becomes narrower at higher energies.

5 Analyticity + Reggeons.

5.1 Duality and Veneziano model.

Now we can come back to the main idea of the approach and try to construct the amplitude from the analytic properties and the Reggeon asymptotic at high energy. Veneziano suggested the amplitude that satisfies the following constraint: it is the sum of all resonances in s - channel with zero width and simultaneously the same amplitude is the sum of the exchanges of all possible Reggeons.

Taking the simplest case of the scattering of scalar particle, the Veneziano amplitude looks as follows:

$$A = g [V(s, t) + V(u, t) + V(s, u)] \quad (50)$$

where

$$V(s, t) = \frac{\Gamma(1 - \alpha(t))\Gamma(1 - \alpha(s))}{\Gamma(1 - \alpha(t) - \alpha(s))} \quad (51)$$

One can see that the Veneziano amplitude has resonances at $\alpha(s) = n+1$ where $n = 1, 2, 3, \dots$, since $\Gamma(z) \rightarrow \frac{1}{z+n}$ at $z \rightarrow -n$. At the same time

$$A \rightarrow_{s \rightarrow \infty} \Gamma(1 - \alpha(t)) [(-\alpha(s))^{\alpha(t)} + (-\alpha(u))^{\alpha(t)}]$$

and therefore reproduces the Reggeon exchange at high energies.

This simple model was the triumph of the whole approach showing us how we can construct the theory using analyticity and asymptotic. The idea was to use the Veneziano model as the first approximation or in other word as a new Born term in the theory and to try to build the new theory starting with the new Born Approximation. The coupling constant g turns out to be dimensionless and smaller than unity. This fact certainly also encouraged the theoreticians in 70's to try this new approach.

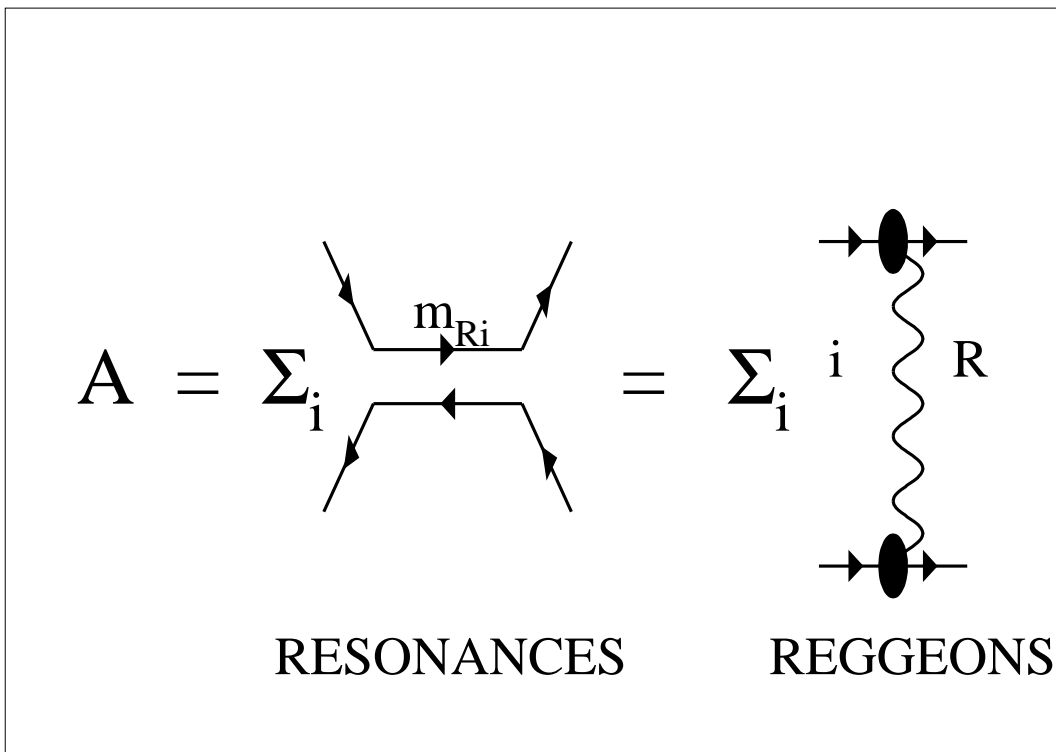


Figure 15: *Duality between the resonances in *s*-channel and the Reggeon exchange in *t*-channel.*

5.2 Quark structure of the Reggeons.

In this section, I would like to remind a consequence of the duality approach, described in Fig.15, namely, any Reggeon can be viewed as the exchange the quark - antiquark pair in t - channel. Indeed, the whole spectrum of observed experimentally resonances can be described as the different kind of excitation of either quark - antiquark pair for mesons or three quarks for baryons. This fact is well known and it is one of the principle experimental results that lied in the foundation of QCD. In Fig.16 we draw the quark diagrams reflecting this selection rules for meson - meson and meson - baryon scattering. One can notice that all these diagrams have quark - antiquark exchange in the t - channel. Therefore, the Reggeon - resonance duality leads to the quark - antiquark structure of the Reggeons.

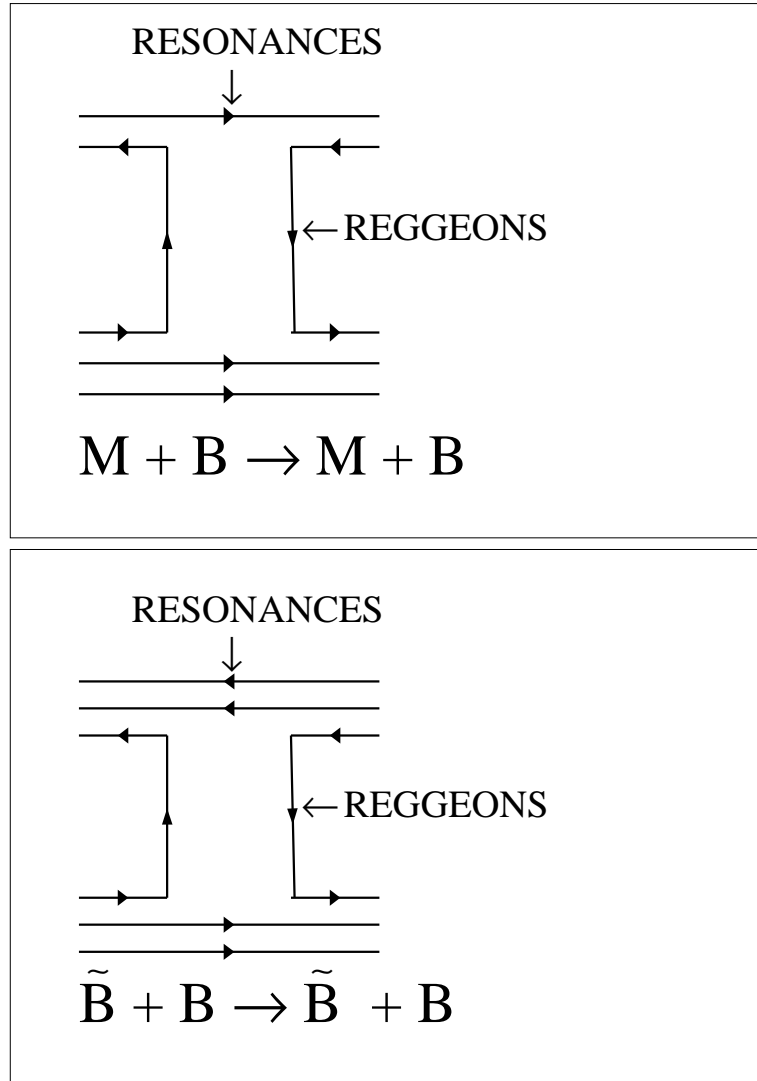


Figure 16: *Quark diagrams for meson - meson and meson - baryon scattering.*

The clear manifestation of these rules is the fact that reggeons do not contribute both to

proton - proton collisions and to K^+p one. For both of these processes we cannot draw the diagram with quark - antiquark exchange in t - channel and /or with three quarks (quark - antiquark pair) in s - channel (see Fig.17).

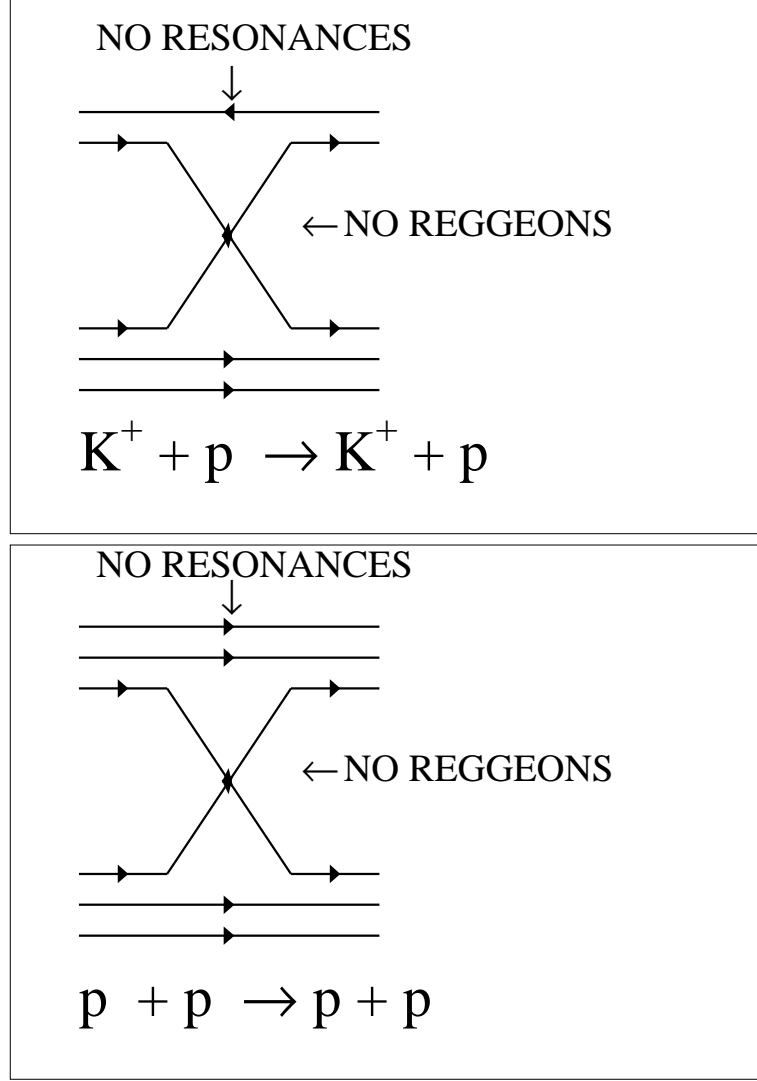


Figure 17: Quark diagrams for proton - proton and K^+p scatterings.

In the pure Reggeon language these quark - antiquark structure of Reggeons leads to so called signature degeneracy. All Reggeons with positive and negative signature have the same trajectory. Actually, it was shown in Fig.14.

Topologically, the duality quark diagrams are so called planar diagrams. It means that they can be drawn in one sheet of paper. It is worthwhile mentioning, that all more complicated diagrams, like exchange of many gluons in side of the planar diagrams, lead to the contributions which contain the maximal power of N_c where N_c is the number of colours. Therefore, in the limit where $\alpha_S \ll 1$ but $\alpha_S N_c \approx 1$ only planar diagrams give the leading contribution.

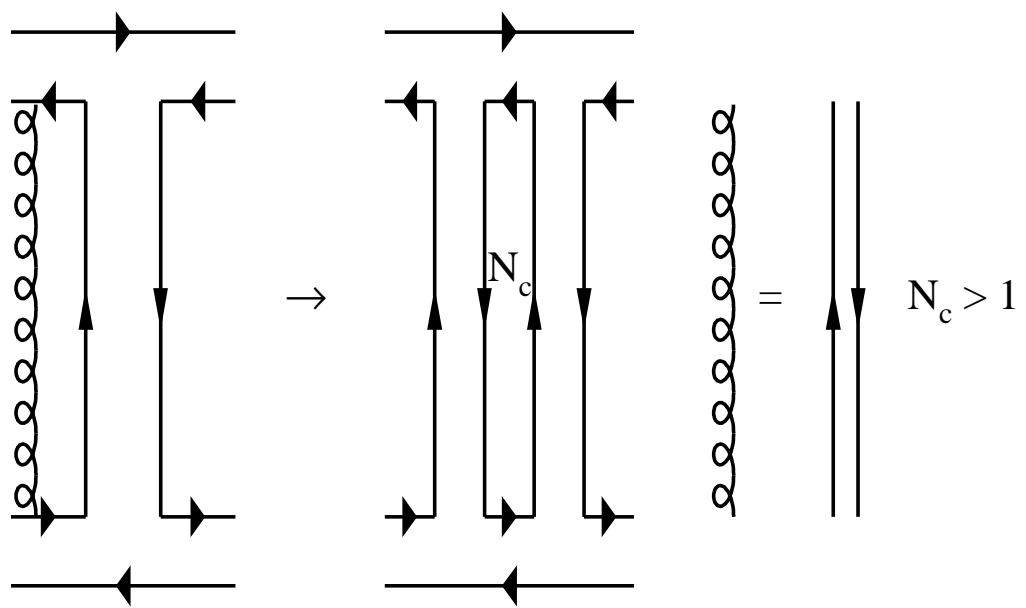


Figure 18: An example of the planar diagram in $N_c > 1$ approximation.

6 The second and the third puzzles: the Pomeron?!

6.1 Why we need the new Reggeon - the Pomeron?

The experiment shows that:

1. *There is no particles (resonances) on the Reggeon trajectory with the value of the intercept which is close to unity ($\alpha(0) \rightarrow 1$).* As it has been mentioned the typical highest value of the intercept is $\alpha(0) \sim 0.5$ which generates the cross section of the order of $\sigma_{tot} \propto s^{\alpha(0)-1} \propto s^{-\frac{1}{2}}$. Therefore, we introduced Reggeons to solve the first puzzle and we found to our surprise that these Reggeons give us the total cross section which falls down with at high energy.

2. *The total cross section is approximately constant at high energy.* It means that fighting against the rise of the cross section due to high spin resonances exchange we were so successful in this struggle that we got a problem to describe a basic experimental fact that the total cross section does not show any decrease with energy.

The above two statement we call the second and the third puzzles that have to be solved in theory. The strategy of the approach was to assume that the Reggeon with the intercept close to 1 exists and tried to understand how and why it would be different from other Reggeons, in particular, why there is no particle on this trajectory. Now let us ask ourselves why we introduce one more Reggeon? And we have to answer: only because of the lack of imagination. In more high words we can say that we did not want to multiply the essentials and even find some philosopher to refer to. However, it does not make any difference and cannot hide the fact that the new Reggeon is just the simplest attempt to understand the constant total cross section at high energy and nothing more.

Now, let me introduce for the first time the word Pomeron. The first definition of the Pomeron:

The Pomeron is the Reggeon with $\alpha(0) - 1 \equiv \Delta \ll 1$

The name of Pomeron was introduced after Russian physicist Pomeranchuk who did a lot to understand this miracle object. By the way, the general name of the Reggeon was given after the Italian physicist Regge, who gave a beautiful theoretical arguments why such objects can exist in the quantum mechanics.

The good message about the Pomeron hypothesis that it is really rich and leads to a huge number of predictions since the Pomeron should show up all properties of the Reggeon exchange (see the previous section). And we have got one more surprise: all these Reggeon properties have been seen experimentally.

6.2 Donnachie - Landshoff Pomeron.

The phenomenology, based on the Pomeron hypothesis turned out to be very successful, survived, at least two decade, and if you even do not like this hypothesis you have to learn it to cope with the huge experimental information on the high energy behaviour of different cross sections.

Let me summarize what we know about the Pomeron from the experiment:

1. $\Delta \simeq 0.08$
2. $\alpha'(0) \simeq 0.25 \text{GeV}^{-2}$

Donnachie and Landshoff gave an elegant description of almost all existing experimental data using the hypothesis of the Pomeron with the above parameters of its trajectory. The fit of the data is quite good but let us use this DL Pomeron as an example to which we are going to apply everything that we have learned.

First regretful property of the DL Pomeron is the fact that it violate the unitarity since $\Delta > 1$. However, the Froissart limit that we obtained, gives $\sigma_{tot} < 30mb N^2 \ln^2 s/s_0$. Taking $N = 1$ and $s_0 = 100 \text{GeV}^2$ we have $\sigma_{tot} < 300 \text{mB}$ for the Tevatron energy. Therefore, at first sight, the theoretical problem with unitarity exists but we are far away from this problem in all experiments even in future.

However, we have to be more careful with such statements, since the unitarity constraint is much richer that the Froissart limit. Indeed, from general unitarity constraint we can derive so called “weak unitarity”, namely

$$Ima_{el}(s, b) \leq 1 . \quad (52)$$

Indeed, it follows directly from the general solution of unitarity constraint which is

$$Ima_{el}(s, b) = 1 - e^{-\frac{\Omega}{2}} \leq 1 . \quad (53)$$

For the DL Pomeron we can calculate the amplitude for the Pomeron exchange in impact parameter representation (see Eq. (48)) and the result is

$$a_{el}^{DL} = \frac{\sigma(s = s_0)}{4\pi [2R_p^2(s = s_0) + \alpha' \ln(s/s_0)]} \left(\frac{s}{s_0}\right)^\Delta e^{-\frac{b^2}{4[2R_p^2(s = s_0) + \alpha' \ln(s/s_0)]}} = \quad (54)$$

$$\frac{\sigma(s = s_0)}{4\pi B_{el}} \left(\frac{s}{s_0}\right)^\Delta e^{-\frac{b^2}{2B_{el}}} ,$$

where B_{el} is the slope for the elastic cross section ($\frac{d\sigma}{dt} = \frac{d\sigma}{dt}|_{t=0} e^{-B_{el}|t|}$). One can see, taking all numbers from Fig.11, that $a_{el}^{DL}(s, b = 0) \sim 1/2$ at $\sqrt{s} \sim 100 \text{GeV}$. For higher energies the DL Pomeron violate the “weak unitarity”.

Therefore, in the range of energies between the fixed target FNAL energies and the Tevatron energy the DL Pomeron cannot be considered as a good approach from the theoretical point of view in spite of the good description of the experimental data. We will discuss this problem later in these lectures in more details.

7 The Pomeron structure in the parton model.

7.1 The Pomeron in the Veneziano model (Duality approach).

As has been mentioned the Pomeron does not appear in the new Born term of our approach. Therefore, the first natural idea was to make an attempt to calculate the next to the Born approximation in the Veneziano model to see can the Pomeron appear in it. The basic equation that we want to use is graphically pictured in Fig.19, which is nothing more than the optical theorem.

However we have to know the Born approximation for the amplitude of production of n particle. Our hope was that we would need to know only a general features of this production amplitude to reach an understanding of the Pomeron structure.

To illustrate the main properties and problems which can arise in this approach let us calculate the contribution in equation of Fig. 19 of the first two particle state ($\sigma_{tot}^{(2)}$). This contribution is equal to:

$$\sigma_{tot}^{(2)} = s^{2(\alpha_R(0)-1)} \int d^2 q'_t \Gamma^2(1 - \alpha(q'^2_t)) \cdot e^{-2\alpha' q'^2_t \ln s} \quad (55)$$

since

$$\Gamma(1 - \alpha(q'^2_t)) \propto \left(-\frac{\alpha(q'^2_t)}{e}\right)^{-2\alpha(q'^2_t)} \rightarrow e^{\alpha' q'^2_t \ln(\alpha' q'^2_t)}$$

one can see that the essential values of q' in the integral is rather big, of the order of $q'^2_t \sim s$. It means that we have to believe in the Veneziano amplitude at the large value of momentum transfer. Of course nobody believed in the Veneziano model as a correct theory at small distance neither 25 years ago nor now.

However we have learned a lesson from this exercise (the lesson!),namely

To understand the Pomeron structure we have to understand better the structure of the scattering amplitude at large values of the momentum transfer or in other words we should know the interaction at small distances.

7.2 The topological structure of the Pomeron in duality approach.

The topological structure of the quark diagrams for the Pomeron is more complicated. Actually, it corresponds to two sheet configuration . It means that we can draw the Pomeron duality diagram not in the sheet of paper but in the surface of a cylinder. For us even more important that the counting the power of N_c leads to the answer which has one power of N_c less that the planar diagram. In Fig.19 you can see a reduction of the duality quark diagram to QCD gluon exchange (gluon “ladder” diagram). A simple counting of N_c factors shows that the amplitude for emission of n -gluon $\propto \alpha_S^2 (2 + n) N_c^{1+n}$. Therefore, the approach

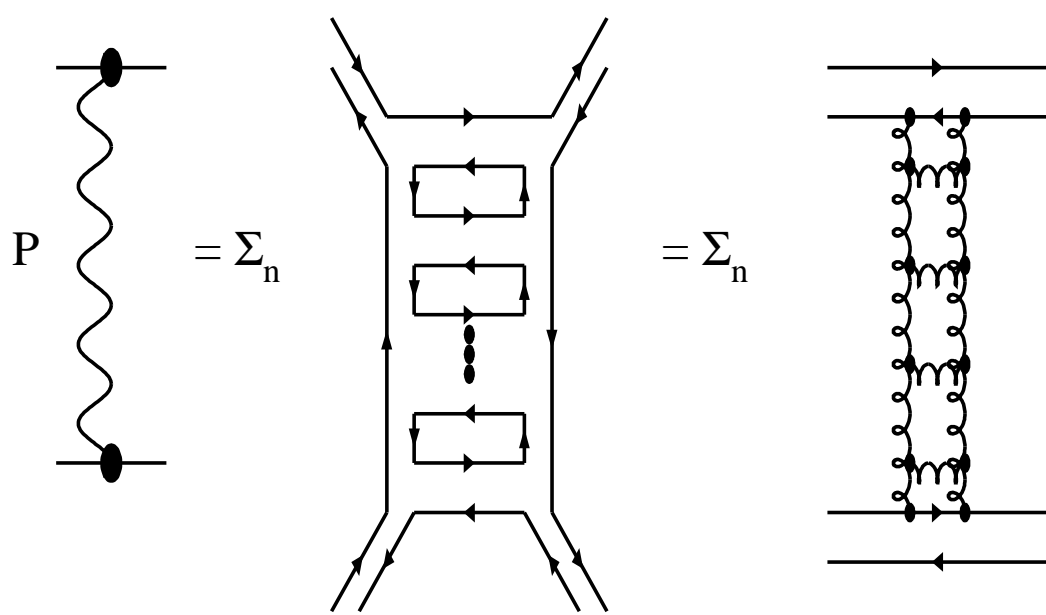
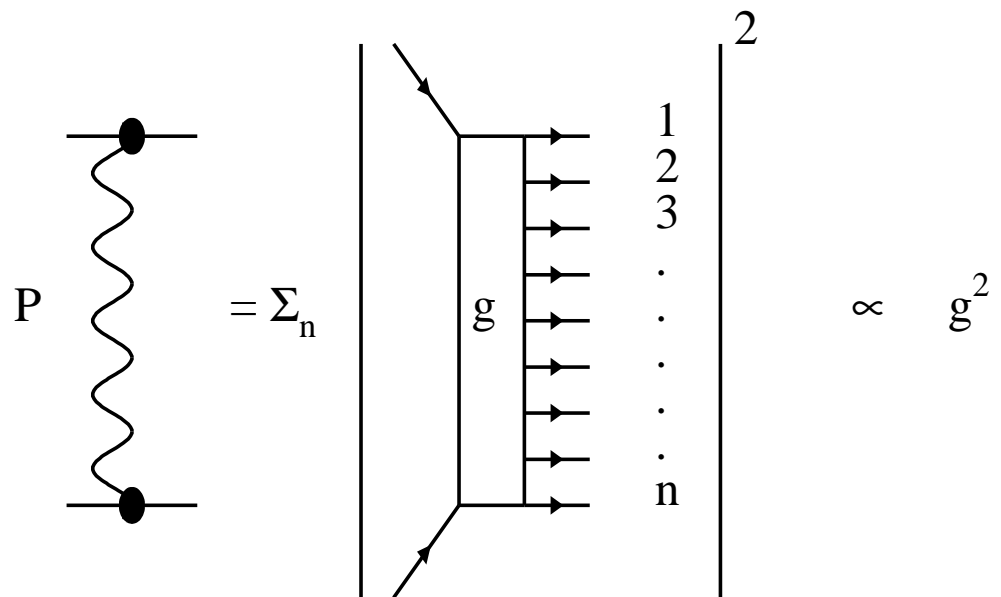


Figure 19: The Pomeron structure in the duality approach. ⁴⁴

becomes a bit messy. Strictly speaking there is no Pomeron in the leading order of N_c , but in spite of the fact that it appears in the next order with respect to N_c the s -dependence can be so strong that it will compensate this smallness. So the estimate for ratio are the following:

$$\frac{\text{Pomeron}}{\text{Reggeon}} \propto \frac{\alpha_S}{N_c} \left(\frac{s}{s_0}\right)^{\Delta - \alpha_R(0)+1} \approx \frac{\alpha_S}{N_c} \left(\frac{s}{s_0}\right)^{\Delta - \alpha_R(0)+1} \approx \frac{\alpha_S}{N_c} \left(\frac{s}{s_0}\right)^{0.51}.$$

7.3 The general origin of $\ln^n s$ contributions.

We show here that the $\ln^n s$ contribution is originated from the phase space and, because of this, such logs appear in any theory (at least in all theories that I know). The main contribution to the equation of Fig.19 comes from very specific region of integration. Indeed, the total cross section can be written as follows:

$$\sigma_{tot} = \Sigma_n \int |M_n^2(x_i p, k_{ti})| \Pi_i \frac{dx_i}{x_i} d^2 k_{ti} \quad (56)$$

where x_i is the fraction of energy that carried by the i -th particle. Let's call all secondary particle partons.

It is clear that the biggest contribution in the above equation comes from the region of integration with strong ordering in x_i for all produced partons, namely

$$x_1 \gg x_2 \gg \dots \gg x_i \gg x_{i+1} \gg \dots \gg x_n = \frac{m^2}{s} \quad (57)$$

Integrating in this kinematic region we can put all $x_i = 0$ in the amplitude M_n . Finally,

$$\begin{aligned} \sigma_{tot} &= \Sigma_n \int \Pi_i d^2 k_{ti} |M_n^2(k_{ti})| \int_{\frac{m^2}{s}}^1 \frac{dx_1}{x_1} \dots \int_{\frac{m^2}{s}}^{x_{i-1}} \frac{dx_i}{x_i} \dots \int_{\frac{m^2}{s}}^{x_{n-1}} \frac{dx_n}{x_n} \\ &= \Sigma_n \int \Pi_i d^2 k_{ti} |M_n^2(k_{ti})| \cdot \frac{1}{n!} \ln^n s \end{aligned} \quad (58)$$

This equation shows one very general property of the high energy interactions, namely the longitudinal coordinates (x_i) and the transverse ones (k_{ti}) turns out to be separated and should be treated differently. The integration over longitudinal coordinates give $\ln^n s$ - term which does not depend on specific theory that we are dealing with, while the transverse momenta integration depends on our theory and it is rather complicated problem to be solved in general. In some sense the above equation reduced the problem of high energy behaviour of the total cross section to the calculation of the amplitude M_n which depend only on transverse coordinates. Assuming, for example, that $\int \Pi d^2 k_{ti} |M_n^2(k_{ti})|^2 \propto \frac{1}{m^2} g^n$ we can derive from the eq.(25)

$$\sigma_{tot} = \frac{1}{m^2} \Sigma_n \frac{g^n}{n!} \ln^n s = \frac{1}{m^2} \cdot s^g \quad (59)$$

which looks just as Pomeron - like behaviour. This example shows the way how the Pomeron can be derived in the theory.

Let us consider a more sophisticated example, so called $g\phi^3$ - theory. This theory has a nice property, namely, the coupling constant is dimension and all integrals over transverse momenta are convergent. Such theory is one of the theoretical realization of Feynman - Gribov parton model, in which was assumed that the mean transverse momentum of the secondary particles (partons) does not depend on energy ($k_{it} = Const(s)$). The parton model is the simplest model for the scattering amplitude at small distances which reproduces the main experimental fact in deep inelastic scattering. For us it seems natural to try this model for the structure of the Pomeron.

Let us try to understand the Pomeron structure in $g\phi^3$ - theory. To do this, let us first formulate the approximation in which we are going to work: the leading logs approximation (LLA). In the LLA we sum in each order of perturbation theory, say g^n , only contributions of the order $(g \ln s)^n$, which are big at high energies. As we have discussed $\ln s^n$ come from the phase space integration at high energy. To have contribution of $(g \ln s)^n$ -type we have to consider so called ladder diagram (see Fig.20). These ladder diagrams give sufficiently simple two dimensional theory for $M_n(k_{it})$, namely the product of bubble as shown in Fig.20.

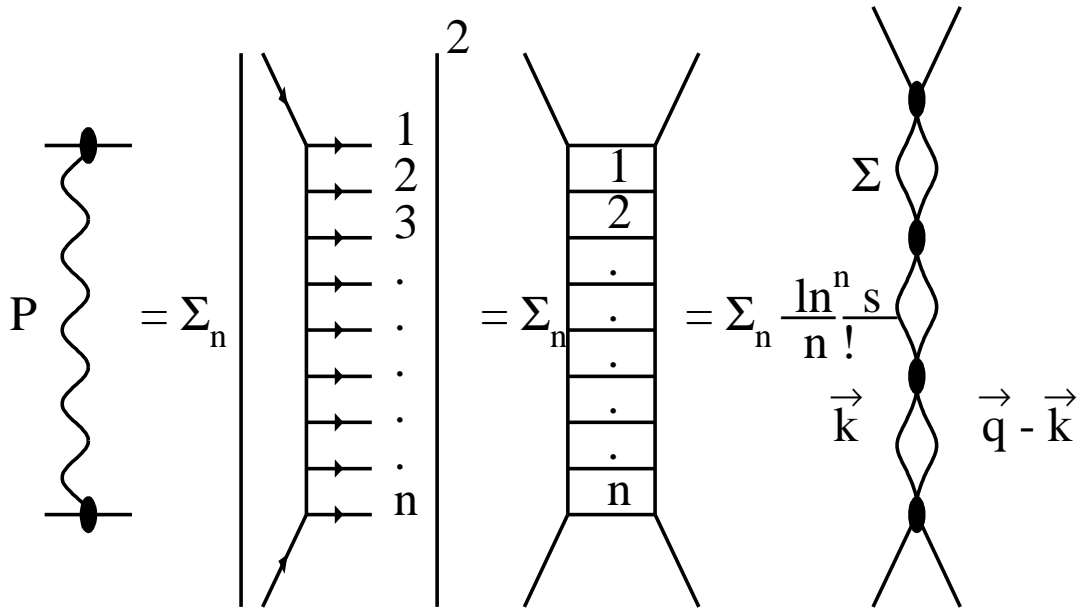


Figure 20: *The Pomeron in the LLA for $g\phi^3$ - theory*

One can see that the cross section of emission of n -partons is equal to *:

$$\sigma^n = \frac{1}{s} \frac{\ln^n(s/\mu^2)}{n!} \alpha \Sigma(q^2) (\Sigma(q^2))^n \quad (60)$$

where $\alpha = \frac{g^2}{4\pi}$ and

$$\Sigma(q^2) = \alpha \int \frac{d^2 k_t}{(2\pi)^2} \frac{1}{(k_t^2 + \mu^2)((k - q)_t^2 + \mu^2)}$$

with μ a mass of parton.

For the total cross section we have:

$$\sigma_{tot} = \sum_{n=0}^{\infty} \sigma^n = \frac{1}{s} \alpha \Sigma(q^2) \left(\frac{s}{\mu^2}\right)^{\Sigma(q^2)}. \quad (61)$$

Therefore, one can see that we reproduce the Reggeon in this theory with trajectory $\Sigma(q^2)$. Could be this Reggeon a Pomeron depends on the value of Σ . For the Pomeron $\Sigma(0) = 1 + \Delta$ as we have discussed.

7.4 Random walk in b .

The simple parton picture reproduces also the shrinkage of the diffraction peak. Indeed, due to the uncertainty principle

$$\Delta b_i k_{ti} \sim 1 \quad (62)$$

or in different form

$$\Delta b_i \sim \frac{1}{\langle k_t \rangle}$$

Therefore after each emission the position of the parton will be shifted on the value of Δb which is the same in average. After n emission we have the picture given in Fig.21a, namely the total shift in b is equal to

$$b_n^2 = \frac{1}{\langle k_t \rangle^2} \cdot n \quad (63)$$

which is typical answer for the random walk in two dimensions (see Fig.21a). The value of the average number of emission n can be estimated from the expression for the total cross section (see Eqs.(60)- (61)), because

$$\sigma_{tot} = \frac{\alpha \Sigma(0)}{s} \Sigma_n \frac{\Sigma^n(0)}{n!} \ln^n \frac{s}{\mu^2} = \sigma_0 \Sigma_n \frac{\langle n \rangle^n}{n!}$$

and the value of $\langle n \rangle \simeq \Sigma(0) \ln s$. If we substitute this value of $\langle n \rangle$ in the eq.(63) We get the radius of interaction

$$R^2 = \langle b_n^2 \rangle = \frac{\Sigma(0)}{\langle k_t \rangle^2} \cdot \ln s = \alpha' \ln s$$

*Here we introduce $\sigma^n(q^2)$ from Eq. (56).

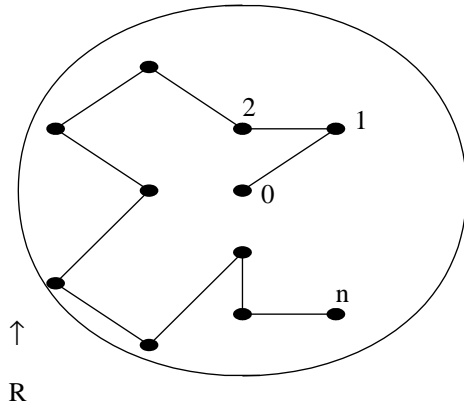


Figure 21-a: *Parton random walk in the transverse plane.*

Therefore, in $g\phi^3$ theory we obtain all typical property of the Pomeron exchange, but the value of the Pomeron intercept is still open question which is crucially correlated with the microscopic theory.

In spite of very primitive level of calculations, especially if you compare them with typical QCD calculations in DIS, this model was a guide for the Pomeron structure for years and, I must admit, it is still the model where we can see everything that we assign to the Pomeron. Therefore, we can formulate the second definition what is the Pomeron, (for completeness I repeat the first definition once more):

What is Pomeron?

A1: Pomeron is the Reggeon with $\alpha_P(0) - 1 = \Delta \ll 1$.

A2: Pomeron is a “ladder” diagram for superconvergent theory like $g\phi^3$.

The second definition turns out to be extremely useful for practical purposes, namely, for development of the Pomeron phenomenology, describing a variety of different processes at high energy. This subject we will discuss in the next section. However, let us first describe the very simple picture of the Pomeron structure that comes out from the second definition.

7.5 Feynman gas approach to multiparticle production.

7.5.1 Rapidity distribution.

Eq. (58) can be rewritten in new variables: transverse momenta and rapidities of produced particles. Let us start from definition of rapidity (y), namely, for particle with energy E and transverse momentum k_t rapidity y is equal:

$$y = \frac{1}{2} \ln \frac{E + p_L}{E - p_L} \rightarrow |_{E \gg \max(k_t, m)} \ln \frac{E}{m_t} , \quad (64)$$

where $m_t^2 = m^2 + k_t^2$.

It is easy to see, that the phase space in Eq. (58) can be written in rapidities in the following way:

$$\sigma_{tot} = \sum_n \int \prod_i d^2 k_{ti} dy_i |M_n^2(k_{ti})| , \quad (65)$$

with strong ordering in rapidities:

$$y_1 > y_2 > \dots > y_{n-1} > y_n .$$

It means that Eq. (61) can be interpreted as the sum over partial cross sections σ^n , each of them is the cross section of production of n particle uniformly distributed in rapidity (see Fig.21b).

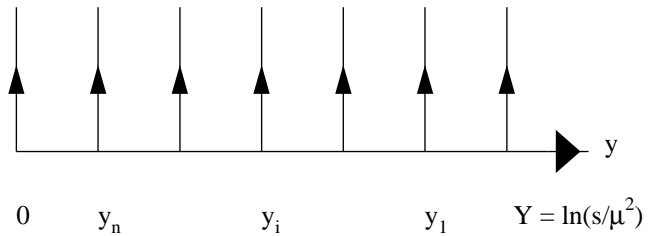


Figure 21-b: *Uniform rapidity distribution of the produced particles in the parton model*

7.5.2 Multiplicity distribution.

Eq. (61) can be rewritten in the form:

$$\sigma_{tot} = \sigma_0 \sum_n \sigma^n = \sigma_0 \sum_n \frac{<n>^n}{n!} = \sigma_0 e^{<n>} , \quad (66)$$

where $<n>$ is the average multiplicity of produced partons (hadrons).

From Eq. (66) one can calculate

$$\frac{\sigma^n}{\sigma_{tot}} = \frac{<n>^n}{n!} e^{-<n>} .$$

This is nothing more than the Poisson distribution Φ . The physical meaning of this distribution is that the produced particles can be considered as a system of free particles without any correlation between them.

7.5.3 Feynman gas.

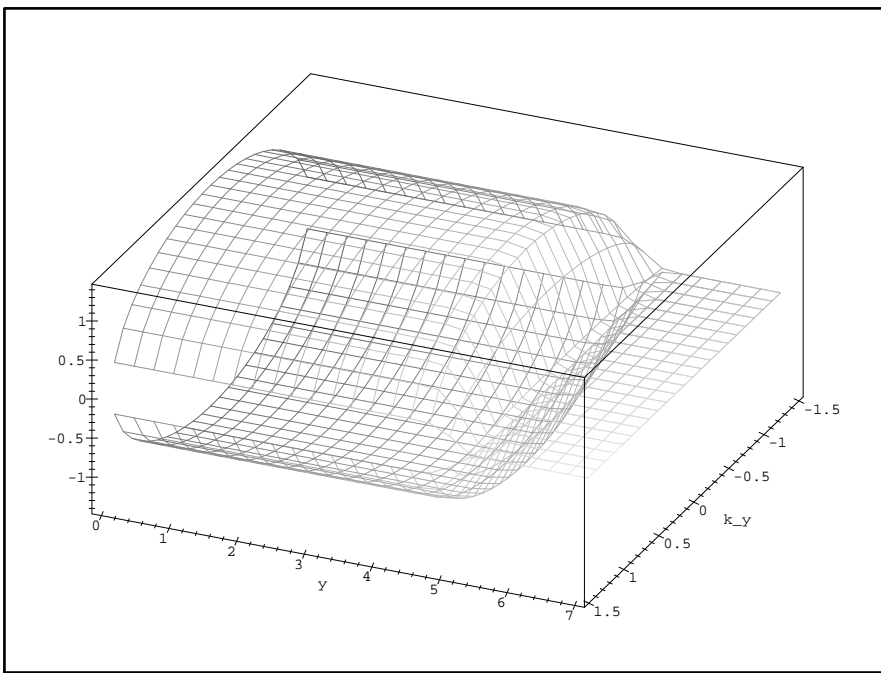
It is clear (from Fig.20, for example) that the transverse momentum distribution of one produced particle does not depend how many other particles has been produced. Now, we can collect everything that has been discussed about particle production in the parton model and draw the simple picture for the Pomeron structure:

The Pomeron exchange has the following simple structure:

1. the dominant contribution comes from the production of large number of particle, namely $n \propto \ln(s/\mu^2)$;
2. the produced particles are uniformly distributed in rapidity;
3. the correlations between produced particles are small and can be neglected in the first approximation, therefore, the final state for the Pomeron exchange can be viewed as the perfect gas (Feynman gas) of partons (hadrons) in the cylinder phase space with the coordinates: rapidity y and transverse momentum (k_t) (see Fig.21c).

This simple picture really generalizes our experience with the parton model and with the experimental data. I am very certain that this picture is our reference point in all our discussions of the Pomeron structure. I think that the real Pomeron is much more complex phenomenon but everybody should know the discussed approximation since only this simple picture leads to the Reggeon with all specific properties: factorization, shrinkage of the diffraction peak and so on.

Figure 21-c: *The cylinder phase space for the Feynman gas approximation.*



8 Space - time picture of interaction in the parton model.

8.1 Collision in space - time representation.

To understand the space - time picture of the collision process in the parton model it turns out to be very instructive to rewrite a simple formula of Eq. (58) in the mixed representation, namely, in variables: transverse momentum k_t and two space - time coordinates $x_+ = ct + z$ and $x_- = ct - z$, where z is the beam direction, for each parton “ i ”. Since amplitude $M_n(k_{ti})$ does not depend on energy and longitudinal momentum, it is easy to write Eq. (58) in such a representation. Indeed, the time - space structure of the n - th term in Eq. (58) reduces to the simple integral (see Fig.21d for all notations):

$$\begin{aligned} & \int \prod_i dt_i dz_i dt'_i dz'_i \int_{\mu}^E \frac{dE_1}{E_1} e^{i(E_1(t_1 + t'_1) - p_{L1}(z_1 + z'_1))} \dots \\ & \int_{\mu}^{E_{i-1}} \frac{dE_i}{E_i} e^{i(E_i(t_i + t'_i) - p_{Li}(z_i + z'_i))} \dots \\ & \int_{\mu}^{E_{n-1}} \frac{dE_n}{E_n} e^{i(E_n(t_n + t'_n) - p_{Ln}(z_n + z'_n))} . \end{aligned} \quad (67)$$

For high energy parton ($E_i \gg \mu$) the longitudinal momentum $p_{Li} = E_i - \frac{m^2 t_i}{2E_i}$, where $m_{ti}^2 = \mu^2 + k_{ti}^2$. Therefore,

$$E_i(t_i + t'_i) - p_{Li}(z_i + z'_i) = p_{+,i}(x_{-,i} - x'_{-,i}) - p_{-,i}(x_{+,i} - x'_{+,i}) ,$$

where $p_{+,i} = \frac{E_i + p_{Li}}{2}$ and $p_{-,i} = \frac{E_i - p_{Li}}{2}$.

For fast partons we have

$$E_i(t_i + t'_i) - p_{Li}(z_i + z'_i) \rightarrow E_i(c(t_i + t'_i) - (z_i + z'_i)) - \frac{m^2 t_i}{4E_i} (c(t_i + t'_i) + (z_i + z'_i)) .$$

Therefore, we can conclude that $c(t_i + t'_i) = (z_i + z'_i) + O(1/E_i)$ at high energy. One can also see that integrand in Eq. (67) does not depend on variables $t_i - t'_i$ and $z_i - z'_i$. Since our amplitude does not depend on energy and longitudinal momenta, it means that we have δ - function with respect of the both above variable. Integrating these two δ - functions we obtain $t_i = t'_i$ and $z_i = z'_i$. After taking the integral over $c(t_i + t'_i) - (z_i + z'_i)$, which leads to extra power of E_i in the dominator, we left with the following integrations:

$$\int dz_1 \int_{\mu}^E \frac{dE_1}{E_1^2} e^{-\frac{m_{t1}^2}{E_1} z_1} \dots \int dz_i \int_{\mu}^{E_{i-1}} \frac{dE_i}{E_i^2} e^{-\frac{m_{ti}^2}{E_i} z_i} \dots \int dz_n \int_{\mu}^{E_{n-1}} \frac{dE_n}{E_n^2} e^{-\frac{m_{tn}^2}{E_n} z_n} . \quad (68)$$

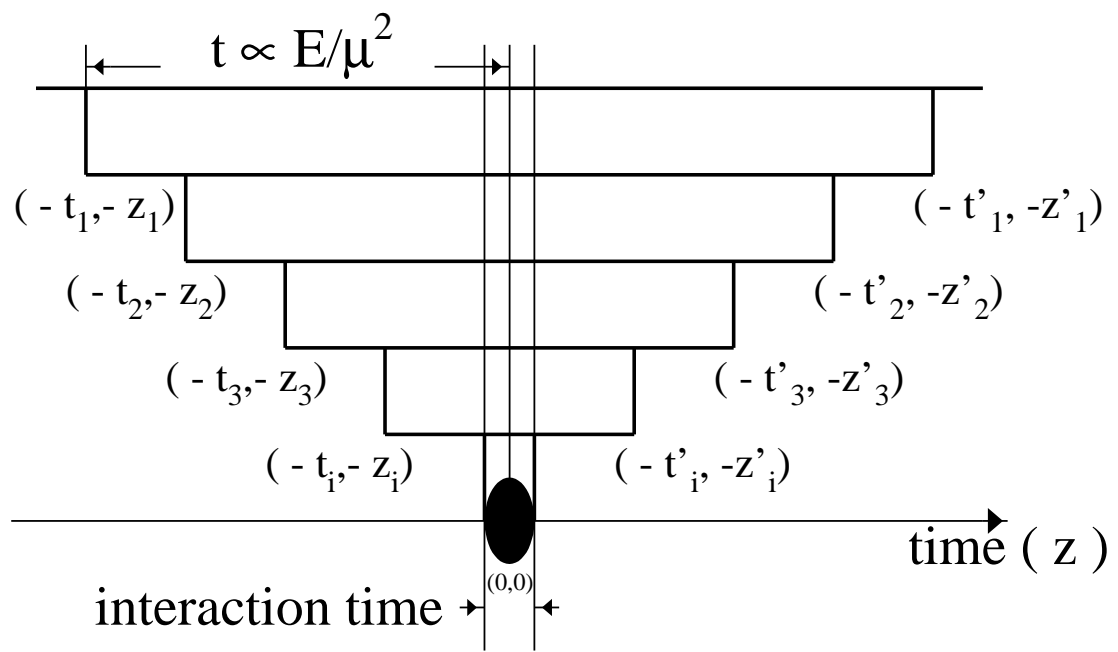


Figure 21-d: *Space - time picture for high energy interaction in the parton model.*

The main contribution in the integral over E_i comes from small E_i due to the factor E_i^2 in the denominator but for $E_i > \frac{z_i}{m_{ti}^2}$ since the integral is suppressed for smaller energies due to oscillations of the exponent.

Finally, Eq. (58) in space - time coordinates can be written in the form which is very similar to the form of Eq. (58), namely,

$$\begin{aligned}\sigma_{tot} &= \Sigma_n \int \Pi_i d^2 k_{ti} |\tilde{M}_n^2(k_{ti})| \int_{\frac{1}{\mu}}^{\frac{s}{m_{ti}^2}} \frac{dz_1}{z_1} \dots \int_{\frac{1}{\mu}}^{z_{i-1}} \frac{dz_i}{z_i} \dots \int_{\frac{1}{\mu}}^{z_{n-1}} \frac{dz_n}{z_n} \\ &= \Sigma_n \int \Pi_i d^2 k_{ti} |\tilde{M}_n^2(k_{ti})| \cdot \frac{1}{n!} \ln^n s.\end{aligned}\quad (69)$$

Fig. 21d shows how looks the high energy interaction in the lab. frame, where the target is in the rest, accordingly to Eq. (69). A long time ($t_1 \propto \frac{s}{2m^2}$, where m is the target mass while m_{ti}^2 is the transverse mass of the first parton) before a collision with the target the fast hadron decays in the system of partons which can be considered as non - interacting ones in the first approximation. The target interacts only with the partons which has energy and /or longitudinal momentum of the order of the target size, which is $\approx 1/\mu$. It takes small time (of the order of $\frac{1}{\mu}$) in comparison with the large time of the whole parton cascade which is of the order of E/μ^2 where E is the energy of incoming hadron. In the ;parton model we neglect the time of interaction (see Fig.21d) in comparison with the time of the whole parton fluctuation. Therefore, we can rewrite Eq. (69) in a general form:

$$\sigma = \sum_n |\Psi_n^{partons}(t)|^2 \sigma(\text{parton} + \text{target})(t), \quad (70)$$

where $\Psi_n^{partons}(t)$ is the partonic wave function (wave function of n - partons) in the moment of interaction t ($t = 0$ in Fig.21d). From Eq. (70) one can see that the target affects only small number of partons with sufficiently low energies while the most properties of the high energy interaction are absorbed in the partonic wave function which is the same for any target. One can recognize our factorization properties of the Pomeron in this picture.

8.2 Probabilistic interpretation.

One can see from Eq. (70) that the physical observable (cross section) can be written as sum of $|\Psi_n|^2$. $|\Psi_n|^2$ has obvious physical meaning, namely, it is probability to find n partons in the parton cascade (in the fast hadron). Therefore, discussing the Pomeron structure in the parton model we can forget about interference diagrams and all other specific features of quantum mechanics. In some sense we can develop a Monte Carlo simulation for the Pomeron content. It happens only because the Pomeron turns out to be mostly inelastic object and we can neglect the contribution of the elastic amplitude to the unitarity constraint.

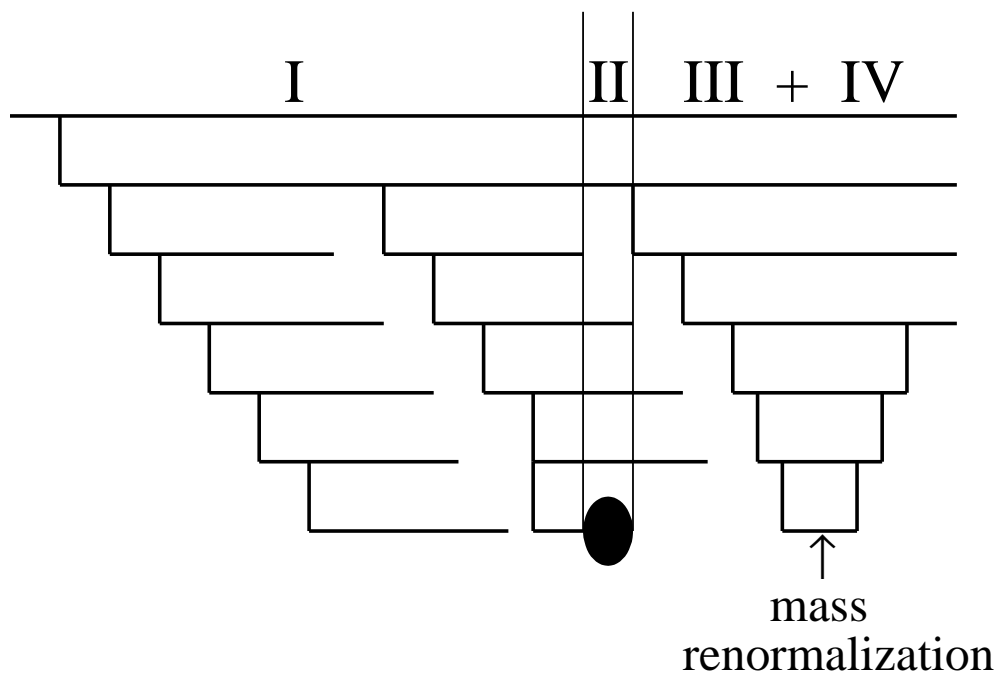


Figure 21-e: *Four stages of high energy interaction in the parton model.*

The second important observation is that for each term in sum of Eq. (70), the transverse and longitudinal degrees of freedom are completely separated and could be treated in a quite different way: simple uniform distribution in rapidity and rather complicated field theory for the transverse degrees of freedom.

8.3 “Wee” partons and hadronization.

Taking this simple probabilistic (parton) interpretation we are able to explain all features of the high energy interaction without explicit calculations. As we have mentioned only very slow parton can interact with the target in the lab. frame. Such active partons we call “wee” partons.

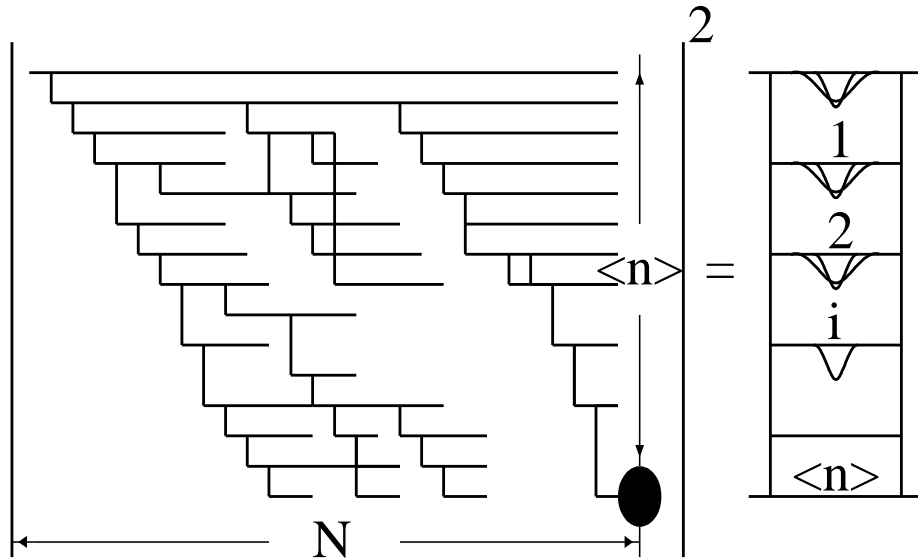


Figure 21-f: “Wee” partons and hadrons.

Therefore, in the parton model the high energy interaction has four clear separated stages (see Fig.21e):

I stage: Time ($t \propto \frac{E}{\mu^2}$) before interaction of the “wee” parton with the target. The fast hadron can be considered as a state of many point-like particle (partons) but all of them are in a very coherent state which we describe by the means of the wave function.

II stage: Short time of interaction of the “wee” parton with the target. The cross section of such interaction depends on the target, but the most important thing that this interaction is doing is that it destroys the coherence of the partonic wave function.

III stage: Free partons in the final state which can be described as Feynman gas in the first approximation.

IV stage: Hadronization or in other words the creation of observed hadrons out of free partons. There is wide spread but wrong opinion that in the simple parton model we have no hadronization stage. We will show in a short while that it is just wrong.

The total cross section of the interaction is equal to

$$\sigma_{tot}(s) = N(\text{“wee” partons}) \sigma(\text{“wee” parton} + \text{target}) . \quad (71)$$

Actually, we can write Eq. (71) in more details including the integration over rapidity of the “wee” parton, namely:

$$\sigma_{tot}(s) = \int dy_{wee} N(y_{wee}) \sigma(y_{wee}) , \quad (72)$$

and we assume that the cross section for “wee” parton - target interaction falls down as a function of y_{wee} much faster than y_{wee} - dependence in N .

We can estimate how N depends on energy. Indeed, even a slight glance on Fig.21f shows that the number of “wee” partons should be very large because each parton can decay in its own chain of partons. Let us assume that we know the multiplicity of partons in one chain (let us denote it by $\langle n \rangle$). One can evaluate that $N \propto e^{\langle n \rangle}$. Therefore,

$$\sigma_{tot} \propto \sigma_0 e^{\langle n \rangle} ,$$

where σ_0 stands for “wee” parton - target interaction cross section.

We have calculated $\langle n \rangle \approx \Sigma(o) \ln s$ in the subsection where we discussed the random walk in the transverse plane. Graphically, we show this calculation in Fig.21f.

The natural question arises why the multiplicity in one chain coincide with the multiplicity of produced particles as it follows from our calculation of $\langle n \rangle$ (see also Fig. 21f). The difference really is in the hadronization stage. Indeed, a “wee” parton interacts with the target. We have N “wee” partons but interacts only one of them. Of course, it could be any, this is why our cross section is proportional to the total number of the “wee” partons. However, if one of the “wee” parton hits the target all other pass the target without interaction. They gather together and contribute to the renormalization of the mass in our field theory (see Figs. 21e and 21f). Therefore, in the simple partonic picture the number of produced “hadrons” is the same as the number of partons in one parton chain. Of course, this is an oversimplified picture of hadronization, but it should be stressed that even in the simplest field theory such as $g\phi^3$ - theory we have a hadronization stage which reduces the number of partons in the parton cascade from $N \propto e^{\langle n \rangle}$ to $\langle n \rangle$.

8.4 Diffraction Dissociation.

As we have discussed the typical final state in the parton model is the inelastic event with large multiplicity and with uniform distributions Φ of produced hadrons in rapidity. All event with small multiplicity, such as diffraction dissociation one, can be considered as a correction to the parton model and they should be small. Indeed, diffraction dissociation event corresponds to such interaction of the “wee” parton with the target which does not destroy the coherence of the partonic wave function for the most of partons in it. This process is shown in Fig.21g. In Fig.21g one can see that the interaction of “wee” parton with the target does not change the wave function for all parton with rapidities $y_i < y_M$ and destroys coherence completely for partons with $y_i > y_M$. The practical way how we will be able to describe such processes we will discuss in the next section.

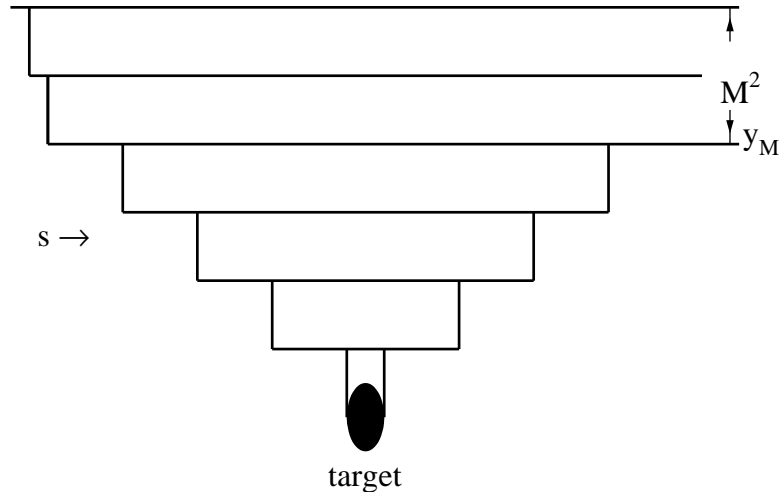


Figure 21-g: *Diffractive dissociation in the parton model.*

9 Different processes in the Reggeon Approach.

9.1 Mueller technique.

Using the second definition (better to say, having the second definition as a guide) we can easily understand a very powerful technique suggested by Al Mueller in 1970. First

observation is that the optical theorem in the LLA looks very simple as shown in Fig.22. Mueller technique can be understood in a very simple way: *for every process try to draw ladder diagrams and use the optical theorem in the form of Fig.22.*

Let us illustrate this technique considering the single inclusive cross section of hadron c with rapidity y_c integrated over its transverse momentum (see Fig.22). Summing over hadrons n_1 and n_2 with rapidities more or less than y_c and using the optical theorem we can rewrite this cross section as product of two cross sections with rapidities (energies) $Y - y_c$ and y_c . Using the Pomeron exchange for the total cross section and introducing a general vertex a we obtain a Mueller diagram for the single inclusive cross section. In spite of the fact that this technique looks very simple it is a powerful tool to establish a unique description of different exclusive and inclusive processes in the Reggeon Approach. Here we want to write down several examples of different processes that can be treated on the same footing in the Reggeon approach.

9.2 Total cross section.

As has been mentioned in one Pomeron exchange approximation the total cross section is given by the following expression (see Fig.23a):

$$\sigma_{tot} = 4\pi g_1(0) g_2(0) \left(\frac{s}{s_0}\right)^\Delta = \sigma(s = s_o) \left(\frac{s}{s_0}\right)^\Delta \quad (73)$$

We would like to remind you that multi Pomeron exchange is very essential in the total cross section but we postpone the discussion of their contribution to the second part of our lectures.

The energy behaviour of the total cross section in the region of not very high energy depends on the contribution of the secondary Reggeons. Very often, nowadays, we introduce the only one secondary Reggeon. It is not correct and we have to be very careful. For example, for $p + p$ total cross section we have the secondary Reggeon with positive signature (P' or f Reggeon) and two Reggeons with negative signature (ω and ρ). The first one is responsible for the energy dependence of the total cross section and it gives the same contribution to $p + p$ and $\bar{p} + p$ collisions. ω - Reggeon gives different sign for these two reactions and it is responsible for the value and energy dependence of the difference $\sigma_{tot}(\bar{p}p) - \sigma_{tot}(pp) \propto \left(\frac{s}{s_0}\right)^{\alpha_\omega(0)-1} \approx \left(\frac{s}{s_0}\right)^{-0.5}$.

Finally, the total cross section can be written in the general form

$$\sigma_{tot} = 4\pi g_1^P(0) g_2^P(0) \left(\frac{s}{s_0}\right)^\Delta + \sum_{R_i} (-1)^S 4\pi g_1^{R_i}(0) g_2^{R_i}(0) \left(\frac{s}{s_0}\right)^{\alpha_{R_i}(0)-1}, \quad (74)$$

where $S = 0$ for positive signature and $S = 1$ for negative signature for particle - particle scattering (for antiparticle - particle scattering all contributions are positive).

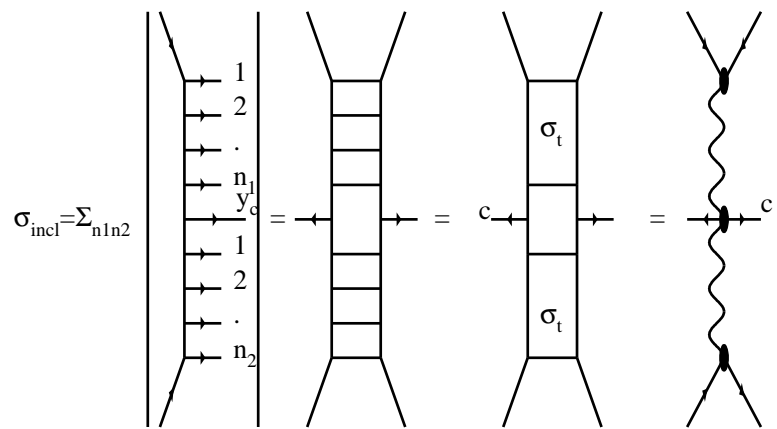
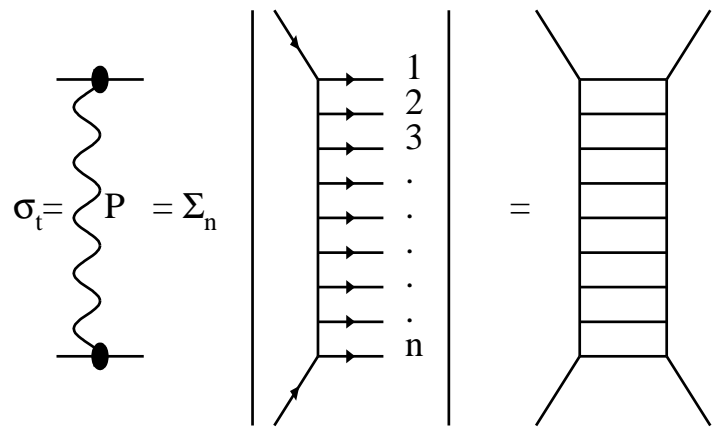


Figure 22: *Optical theorem and inclusive production in the LLA for $g\phi^3$ -theory (parton model).*

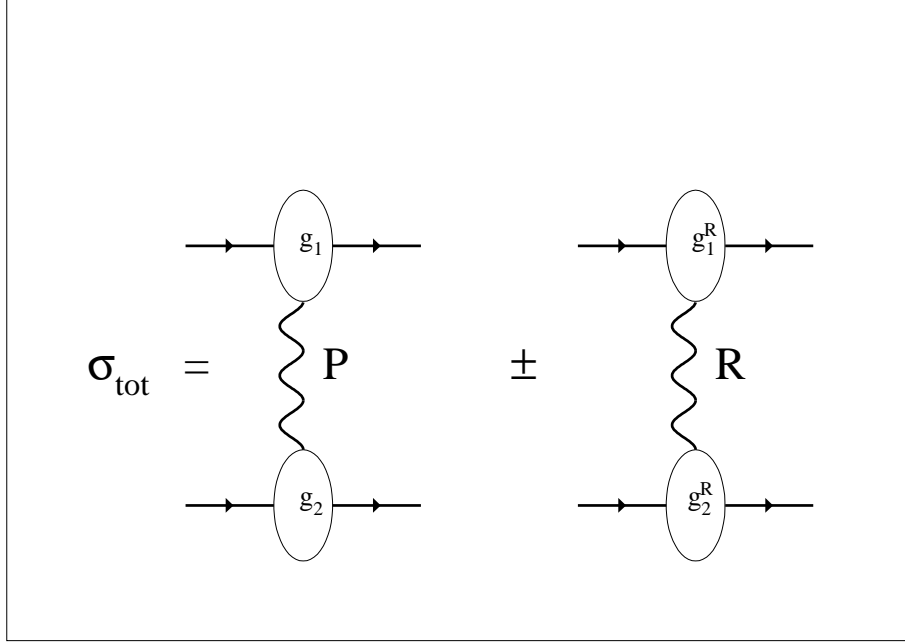


Figure 23-a: *Total cross section in the Mueller technique.*

9.3 Elastic cross section.

Collecting everything that we have learned on Reggeon (Pomeron) exchange we can show that for one Pomeron exchange the total elastic cross section is equal to (see Fig.23b)

$$\sigma_{el} = \frac{\sigma_{tot}^2}{16\pi B_{el}}$$

where

$$B_{el} = 2R_{01}^2 + 2R_{02}^2 + 2\alpha'_P \ln s/s_0$$

in the exponential parameterization for the vertices.

Interesting to notice that this formula is written in the approximation when we neglected the real part of the amplitude. The correct formula is

$$\sigma_{el} = \frac{\sigma_{tot}^2}{16\pi B_{el}} (1 + \rho^2) ,$$

where $\rho = \frac{ReA(s,t)}{ImA(s,t)}$. For the Pomeron Δ is small (see first definition) and

$$\rho = \frac{\pi}{2} \frac{1}{ImA(s,t)} \frac{dImA(s,t)}{d\ln s} = \frac{\pi}{2} \Delta .$$

For the secondary trajectories we have to take into account the signature factors (η_+ or η_-) and calculate the real part of the amplitude.

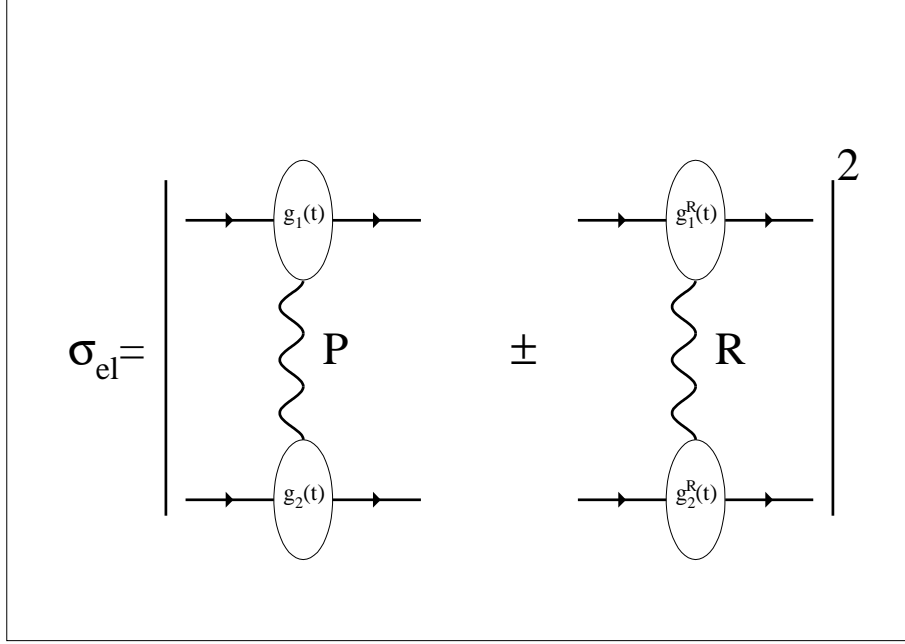


Figure 23-b: *Elastic cross section in the Mueller technique.*

9.4 Single diffraction dissociation

The cross section of the single diffraction (see Fig.23c) has the following form M^2 is large):

$$\frac{M^2 d\sigma_{SD}}{dM^2 dt} = \frac{g_p^2(t)}{4} \left(\frac{S}{M^2}\right)^{2\Delta} \sigma_{tot} (2 + P) , \quad (75)$$

where σ_{tot} is the total cross section of the Pomeron and hadron 2.

At first sight, it is strange that the Pomeron exchange depends on the ratio $\frac{s}{M^2}$. In the LLA for $g\phi^2$ - theory (parton model) this processes is shown in Fig.23 and the Pomeron exchange certainly depends energy $s' = x_i p_2 m_1$ in the rest frame of hadron 1(in lab. frame). In the LLA

$$x_1 \gg x_2 \gg \dots \gg x_i$$

and

$$M^2 = \left(\sum_{l=1}^i p_{0l}\right)^2 - \left(\sum_{l=1}^i p_{Ll}\right)^2 \approx \frac{p_t^2}{x_i} .$$

It means that in the framework of the parton model where $\langle p_t^2 \rangle$ does not depends on energy,

$$x_i \approx \frac{\langle p_t^2 \rangle}{M^2}$$

and

$$s' = 2x_i p_2 m_1 = \langle p_t^2 \rangle \cdot \frac{s}{M^2} .$$

We absorb some of factors in the definition of the cross section in Eq. (75).

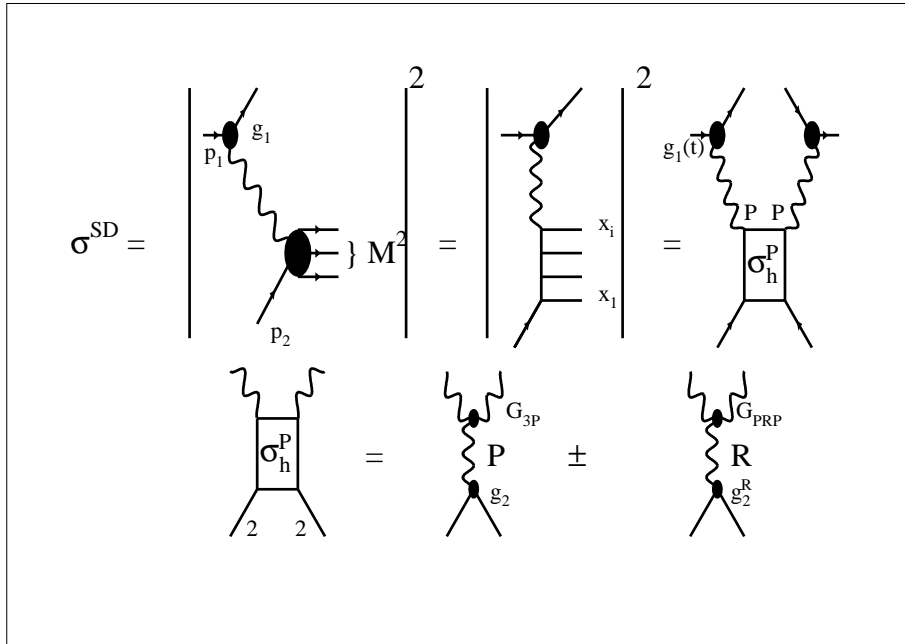


Figure 23-c: *Single Diffraction in the Mueller technique.*

The next question is how well we define the normalization of the Pomeron - hadron cross section. The natural condition for such a normalization is that the cross section, defined in Eq. (75), should coincide with the cross section of the interaction of hadron 2 with the resonance (R) at $t = m_R^2$. Of course, when m_R is small all formulae give the same answer. However, let us consider ρ - trajectory and compare the exchange of the ρ - Reggeon at $t = 0$ in two different model: Veneziano model and simple formula of Eq. (42). Taking $\alpha_\rho(t = 0) = 0.5$ we see that cross section in the Veneziano model in π times bigger than in Eq. (42). Therefore, in the reality even for Reggeons we have a problem with normalization. In the case of the Pomeron situation even worse since we even do not know there is at least one resonance on the Pomeron - trajectory. My personal opinion we have to make a common agreement what we will cross section but we should be very careful in comparison the value of the cross section with normal hadron - hadron cross sections.

In the region of big mass M^2 we can apply to the Pomeron - hadron cross section the same expansion with respect to the Pomeron + Reggeons exchange (see Eq. (74))

$$\frac{M^2 d\sigma_{SD}}{dM^2} = \frac{\sigma_0}{2\pi R^2(\frac{s}{M^2})} \cdot \left(\frac{s}{M^2}\right)^{2\Delta} \cdot \left[G_{3P}(0) \cdot \left(\frac{M^2}{s_0}\right)^\Delta + G_{PPR}(0) \left(\frac{M^2}{s_0}\right)^{\alpha_R(0)-1} \right] \quad (76)$$

Let me summarize what we learned experimentally about triple Pomeron vertex:

1. the value of it is smaller than the value of g_i (the hadron - Pomeron vertex), approximately, $G_{3P} \approx 0.1 g_i$;
2. the dependence on t of the triple Pomeron vertex can be characterized by the radius of the triple Pomeron vertex r_0 , which turns out to be rather small, namely, $r_0^2 \leq 1 \text{ GeV}^{-2}$.

It is easy to show that in exponential parameterization for vertices (see Eq. (48))

$$R^2\left(\frac{s}{M^2}\right) = 2R_{01}^2 + 2r_0^2 + 2\alpha'_P \ln(s/M^2) .$$

9.5 Non-diagonal contributions.

Eq.(76) gives the correct descriptions of the energy and mass behaviour of the SD cross section in the Reggeon phenomenology but only at $\frac{s}{M^2} \ll 1$. If it is not the case and $\frac{s}{M^2} \approx 1$ we have to modify Eq.(76) including secondary Reggeons. It means that we have to substitute in Eq.(76)

$$\left(\frac{s}{M^2}\right)^\Delta \rightarrow \left(\frac{s}{M^2}\right)^\Delta + \sum_i \left(\left(\frac{s}{M^2}\right)^{\alpha_{R_i}(0)-1}\right)$$

where i denotes the Reggeon with trajectory $\alpha_{R_i}(t)$. As one can see the s - dependence of Eq. (76) is only governed by the Pomeron ($M^2 d\sigma_{SD}/dM^2 \propto s^{2\Delta}$) while Eq. (76-b) leads to more general energy dependence, namely,

$$\frac{M^2 d\sigma_{SD}}{dM^2} \propto \left\{ \left(\frac{s}{M^2}\right)^\Delta \pm A_R \left(\frac{s}{M^2}\right)^{\alpha_R(0)-1} \right\}^2 . \quad (76\text{-a})$$

Therefore the general equation has a form:

$$\frac{M^2 d\sigma_{SD}}{dM^2 dt} = \sum_{i,j,k} g_i g_j g_k G_{ijk} \left(\frac{s}{M^2}\right)^{\Delta_i} \left(\frac{M^2}{s_0}\right)^{\Delta_j} \left(\frac{s}{M^2}\right)^{\Delta_k} , \quad (76\text{-b})$$

where i,j and k denote all Reggeons including the Pomeron and $\Delta_l = \alpha_l(0) - 1$ with $l = i,j$ and k .

We can see from Eq. (76-b) as well as from Eq. (76-a) that the first correction to the Pomeron induced energy behaviour comes from so called interference or non-diagonal (N-D) term, which can be written in a general form:

$$\frac{M^2 d\sigma_{SD}^{N-D}}{dM^2 dt} = \sigma_{P+p \rightarrow R+p}(M^2) g_P g_R \left(\frac{s}{M^2}\right)^{\Delta_P} \left(\frac{s}{M^2}\right)^{\Delta_R} , \quad (76\text{-c})$$

where P stands for the Pomeron and R for any secondary Reggeon. $\sigma_{P+p \rightarrow R+p}(M^2)$ can be written as a sum of the Reggeon contributions as

$$\sigma_{P+p \rightarrow R+p}(M^2) = g_P G_{PPR} \left(\frac{M^2}{s_0}\right)^{\Delta_P} \pm g_R G_{PPR} \left(\frac{M^2}{s_0}\right)^{\Delta_R} . \quad (76\text{-d})$$

It is clear that the non-diagonal term gives the first and the most important correction which have to be taken into account in any phenomenological approach to provide a correct determination of the diffractive dissociation contribution. By definition, we call diffractive

dissociation only the contribution which survives at high energy or, in other words, it corresponds to the Pomeron exchange term in the Reggeon phenomenology. Unfortunately, we know almost nothing about this non-diagonal term. We cannot guarantee even the sign of the contribution. This lack of our knowledge I tried to express putting \pm in the above equations. Let me discuss here this “almost nothing”.

First, we can derive an inequality for $\sigma_{P+p \rightarrow R+p}(M^2)$ using the generalized optical theorem that we discussed in section 9.1. By definition

$$\sigma_{P+p \rightarrow R+p}(M^2) = \frac{1}{2} \sum_{n,q} \{ g_P(M^2, n, q) \cdot g_R^*(M^2, n, q) + g_P(M^2, n, q) \cdot g_R^*(M^2, n, q) \},$$

where n is the number of produced particles with mass M and q is all other quantum numbers of the final state. Notice that factor $1/2$ in front is due to the definition in Eq. (76-b) where we sum separately over PR and RP contributions.

Due to obvious inequality

$$\sum_{n,q} |g_P(M^2, n, q) - z g_R(M^2, n, q)|^2 \geq 0$$

at any value of z one can see that

$$\sigma_{P+p \rightarrow R+p}^2(M^2) \leq \sigma_{P+p \rightarrow P+p}(M^2) \cdot \sigma_{R+p \rightarrow R+p}(M^2) \quad (76-e)$$

Using Eq. (76-d) and analogous decomposition for $p + p$ and $R + p$ cross sections, we can easily derive from Eq. (76-e) that

$$G_{PPR}^2 \leq G_{PPP} \cdot G_{RPR}; \quad G_{PRR}^2 \leq G_{PRP} \cdot G_{RRR}. \quad (76-f)$$

Actually, Eq. (76-f) is the only reliable knowledge on the interference (non-diagonal) term. However, in the simple parton model or/and in the LLA of $g\phi^3$ -theory we know that the sign of the non-diagonal vertices is positive and inequality of Eq. (76-f) is saturated or, in other words, we have

$$G_{PPR}^2 = G_{PPP} \cdot G_{RPR}; \quad G_{PRR}^2 = G_{PRP} \cdot G_{RRR}. \quad (76-g)$$

The same result we can obtain in other models where we assume that the Pomeron scale is larger than the typical hadron size, for example, in the additive quark model. However, in general we have no proof for Eq. (76-g) and, therefore, we can recommend only to introduce a new parameter δ and use the following form for the phenomenology:

$$G_{PPR} = \sin\delta_P \cdot \sqrt{G_{PPP} \cdot G_{RPR}}; \quad G_{PRR} = \sin\delta_R \cdot \sqrt{G_{PRP} \cdot G_{RRR}}. \quad (76-h)$$

I think, this section is a good illustration how badly we need a theory for the high energy scattering.

9.6 Double diffraction dissociation.

From Fig.23d one can see that the cross section of the double diffraction dissociation (DD) process is equal to:

$$\frac{M_1^2 M_2^2 d^2 \sigma_{DD}}{dM_1^2 dM_2^2} = \frac{\sigma_0}{2\pi R^2(\frac{ss_0}{M_1^2 M_2^2})} \cdot G_{3P}^2(0) \cdot \left(\frac{ss_0}{M_1^2 M_2^2}\right)^{2\Delta} \cdot \left(\frac{M_1^2}{s_0}\right)^\Delta \cdot \left(\frac{M_2^2}{s_0}\right)^\Delta \quad (77)$$

in the region of large values of produced masses (M_1 and M_2).

Actually, to explain Eq. (77) we need only to comment why our formula depends on energy as a function of the argument

$$s'' \propto \frac{ss_0}{M_1^2 M_2^2}.$$

Repeating the simple calculation of the previous subsection we can see that (see Fig.23d):

$$\begin{aligned} x_i^1 &= \frac{\langle p_t^2 \rangle}{M_1^2} ; \\ x_{i'}^2 &= \frac{\langle p_t^2 \rangle}{M_2^2} ; \end{aligned} \quad (78)$$

and

$$s'' = 2 x_i^1 x_{i'}^2 p_{1\mu} p_{2\mu} = (\langle p_t^2 \rangle)^2 \frac{s}{M_1^2 M_2^2} \approx s_0 \frac{s s_0}{M_1^2 M_2^2}.$$

The second remark is that $R^2(\frac{ss_0}{M_1^2 M_2^2})$ in Eq. (77) is equal to

$$R^2\left(\frac{s s_0}{M_1^2 M_2^2}\right) = 2 r_0^2 + 2\alpha'_P \ln(ss_0/M_1^2 M_2^2)$$

in exponential parameterization of the vertices (see Eq. (48)).

9.7 Factorization for diffractive processes.

Comparing the cross section for double and single diffraction as well as for elastic cross section one can get the following factorization relation:

$$\frac{M_1^2 M_2^2 d^2 \sigma_{DD}}{dM_1^2 dM_2^2} = \frac{\frac{M_1^2 d\sigma_{SD}}{dM_1^2} \frac{M_2^2 d\sigma_{SD}}{dM_2^2}}{\sigma_{el}} \cdot \frac{R^2\left(\frac{s}{M_1^2}\right) R^2\left(\frac{s}{M_2^2}\right)}{R^2\left(\frac{ss_0}{M_1^2 M_2^2}\right) R_{el}^2(s)} \quad (79)$$

where

$$R_{el}^2 = 2R_{01}^2 + 2R_{02}^2 + 2\alpha'_P \ln(s/s_0)$$

The structure of the event which corresponds to double diffraction is pictured in Fig.24 in logo - plot. In the region of rapidity Δy we have no produced particles.

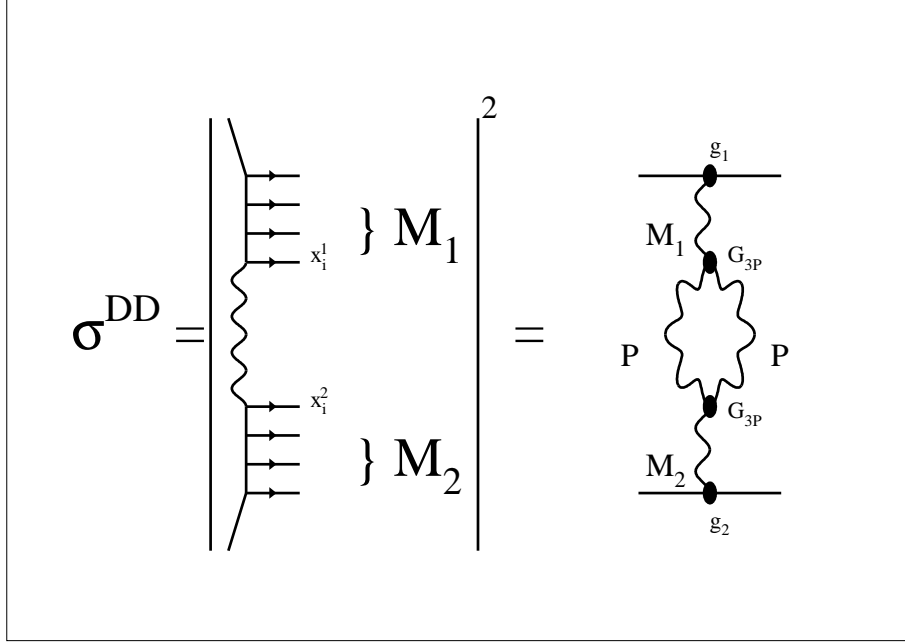


Figure 23-d: *Double Diffraction in the Mueller technique.*

9.8 Central Diffraction.

In this process we produced the bunch of secondary particle in the central rapidity region, while there are no secondary particles in other regions in rapidity.

The cross section for the production of the bunch of particles of the mass M in proton - proton collision can be written in the form:

$$M^2 \frac{d\sigma}{dM^2} = \sigma_{PP} \sigma_{pp}^2 \frac{1}{R_{0p}^2 + \alpha'_P(0) \ln(s/M^2)} \frac{1}{2\alpha'_P(0)} \ln\left(\frac{R_{0p}^2 + \alpha'_P(0) \ln(s/M^2)}{R_{0p}^2}\right). \quad (80)$$

The last factor in Eq. (80) arises from the integration over rapidity y_1 of the factor $1/(R_{0p}^2 + \alpha'_P(Y - y_1))(R_{0p}^2 + \alpha'_P(Y - y_1))$ which comes from the integrations over t_1 and t_2 (see Fig.23e).

9.9 Inclusive cross section.

As we have discussed the inclusive cross section accordingly to the Mueller theorem can be described by the diagram of Fig.22. For reaction

$$a + b \rightarrow c(y) + \text{anything}$$

the inclusive cross section can be written in a very simple form:

$$\frac{d\sigma}{dy_c} = a \cdot \sigma_{tot} \quad (81)$$

where a is the new vertex for the emission of the particle c .

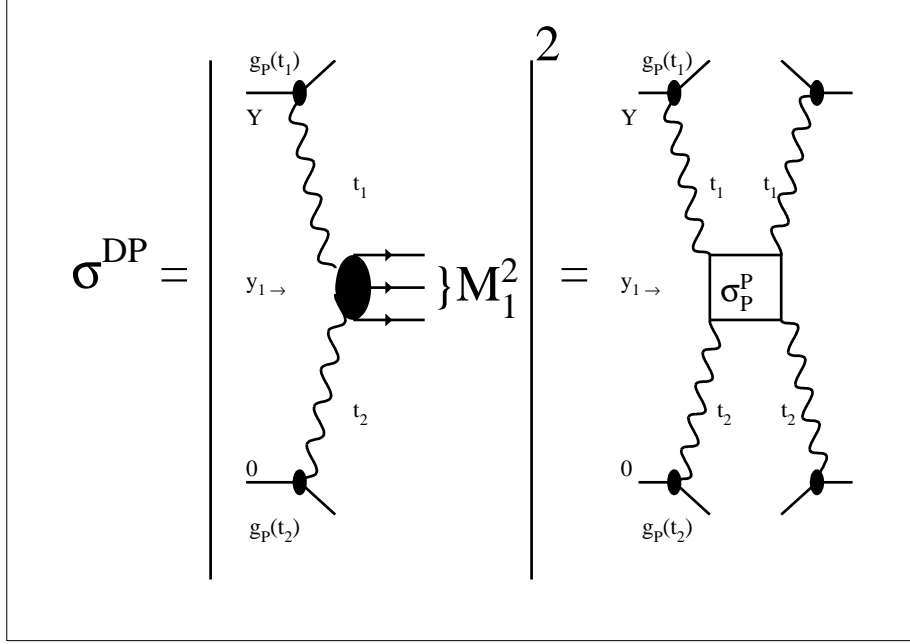


Figure 23-e: *Central Diffraction in the Mueller technique.*

9.10 Two particle rapidity correlation.

The Reggeon approach we can use for the estimates of the two particle rapidity correlation function, which is defined as:

$$R = \frac{\frac{d^2\sigma(y_1, y_2)}{\sigma_{tot} dy_1 dy_2}}{\frac{d\sigma(y_1)}{\sigma_{tot} dy_1} \frac{d\sigma(y_2)}{\sigma_{tot} dy_2}} - 1 \quad (82)$$

where $\frac{d^2\sigma}{dy_1 dy_2}$ is the double inclusive cross section of the reaction:

$$a + b \rightarrow 1(y_1) + 2(y_2) + \text{anything}$$

The double inclusive cross section can be described in the Reggeon exchange approach by two diagrams (see Fig.23g). It is easy to notice that the first diagram cancels in the definition of the correlation function but the second one survives and gives the correlation function in the form:

$$R(\Delta y = |y_1 - y_2|) = \frac{a_{PR}^2}{a_{PP}^2} \cdot e^{(1-\alpha_R(0)) \Delta y} \quad (83)$$

All notations are clear from Fig.23g.

It should be stressed that the Reggeon approach gives the estimates for the correlation length (L_{cor}). Namely, we can rewrite the above formula in the form:

$$R = SR \cdot e^{-\frac{\Delta y}{L_{cor}}} ,$$

and from our Reggeon formula we have $L_{cor} \simeq 2$. We would like to draw your attention to the fact that this formula describes the correction to the Feynman gas model, but one can see that corrections die at large difference in rapidity.

We would like to stress that the correlation function depends strongly on the value of shadowing corrections (many Reggeon exchange) but this problem we will discuss later.

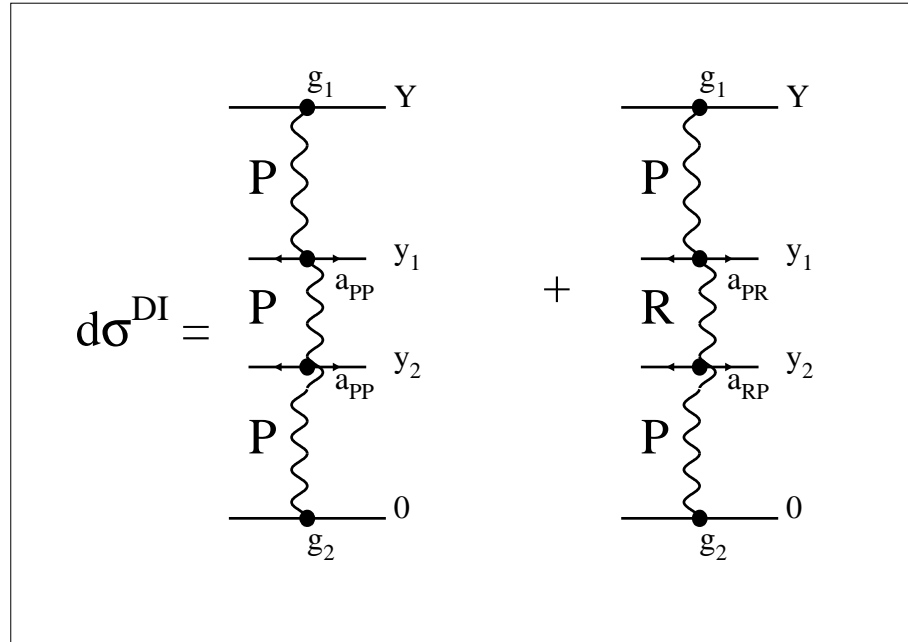


Figure 23-f: Double inclusive production in the Mueller technique.

10 Why the Donnachie - Landshoff Pomeron is not the right one.

We have discussed in details that the DL Pomeron gives the amplitude $a(s, b)$ which reaches unity just around the corner, namely, at energies slightly higher than the Tevatron energies (see Fig.25). Let us discuss in more details what kind of information on the hadron - hadron collisions we can obtain from the value of $a(s, b = 0)$. At the Tevatron energies $Im a(s, b = 0) = 1 - \exp(-\frac{\Omega}{2}) \approx 0.95$. Therefore, $\Omega \approx 6$, which is rather large value. Indeed, we can calculate the value of $G_{in}(s, b = 0) = 1 - \exp(-\Omega)$ which is equal to 0.9975 and it is close to the unitarity limit ($G_{in} < 1$). Using the unitarity constraint we see that

$$Im a(W = 1800 \text{ GeV}, b = 0) = 45\% \text{ (elastic)} + 50\% \text{ (inelastic)}$$

This fact certainly contradicts the parton model structure of the Pomeron, in which the Pomeron is originated predominantly from inelastic multiparticle production processes. Nevertheless, we have to admit that the above observation cannot rule out the first definition of the Pomeron as the Reggeon with the intercept close to 1.

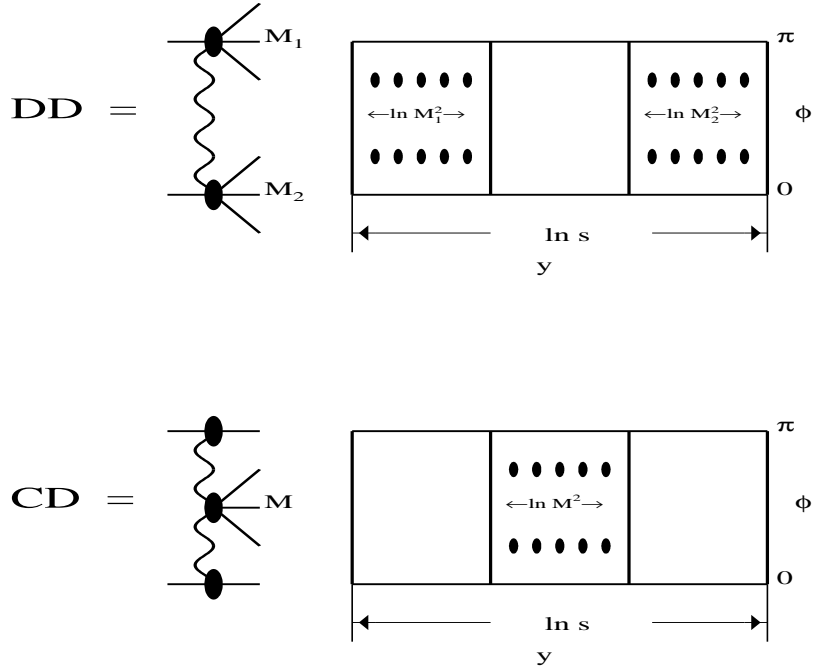


Figure 24: *Lego - plot for Double and Single Diffraction.*

However, there are experimental data which disagree with the DL Pomeron, namely, the data on single diffraction in the proton - proton (antiproton) collisions. In the Pomeron exchange approach, the cross section of the single diffraction dissociation as well as elastic scattering cross section behaves as

$$\sigma^{SD} \propto \sigma^{el} \propto \left(\frac{s}{s_0}\right)^{2\Delta},$$

where $\Delta = \alpha_P(0) - 1$. Recalling that $\sigma_{tot} \propto \left(\frac{s}{s_0}\right)^\Delta$, we see that we expect

$$\frac{\sigma^{el}}{\sigma_{tot}} \propto \frac{\sigma^{SD}}{\sigma_{tot}}; \quad (84)$$

$$\frac{\sigma^{SD}(t=0)}{\sigma^{el}(t=0)} = Const(s).$$

One can see from Fig.26 that the experimental data does not show anything like these predictions.

Therefore, we can conclude without any hesitation that despite the DL Pomeron describes a lot of experimental data it cannot be considered as a serious candidate for the Pomeron exchange. The problem how to heal the DL Pomeron is related to the problem of shadowing corrections which I am not able to touch in these lectures because of lack of time.

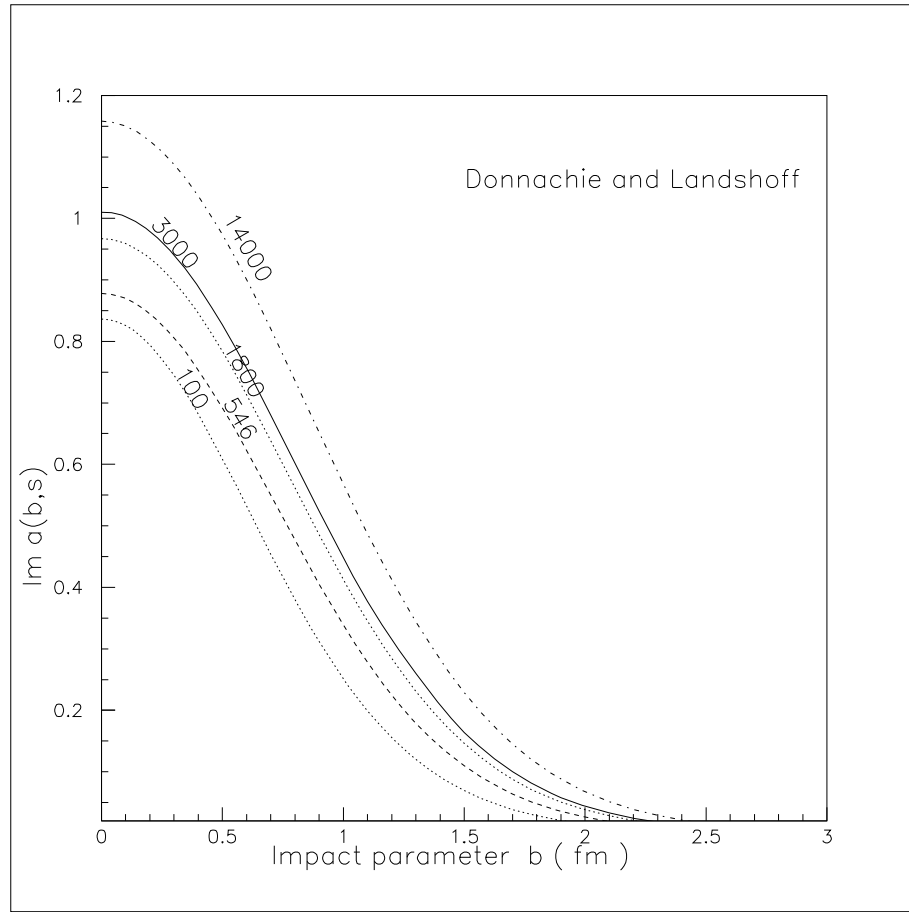


Figure 25-a: *Impact parameter profile for the Donnachie - Landshoff Pomeron at different values of $W = \sqrt{s}$. I am very grateful to E.Gotsman, who did and gave me this picture.*

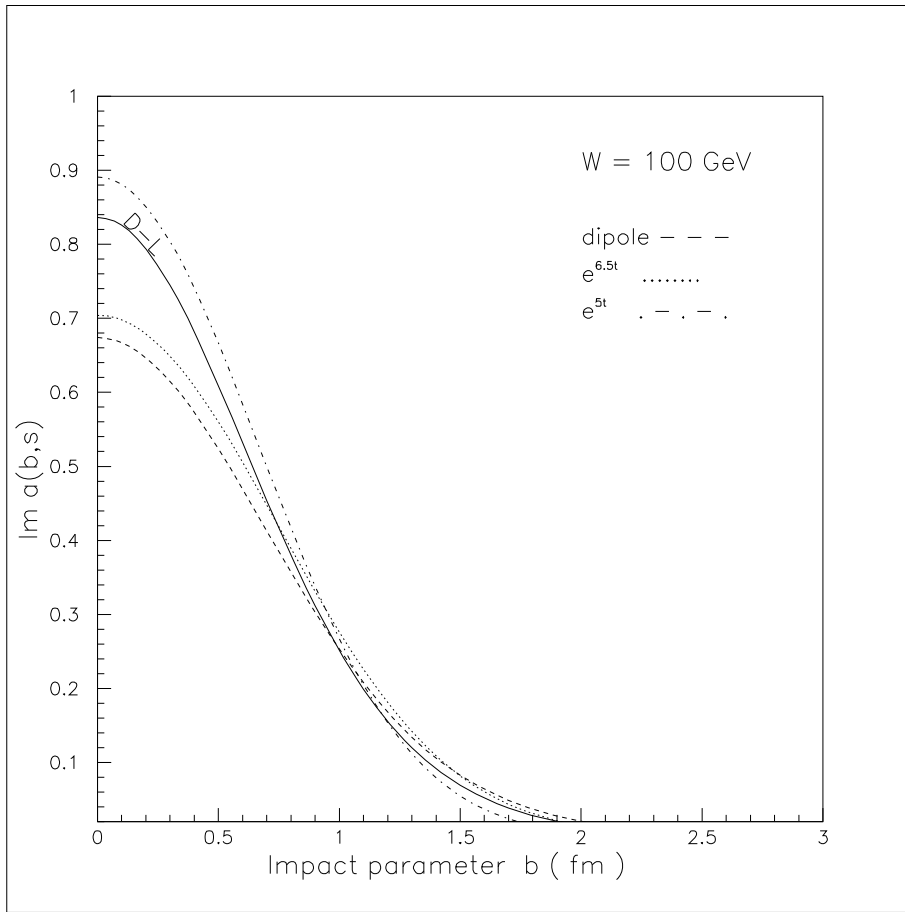


Figure 25-b: Impact parameter profile for the Donnachie - Landshoff Pomeron and other models for the Pomeron at $W = \sqrt{s} = 100 \text{ GeV}$. I am very grateful to E. Gotsman, who did and gave me this picture.

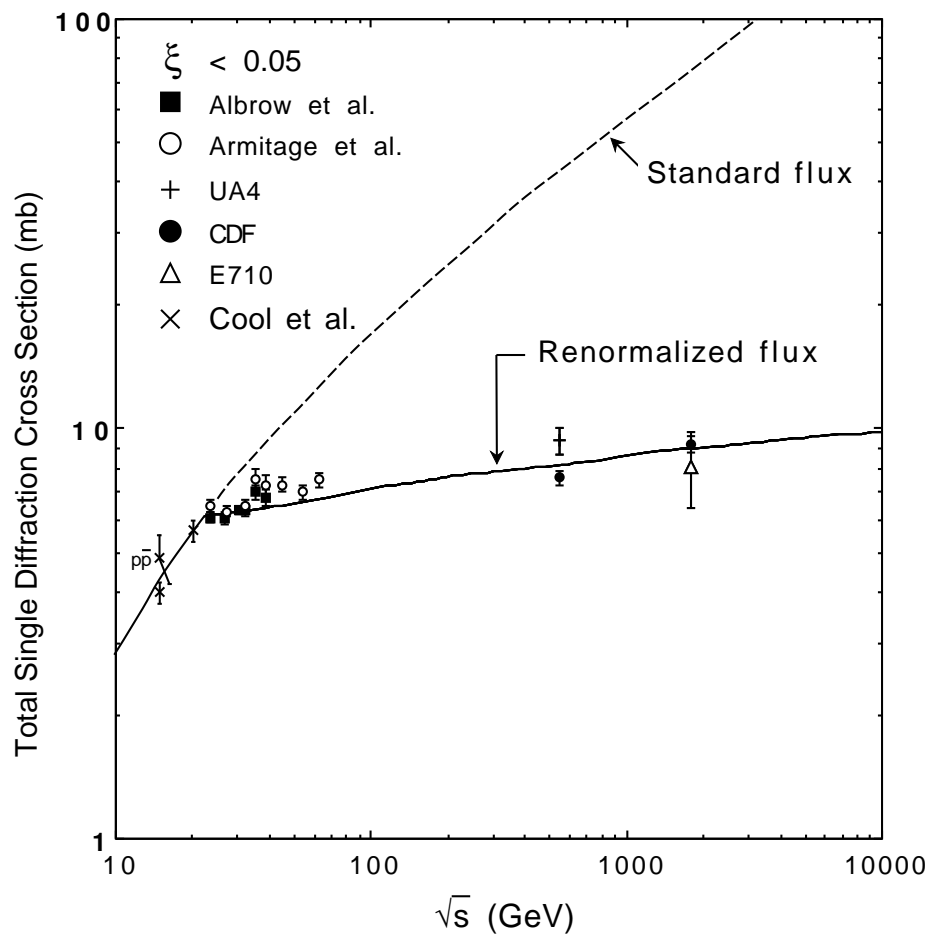


Figure 26: Experimental data on σ_{SD} as a function of center mass energy. The dashed curve is the triple-Pomeron prediction while the solid one is one of the model which fits the data. Picture is taken from one of numerous talks of D. Goulianos.

11 Pomeron in photon - proton interaction.

The photon - hadron interaction has two aspects which makes it quite different from the hadron - hadron interaction (at least at first sight). First, the total cross section is of the order of $\alpha_{em} \approx 1/137 \ll 1$ and, therefore, we can neglect the elastic cross section which is in extra α_{em} times smaller. Therefore, we need to understand how looks the unitarity constraint here. I want to recall that for hadron - hadron collisions the square of scattering amplitude enters the unitarity constraint. Second, we have a unique way to study the dependence of the cross section on the mass of incoming particle changing the virtuality of photon. As everybody knows at large virtualities we are dealing with deep inelastic scattering (DIS) which has a simple partonic interpretation. I would like to remind you that DIS will be a subject of the third and fourth parts of my lectures, if any. Here, let us try to understand how to incorporate the Reggeon exchange for photon - proton interaction at high energy.

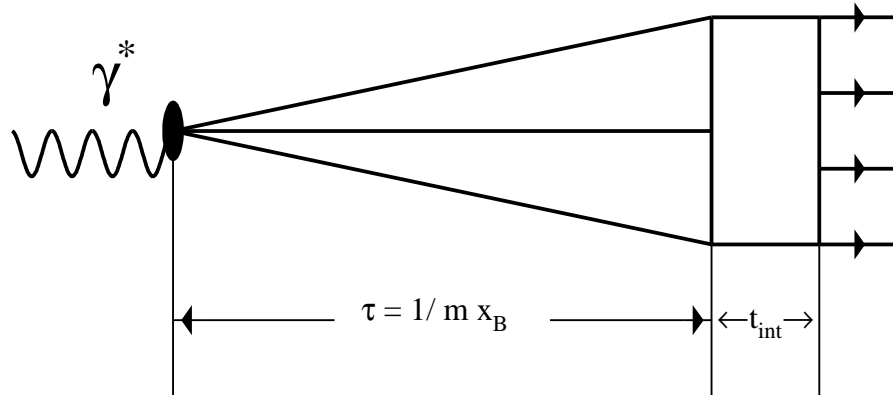


Figure 27: *Two stages of photon - hadron interaction at high energy.*

11.1 Total cross section.

Gribov was the first who observed that a photon (even virtual one) fluctuates into hadron system with the life time (coherence length) $\tau = l_c = \frac{1}{m x_B}$ where $x_B = \frac{Q^2}{s}$, Q^2 is the photon virtuality and m is the mass of the target. This life time is much larger at high energy

than the size of the target and therefore, we can consider the photon - proton interaction as a processes going in two stages:

(1) $\gamma^* \rightarrow \text{hadrons}$ transition which is not affected by the target and, therefore, looks similar to the electron - positron annihilation;

and

(2) *hadron - target* interaction, which can be treated as normal hadron - hadron interaction, for example, in the Pomeron (Reggeon) exchange approach (see Fig.27).

The resulting photon - nucleon cross section can be written as:

$$\sigma(\gamma^* N) = \frac{\alpha_{em}}{3\pi} \int \frac{R(M^2) M^2 d M^2}{(Q^2 + M^2)^2} \sigma_{M^2 N}(s) . \quad (85)$$

Here $R(M^2)$ is defined as the ratio

$$R(M^2) = \frac{\sigma(e^+ e^- \rightarrow \text{hadrons})}{\sigma(e^+ e^- \rightarrow \mu^+ \mu^-)} . \quad (86)$$

The notation is illustrated in Fig.28 where M^2 is the mass squared of the scattered hadronic system, $\Gamma^2(M^2) = R(M^2)$ and $\sigma_{M^2 N}(s)$ is the cross section for the hadronic system to scatter off the nucleonic target.

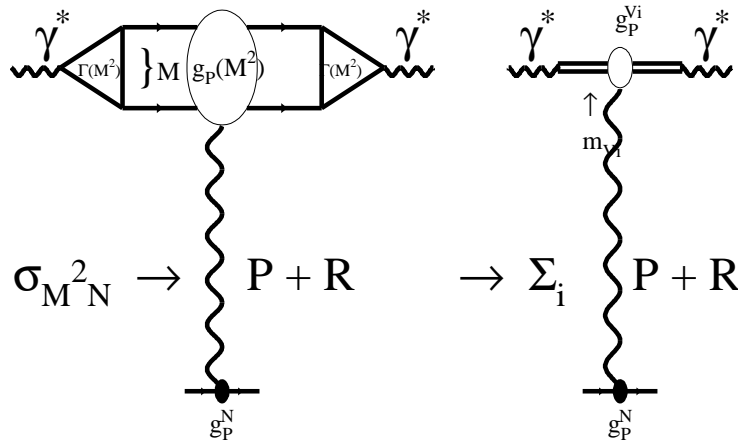


Figure 28: *Gribov's formula for DIS.*

In Fig.29 one can see the experimental data on $R(M^2 = s)$. It is clear that $R(M^2)$ can be described in two component picture: the contribution of resonances such as $\rho, \omega, \phi, J/\Psi, \Psi'$ and so on and the contributions of quarks which give more less constant term but it changes abruptly with each new open quark - antiquark channel.

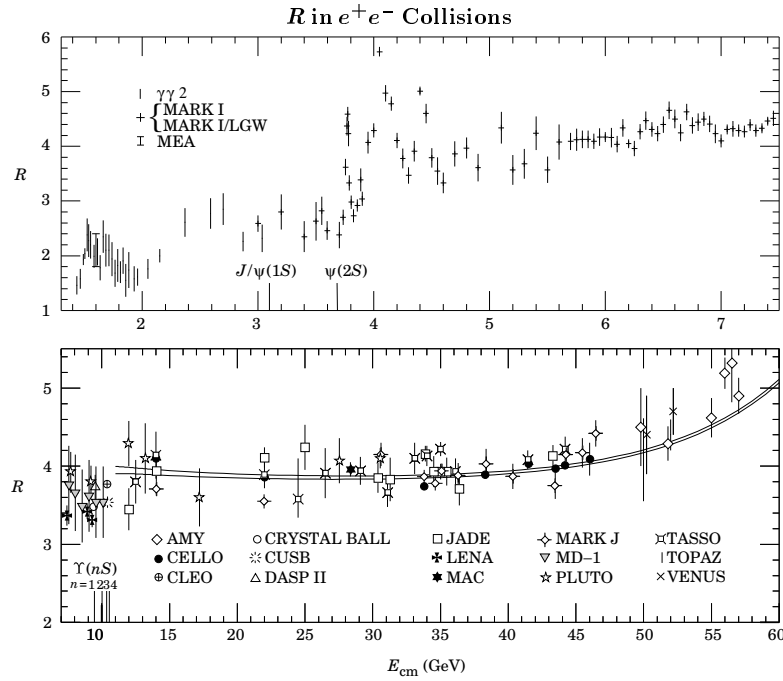


Figure 36.16: Selected measurements of $R \equiv \sigma(e^+e^- \rightarrow \text{hadrons})/\sigma(e^+e^- \rightarrow \mu^+\mu^-)$, where the annihilation in the numerator proceeds via one photon or via the Z . Measurements in the vicinity of the Z mass are shown in the following figure. The denominator is the calculated QED single-photon process; see the section on Cross-Section Formulae for Specific Processes. Radiative corrections and, where important, corrections for two-photon processes and τ production have been made. Note that the ADONE data ($\gamma\gamma 2$ and MEA) is for ≥ 3 hadrons. The points in the $\psi(3770)$ region are from the MARK I—Lead Glass Wall experiment. To preserve clarity only a representative subset of the available measurements is shown—references to additional data are included below. Also for clarity, some points have been combined or shifted slightly ($< 4\%$) in E_{cm} , and some points with low statistical significance have been omitted. Systematic normalization errors are not included; they range from $\sim 5\text{--}20\%$, depending on experiment. We caution that especially the older experiments tend to have large normalization uncertainties. Note the suppressed zero. The horizontal extent of the plot symbols has no significance. The positions of the $J/\psi(1S)$, $\psi(2S)$, and the four lowest Υ vector-meson resonances are indicated. Two curves are overlaid for $E_{\text{cm}} > 11$ GeV, showing the theoretical prediction for R , including higher order QCD [M. Dine and J. Sapirstein, Phys. Rev. Lett. **43**, 668 (1979)] and electroweak corrections. The Λ values are for 5 flavors in the $\overline{\text{MS}}$ scheme and are $\Lambda_{\overline{\text{MS}}}^{(5)} = 60$ MeV (lower curve) and $\Lambda_{\overline{\text{MS}}}^{(5)} = 250$ MeV (upper curve). (Courtesy of F. Porter, 1992.) References (including several references to data not appearing in the figure and some references to preliminary data):

AMY: T. Mori *et al.*, Phys. Lett. **B218**, 499 (1989);
 CELLO: H.-J. Behrend *et al.*, Phys. Lett. **144B**, 297 (1984);
 and H.-J. Behrend *et al.*, Phys. Lett. **183B**, 400 (1987);
 CLEO: R. Giles *et al.*, Phys. Rev. **D29**, 1285 (1984);
 and D. Besson *et al.*, Phys. Rev. Lett. **54**, 381 (1985);
 CUSB: E. Rice *et al.*, Phys. Rev. Lett. **48**, 906 (1982);
 CRYSTAL BALL: A. Osterheld *et al.*, SLAC-PUB-4160;
 and Z. Jakubowski *et al.*, Z. Phys. **C40**, 49 (1988);
 DASP: R. Brandelik *et al.*, Phys. Lett. **76B**, 361 (1978);
 DASP II: Phys. Lett. **116B**, 383 (1982);
 DCF: G. Cosme *et al.*, Nucl. Phys. **B152**, 215 (1979);
 DHHM: P. Bock *et al.* (DESY-Hamburg-Heidelberg-
 MPI München Collab.), Z. Phys. **C6**, 125 (1980);
 gamma2: C. Bacci *et al.*, Phys. Lett. **86B**, 234 (1979);
 HRS: D. Bender *et al.*, Phys. Rev. **D31**, 1 (1985);
 JADE: W. Bartel *et al.*, Phys. Lett. **129B**, 145 (1983);
 and W. Bartel *et al.*, Phys. Lett. **160B**, 337 (1985);
 LENA: B. Niczyporuk *et al.*, Z. Phys. **C15**, 299 (1982).
 MAC: E. Fernandez *et al.*, Phys. Rev. **D31**, 1537 (1985);
 MARK J: B. Adeva *et al.*, Phys. Rev. Lett. **50**, 799 (1983);
 and B. Adeva *et al.*, Phys. Rev. **D34**, 681 (1986);
 MARK I: J. L. Siegrist *et al.*, Phys. Rev. **D26**, 969 (1982);
 MARK I + Lead Glass Wall: P.A. Rapidis *et al.*,
 Phys. Rev. Lett. **39**, 526 (1977); and P.A. Rapidis, thesis,
 SLAC-Report-220 (1979);
 MARK II: J. Patrick, Ph.D. thesis, LBL-14585 (1982);
 MD-1: A.E. Blinov *et al.*, Z. Phys. **C70**, 31 (1996);
 MEA: B. Esposito *et al.*, Lett. Nuovo Cimento **19**, 21 (1977);
 PLUTO: A. Bäcker, thesis, Gesamthochschule Siegen,
 DESY F33-77/03 (1977); C. Gerke, thesis, Hamburg Univ. (1979);
 Ch. Berger *et al.*, Phys. Lett. **81B**, 410 (1979);
 and W. Lackas, thesis, RWTH Aachen, DESY Pluto-81/11 (1981);
 TASSO: R. Brandelik *et al.*, Phys. Lett. **113B**, 499 (1982);
 and M. Althoff *et al.*, Phys. Lett. **138B**, 441 (1984);
 TOPAZ: I. Adachi *et al.*, Phys. Rev. Lett. **60**, 97 (1988); and
 VENUS: H. Yoshida *et al.*, Phys. Lett. **198B**, 570 (1987).

Figure 29: Experimental behaviour of $R(M^2 = E_{\text{cm}}^2)$ (Particle Data Group 1996).

For σ_{M^2N} we can use the Reggeon exchange approach which gives for the total cross section Eq. (74) where only vertices g_P and g_R depend on M^2 .

If we take into account only the contribution of the ρ - meson and ω - meson resonances in $R(M^2)$ we obtain the so called vector dominance model (VDM) which gives for the total cross section the following formula:

$$\sigma_{tot}(\gamma^* + p) = \frac{\alpha_{em}}{3\pi} \sigma_{tot}(\rho + p) \sum_i R(M^2 = m_{V_i}^2) \left\{ \frac{m_{V_i}^2}{Q^2 + m_{V_i}^2} \right\}^2 \quad (87)$$

where m_{V_i} is the mass of vector meson, Q^2 is the value of the photon virtuality and $R(M^2 = m_{V_i}^2)$ is the value of the R in the mass of the vector meson which can be rewritten through the ratio of the electron - positron decay width to the total width of the resonance.

One can see from Eq. (87), that the VDM gives the $\frac{1}{Q^4}$ behaviour of the total cross section. Such a behaviour is in clear contradiction with the experimental data which shows approximately $\frac{1}{Q^2}$ dependence at large values of Q^2 . It should be stressed that the background contribution to Eq. (85) leads to experimental Q^2 - dependence. Indeed, for $M^2 > m_\rho^2$ we can consider $R(M^2)$ as a constant ($R^2(M^2) \approx 2$, see Fig.29) as far as Q^2 - dependence is concerned. Assuming that σ_{M^2N} does not depend on M^2 , we have

$$\sigma_{tot}(\gamma^* + p) = \frac{\alpha_{em}}{3\pi} \sigma_{tot}(\rho + p) 2 \ln\left(\frac{Q^2 + M_0^2}{Q^2 + m_\rho^2}\right), \quad (88)$$

where M_0 is the largest mass up to which we can consider that σ_{M^2N} is independent of M^2 . Directly from Eq. (88) one can see that

$$\sigma_{tot}(\gamma^* + p) = \frac{2\alpha_{em}}{3\pi} \sigma_{tot}(\rho + p) \frac{M_0^2 - m_\rho^2}{Q^2}.$$

The value of M_0 is the new scale of our approach which separate the “soft” (long distance) processes from the “hard” (small distance) ones. Actually, any discussion of this problem is out of the schedule of these lectures and I want only to point out that the QCD leads to the cross section which falls down as $\frac{1}{M^2}$ at large M^2 .

To write explicitly the Pomeron (Reggeon) contribution to photon - nucleon cross section we have to specify the energy variable. I hope, that I have discussed this issue in so many details that I can guess that energy variable s/M^2 will be familiar for a reader.

Therefore, finally, the contribution of the Pomeron as well as any Reggeon to photon - nucleon scattering has the following form:

$$\sigma(\gamma^* N) = \frac{\alpha_{em}}{3\pi} \int \frac{R(M^2) M^2 d M^2}{(Q^2 + M^2)^2} g_P(M^2) g_P^N \left(\frac{s}{M^2} \right)^{\alpha_P(0) - 1}. \quad (89)$$

I would like to draw your attention once more to the very important feature of Eq. (89), namely, the mass dependence is concentrated only in the dependence of vertex $g_P(M^2)$ and in the energy variable s/M^2 . It is interesting to notice that the integral over M^2 converges even if $g_P(M^2)$ does not depend on M^2 , but it should be stressed that at large M^2 we are dealing with the small distance physics where the powerful methods of perturbative QCD have to be applied.

11.2 Diffractive dissociation

Diffractive dissociation is the process in which in the final state we have a large rapidity gap (see Fig.30). This process can be described using the same approach as in Eq. (85), namely, the dispersion relation with respect to M^2 in Fig.30. However, it is useful to discuss separately two cases: the exclusive final state with restricted number of hadrons and inclusive diffraction dissociation without any selection in the final state. To understand the difference between these two cases, let me recall, that, accordingly to the second definition of the Pomeron, the typical final state in the diffractive processes is still the parton “ladder”, namely, the final state hadrons are uniformly distributed in rapidity. In other word for fixed but large mass M of the final state the typical multiplicity of produced hadron $N \propto a \ln M^2$, where a is the parton density in rapidity (the number of particles in the unit rapidity interval). Therefore, the final state with fixed number of hadrons (partons) has a suppression which is proportional to $\exp(-a \ln M^2)$. It means that for the exclusive process with fixed number of the hadrons in the final state we have to find a new mechanism different from normal parton one. This mechanism is rather obvious since the large value of M could be due to the large value of the parton (hadron) transverse momenta (k_{it} in the final state which are of the order of M ($k_{it}^2 \approx M^2$)). Concluding this introduction to the DD processes in Reggeon approach, we should emphasize that

- (i) for exclusive final state with fixed number of hadrons (partons) the large diffractive mass is originated by the parton (hadron) interaction at small distances;
- (ii) while the inclusive DD in the region of large mass looks like the normal inclusive process in the parton model with uniformed distribution of the secondary hadrons in rapidity and with restricted hadron transverse momentum which does not depend on M .

11.3 Exclusive (with restricted number of hadrons) final state.

For this process we can use the Gribov’s formula (see Fig.30) and even more, for large values of mass we can calculate the transition from virtual photon to quark - antiquark pair in perturbative QCD. So, here, for the first time in my lecture I recall our microscopic theory - QCD, but, actually, we will discuss here only a very simple ideas of QCD, namely, the fact that the correct degrees of freedom are quark and gluons.

Let us start with the definition of all variables:

1. The Bjorken x variable is given by

$$x_B = x = \frac{Q^2}{s} ;$$

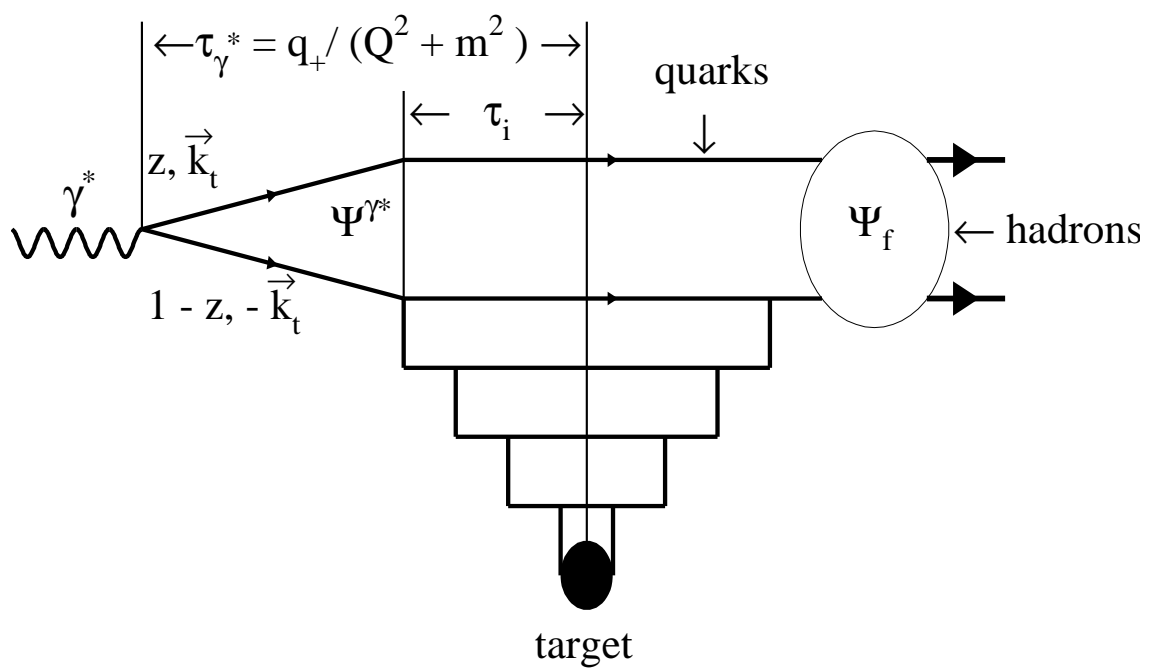


Figure 30: *Gribov's formula for diffractive dissociation (DD) in DIS.*

2. As usual, we introduce

$$x_P = \frac{Q^2 + M^2}{s},$$

which is the longitudinal fraction of the photon energy carried by the Pomeron;

$$3. \beta = \frac{Q^2}{Q^2 + M^2} = \frac{x_B}{x_P};$$

4. The transverse momenta of the out going quark and antiquark are denoted by $\pm \vec{k}_t$, and those of the exchanged partons (gluons) by $\pm \vec{l}_t$;

5. It is convenient to use light - cone perturbation theory and to express the particle four momenta in the form:

$$k_\mu = (k_+, k_-, \vec{k}_t),$$

where $k_\pm = k_0 \pm k_3$;

6. In the frame in which the target is essentially at rest we have

$$\begin{aligned} q_\mu &= (q_+, -\frac{Q^2}{q_+}, \vec{0}_t); \\ k_\mu &= (k_+, -\frac{m_t^2}{k_+}, \vec{k}_t); \\ l_\mu &= (l_+, -\frac{l_t^2}{l_+}, \vec{l}_t); \end{aligned}$$

with $m_t^2 = m_Q^2 + k_t^2$ where m is the quark mass.

The Gribov factorization (Gribov's formula) follows since the time of quark - antiquark fluctuation τ_{γ^*} is much longer than the time of interaction with partons (τ_i). It is instructive to illustrate why this is so. Accordingly to the uncertainty principle the fluctuation time is equal to:

$$\tau_{\gamma^*} \sim \left| \frac{1}{q_- - k_{1-} - k_{2-}} \right| = \frac{q_+}{Q^2 + M^2}, \quad (90)$$

where k_1 and k_2 are four momenta of the quarks of mass m , and

$$M^2 = \frac{m^2 + k_t^2}{z(1-z)}.$$

To estimate the interaction time we calculate the typical time of the emission of parton with momentum l_μ from quark k_1 , which is

$$\tau_i = \left| \frac{1}{k_{1-} - k'_{1-} - l_-} \right| = \left| \frac{q_+}{\frac{m_t^2}{z} - , \frac{m_t^2}{z'} - \frac{l_t^2}{\alpha}} \right|, \quad (91)$$

where $\alpha = \frac{l_+}{q_+}$ and $z' = z - \alpha$. In leading log s approximation in which we have obtained the Pomeron, we have $\alpha \ll z$ and hence

$$\tau_i = \frac{\alpha q_+}{l_t^2} \ll \tau_{\gamma^*}.$$

Therefore, we can write the Gribov's formula as it is given in Fig.30, namely:

$$M(\gamma^* + p \rightarrow M^2 + [LRG] + p) = \int d^2 k_t \int_0^1 dz \Psi^*(z, k_t, Q) A_P(M^2, s) \Psi_{final}(\bar{q}q \rightarrow \text{hadrons}) , \quad (92)$$

where LRG stands for large rapidity gap.

The wave function of the virtual photon can be written in the following way:

$$\Psi^*(z, k_t, Q) = -e Z_f \frac{\bar{u}(k_t, z) \gamma \cdot \epsilon v(-k_t, 1-z)}{\sqrt{z(1-z)}} \frac{1}{Q^2 - M^2} , \quad (93)$$

where $\vec{\epsilon}$ is the photon polarization: for longitudinal polarized photon we have

$$\epsilon_L = \left(\frac{q_+}{Q}, \frac{Q}{q_+}, \vec{0}_t \right)$$

while for transverse polarized photon($\vec{\epsilon}_t$) we will use the basis of circular polarization vectors :

$$\epsilon_{\pm} = \frac{1}{\sqrt{2}} (0, 0, 1, \pm i) .$$

To evaluate Eq. (93) with $\epsilon = \epsilon_L$ we first note that

$$q^{\mu} \bar{u} \gamma_{\mu} v = \frac{1}{2} (q_+ \bar{u} \gamma_- v + q_- \bar{u} \gamma_+ v) = 0$$

so that we have

$$\bar{u} \gamma_- v = \frac{Q^2}{q_+^2} \bar{u} \gamma_+ v .$$

We can use this identity to evaluate the wave function:

$$\bar{u} \gamma \cdot \epsilon_L v = \frac{1}{2} \left\{ \frac{q_+}{Q} \bar{u} \gamma_- v + \frac{Q}{q_+} \bar{u} \gamma_+ v \right\} = \frac{Q}{q_+} \bar{u} \gamma_+ v = 2Q \sqrt{z(1-z)} \delta_{\lambda, -\lambda'} ,$$

where we λ is helicity of the antiquark while λ' is helicity of the quark (we omitted helicities in the most of our calculations but put them correctly in the answer). Coming back to Eq. (93) one can see that:

$$\Psi_L^* = -e Z_f \frac{4Q \delta_{\lambda, -\lambda'}}{Q^2 + M^2} . \quad (94)$$

For the transverse polarized photon with helicity $\lambda_{\gamma} = \pm 1$ we can obtain the answer:

$$\Psi_T^* = -e Z_f \frac{\delta_{\lambda, -\lambda'} \{(1-2z)\lambda_{\gamma} \pm 1\} \vec{\epsilon}_{\pm} \cdot \vec{k}_t + \delta_{\lambda, \lambda'} m \lambda_{\gamma}}{[z(1-z)] (Q^2 + M^2)} . \quad (95)$$

To obtain the expression for the diffractive dissociation cross section we have to square our amplitude and sum over all quantum numbers of the final state (with fixed mass M).

Assuming that experimentally no selection has been made or in other words Ψ_{final} does not describe a specific state with definite angular momentum, we can sum over helicities and obtain the following answers:

$$\frac{d\sigma_L^{SD}}{dM^2 dt} = \frac{\alpha_{em}}{48\pi^3} \frac{Q^2 R_L^{exclusive}(M^2)}{\{Q^2 + M^2\}^2} g_P^2(M^2) g_p^2 \left(\frac{s}{Q^2 + M^2} \right)^{2\Delta}; \quad (96)$$

$$\frac{d\sigma_T^{SD}}{dM^2 dt} = \frac{\alpha_{em}}{48\pi^3} \frac{M^2 R_T^{exclusive}(M^2)}{\{Q^2 + M^2\}^2} g_P^2(M^2) g_p^2 \left(\frac{s}{Q^2 + M^2} \right)^{2\Delta}; \quad (97)$$

where $R_{L,T}(M^2)$ is defined as ratio

$$R_{L,T}(M^2) = \frac{\sigma(e^- + e^+ \rightarrow \text{hadrons with mass } M)}{\sigma(e^- e^+ \rightarrow \mu^- \mu^+)}. \quad (98)$$

You can see that Eq. (96) and Eq. (97) give us a possibility to measure experimentally the dependence of $g(M^2)$ on mass M and therefore to find out the value of the separation scale M_0 . As we have discussed, this scale separate the long distance (nonperturbative, “soft”) physics from the short distance one (perturbative, “hard”). I think, that I do not even need to mention how it is important to have such sort of information for our understanding of nonperturbative QCD contribution to find a way out of the Reggeon phenomenology.

11.4 Inclusive diffraction

The diffractive production of the large mass in $\gamma^* p$ in the Reggeon approach looks quite similar to the diffractive dissociation in hadron - hadron collisions. We can safely apply the triple Reggeon phenomenology and the formulae have the same form as Eq. (76), namely

$$\frac{M^2 d\sigma_{SD}(\gamma^* p)}{dM^2} = \frac{\sigma_0}{2\pi R^2(\frac{s}{M^2})} \cdot \left(\frac{s}{M^2} \right)^{2\Delta} \cdot [g_P^{\gamma^*} \cdot G_{3P}(0) \cdot \left(\frac{M^2}{s_0} \right)^\Delta + g_R^{\gamma^*} \cdot G_{PPR}(0) \left(\frac{M^2}{s_0} \right)^{\alpha_{R(0)}-1}]. \quad (98)$$

The difference is the only one, namely, we can write the Gribov’s formula for vertex $g_{P,R}^{\gamma^*}$. Indeed,

$$g_{P,R}^{\gamma^*}(Q^2) = \frac{\alpha_{em}}{3\pi} \int^{M_0^2} \frac{R(M'^2) M'^2 dM'^2}{(Q^2 + M'^2)^2} g_{P,R}(M^2) \left(\frac{s_0}{M'^2} \right)^{\alpha_{P,R(0)}-1}. \quad (99)$$

We introduce explicitly the separation scale M_0 to demonstrate that we trust this formula only in the region of sufficiently small mass while at large masses this integral should be treated in perturbative QCD.

I would like to draw your attention to the fact that the Q^2 dependence is concentrated only in vertex $g_{P,R}^{\gamma^*}$ and one of prediction of the Pomeron approach is the fact that large mass diffraction has the same Q^2 dependence as the total $\gamma^* p$ cross section. Surprisingly the HERA data are not in contradiction with this prediction.

However, it should be stressed that the Pomeron approach can be trusted only for rather small virtualities while at large Q^2 perturbative QCD manifests itself as more powerful and reliable tool for both the DIS total cross sections and diffractive dissociation in DIS. The challenge for everybody who is trying to understand the photon - hadron interaction is to find the region of applicability of pQCD and to separate “soft” and “hard” interactions. This task is impossible without a certain knowledge of the Reggeon phenomenology.

12 Shadowing Corrections (a brief outline).

12.1 Why Pomeron is not enough?

I hope, that I have given a lot of information on the Reggeon phenomenology. Now, I want to touch several difficult and important topics and, in particular, I want to explain why the Pomeron hypothesis is not sufficient. The consistent discussion of these topics will be done in the second part of my lectures, but I would like to give here a brief review of the shadowing corrections (SC) properties to discuss the experimental way of the study of the Pomeron structure which I will present in the next section.

It turns out that the simple hypothesis that *the Pomeron gives you the asymptotic behaviour of the scattering amplitude is not correct*. To illustrate this fact let us consider the single diffraction dissociation in the region of large mass M (see Fig.23c). In this kinematic region we can use the simple triple Pomeron formula for such a cross section. Using Eq.(76b) and exponential parameterization for t - dependence of all vertices, we can write the following expression for the single diffraction cross section:

$$SDSC \frac{M^2 d^2 \sigma_{SD}}{dM^2 dt} = (g_P^p(0))^3 \cdot G_{PPP}(0) \cdot e^{2(R_0^2 + r_0^2 + \alpha'_P \ln(s/M^2))t} \left(\frac{s}{M^2}\right)^{2\Delta_P} \left(\frac{M^2}{s_0}\right)^{\Delta_P}, \quad (100)$$

where R_0^2 and r_0^2 give the t -dependence of the Pomeron - proton form factor and the triple Pomeron vertex respectively. Let us calculate the total diffractive dissociation cross section in large mass M region ($M \geq M_0$).

$$\begin{aligned} \sigma_{SD}(M \geq M_0) &= \quad (101) \\ \int_{-\infty}^0 dt \int_{M_0^2}^s dM^2 \frac{d^2 \sigma_{SD}}{dM^2 dt} &= \frac{(g_P^p(0))^3 \cdot G_{PPP}(0)}{2(R_0^2 + r_0^2 + \alpha'_P \ln(s/M_0^2))} \cdot \left(\frac{s^2}{s_0 M_0^2}\right)^{\Delta_P}. \end{aligned}$$

Therefore, one sees that $\sigma_{sd} \propto s^{2\Delta_P}$ while the total cross section is proportional to s^{Δ_P} . It means that something is deeply wrong in our approach which leads to the cross section of diffractive dissociation which larger than the total cross section. For $\Delta_P > 0$ we can take simpler example like the elastic cross section or cross section of the diffractive dissociation in the region of small masses ($M \leq M_0$) but what is important to notice is the fact that the diffractive dissociation in large masses leads to the cross section which increases with energy even if $\Delta_P = 0$. Indeed, repeating all calculations in Eq. (101) for $\Delta = 0$ we can see that

$$\sigma_{SD} \propto \ln \ln s.$$

Therefore we have to reconsider our approach and take into account the interaction between Pomerons, in particular with the triple Pomeron vertex. I do not want to discuss this deep problem here and I will postpone it to the second part of the lectures. I would like to show here that the Pomeron interactions between Pomerons and with particles is a natural outcome of the parton space - time picture that we have discussed in section 8.

12.2 Space - time picture of the shadowing corrections.

To understand, why we have to deal with the SC, we have to look back at Figs.21e and 21f. When I discussed these pictures in sections 8.2 and 8.3, I, as a skillful lecturer, cheated you a bit or better to say I did not stress that we had an assumption that only one “wee” parton interacts with a target. Now, let ask ourselves why only one? What is going to happen if, let us say, two “wee” partons interact with our target? Look, for example, in Fig. 21e. If two “wee” partons interact with the target the coherence in two “ladders” will be destroyed. Squaring this amplitude with two incoherent “ladders”, one can see that we obtain the diagram in which two initial hadrons interact by exchange of two Pomerons. Here, I used the second definition of the Pomeron, namely, Pomeron = “ladder”.

Therefore, the whole picture of interaction looks as follows. The fast hadron decays in a huge number of partons and this partonic fluctuation lives long time $t \propto \frac{E}{\mu^2}$ (see Fig.21d). During this time each parton can create its own chain of partons and, as we have discussed, all such creations result in production of N “wee” partons, which can interact with the target with a normal cross section (σ_0). Assuming that only one “wee” parton interacts with the target we obtained Eq.(72), namely, $\sigma_{tot}^P = \sigma_0 \cdot N$. This process we call the Pomeron exchange.

However, several “wee” partons can interact with the target. For example, let us assume that two “wee” partons interact with the target. The cross section will be equal to $\sigma_{tot}^P \cdot W$, where W is the probability for the second “wee” parton to meet and interact with the target. As we have discussed in section 7.4 all “wee” partons are distributed in the area in the transverse plane which is equal $\pi R^2(s)$ and $R^2 \rightarrow \alpha'_P \ln(s)$. Therefore, the cross section of the two “wee” parton interaction is equal

$$\sigma^{(2)} = \sigma_0 \cdot N \cdot \frac{\sigma_0 \cdot N}{\pi R^2(s)} . \quad (102)$$

If $\Delta_P > 0$ this cross section tens to overshoot the one “wee” parton cross section. However, if $\Delta = 0$ $\sigma^{(2)}$ turns to be much smaller than σ_{tot}^P , namely,

$$\sigma^{(2)} = \frac{(\sigma_{tot}^P)^2}{\pi R^2(s)} . \quad (103)$$

Actually, Eq. (103) was our hope why nevertheless the Pomeron hypothesis could survive. However, let me recall that the problem with the triple Pomeron interaction and with the large mass diffraction dissociation as the first manifestation of such an interaction will still remain even if $\Delta_P = 0$.

Now let us ask ourselves what should be a sign for $\sigma^{(2)}$ contribution to the total cross section. Strange question, isn't it. My claim is that sign should be negative. Why? Let us remember that the total cross section is just probability that incoming particle has at least one interaction. Therefore, our interaction in the parton model is the scattering of the flux of N "wee" partons with a target. To calculate the total cross section we need only to count that at least one interaction has happened. However, we overestimate the value of the total cross section since we thought that every parton from the total number of "wee" parton N is able to interact with the target. Actually, the second parton cannot interact with the target if it is just behind the first one. The probability to find the second parton just behind the first is equal to W which we have estimated. Therefore, the correct answer is the the flux of "wee" partons that can interact with the target is equal to

$$FLUX = N \cdot (1 - W) = N \cdot \left(1 - \frac{\sigma_{tot}^P}{\pi R^2(s)}\right)$$

which leads to the total cross section:

$$\sigma_{tot} = \sigma_{tot}^P - \frac{(\sigma_{tot}^P)^2}{\pi R^2(s)}. \quad (104)$$

I hope that everybody recognizes the famous Glauber formula.

Therefore, *the shadowing corrections are the Glauber screening for the flux of "wee" partons.*

If $W \ll 1$ we can restrict ourselves by calculation of interaction of two "wee" partons with the target. However, if $W \approx 1$ we face a complicated and challenging problem of calculating all SC. We are far away from any solution of this problem especially in the "soft" interaction. Here, I am only going to demonstrate you how the SC works and what qualitative manifestation of the SC can we expect in the high energy scattering.

12.3 The AGK cutting rules.

The Abramovsky - Gribov - Kancheli (AGK)cutting rules give the generalization of the optical theorem for the case of the multi Pomeron exchange.

Indeed, the optical theorem for one Pomeron exchange ($\sigma_1^{(1)}$ in Fig. 32) decipher the Pomeron structure and says that the Pomeron contribution to the total cross section closely related to the inelastic cross section with large number of hadrons (partons) $\langle n_P \rangle$ which in the first approximation are uniformly distributed in rapidity (Feynman gas hypothesis).

In the case of two "wee" parton interaction or, in other words, in the case of two Pomeron exchange there are three different contributions to the total cross section if we analyze them from the point of view of the type of the inelastic events.

They are (see Fig.32):

1. The diffractive dissociation ($\sigma_2^{(0)}$) processes in which we have a very small multiplicity of the particles in the final state. The clear signature of these processes is the fact that no particles are produced in the large gap in rapidity (see Fig.32 and the lego - plot for $\sigma_2^{(0)}$ typical event).
2. The production of the secondary hadrons with the same multiplicity as for one Pomeron exchange (see $\sigma_2^{(1)}$ in Fig.32). This event has the same multiplicity ($\langle n_P \rangle$) as the one Pomeron exchange (compare $\sigma_2^{(1)}$ with $\sigma_1^{(1)}$ in Fig.32).
3. The production of the secondary hadrons with multiplicity in two times larger than for one Pomeron exchange (see $\sigma_2^{(2)}$ in Fig.32).

The AGK cutting rules claim:

$$\sigma_2^{(0)} \div \sigma_2^{(1)} \div \sigma_2^{(2)} = 1 \div -4 \div 2 \quad (105)$$

Two important consequences follow from the AGK cutting rules:

1. The total cross section of the diffraction dissociation (DD) is equal to the contribution of two Pomeron exchange to the total cross section ($\sigma_{tot}^{(2P)}$) with opposite sign:

$$\sigma^{(DD)} = -\sigma^{(2P)}$$

2. The two Pomeron exchange does not contribute to the total inclusive cross section in central kinematic region. Indeed only two processes $\sigma^{(1)}$ and $\sigma^{(2)}$ are the sources of the produced particle in the central region. It means that the total inclusive cross section due to two Pomeron exchange is equal to

$$\sigma_{inc} = \sigma^{(1)} + 2\sigma^{(2)} = 0$$

Factor 2 comes from the fact that the particle can be produced from two different parton showers (see $\sigma_2^{(2)}$ in Fig. 32).

Now let me give you a brief proof of the AGK cutting rules for the case of hadron - deuteron interaction (see Fig.31). For simplicity let us assume that $G_{in}(b_t) = \kappa = Const(b_t)$ for $b_t < R_N$ and $G_{in} = 0$ for $b_t > R_N$, so the inelastic cross section for hadron - nucleon interaction is equal to

$$\sigma_N^{inel} = \kappa S$$

where S is the area of the nucleon ($S = \pi R_N^2$). To calculate the elastic cross section we need to use the unitarity constraint in b_t (see Eq.(20)) and the answer is

$$\sigma_N^{el} = \left(\frac{\kappa}{2}\right)^2 S$$

Note that the flux of incoming particles after the first interaction becomes $(1 - \kappa)$ we can calculate the total inelastic interaction with the deuteron, namely

$$\sigma_D^{inel} = \kappa S + \kappa(1 - \kappa)S = 2\sigma_N^{inel} - \kappa^2 S$$

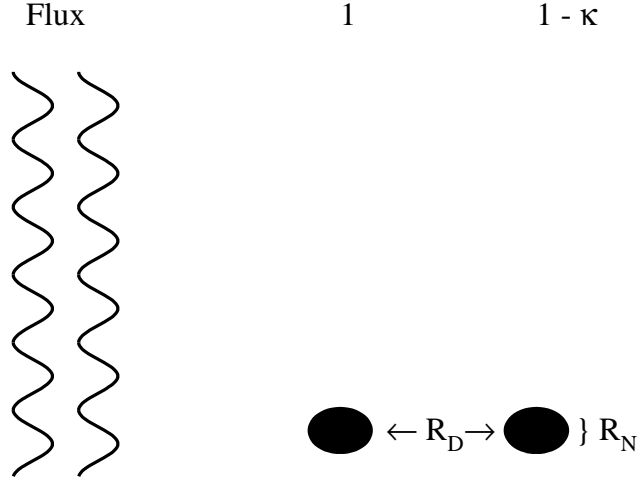


Figure 31: *Hadron - deuteron interaction.*

Using unitarity we have to calculate the elastic cross section for the interaction with deuteron which is equal to

$$\sigma_D^{el} = \left(\frac{2\kappa}{2}\right)^2 S$$

I would like to draw your attention to the fact that in calculation of the elastic cross section we cannot use our probabilistic arguments and we have to use the unitarity constraint of Eq.(20). Therefore the total cross section for hadron - deuteron interaction can be presented in the form:

$$\sigma_D^{tot} = 2\sigma_N^{tot} - \Delta\sigma$$

where

$$\Delta\sigma = \Delta\sigma^{inel} + \Delta\sigma^{el} = -\frac{\kappa^2}{2} S = -\frac{(\sigma_N^{inel})^2}{2\pi R^2}$$

Everybody can recognize the usual Glauber formula for hadron - deuteron interaction.

As has been mentioned we have two sources of the inelastic cross section which are pictured in Fig. 32 for the case of the deuteron. The cross section of the inelastic process with double multiplicity is easy to calculate, because it is equal to the probability of two inelastic interaction:

$$\Delta\sigma_2^{(2)} = \kappa^2 \cdot S$$

To calculate $\sigma_2^{(1)}$ we have to remember that

$$\Delta\sigma^{inel} = \sigma_2^{(2)} + \sigma^{(1)2} = -\kappa S$$

Therefore $\sigma_2^{(1)} = -2\kappa S$. Remembering that $\Delta\sigma_2^{(0)} = \sigma_D^{el} - 2\sigma_N^{el}$ we get

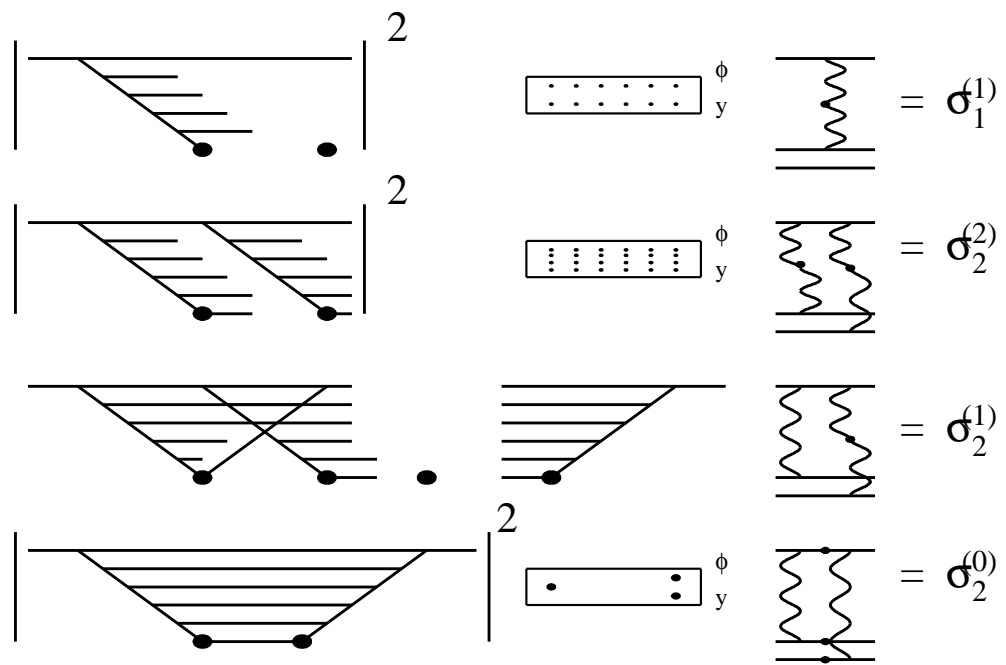


Figure 32: *The AGK cutting rules for hadron - deuteron interaction. Dots mark cut Pomerons and particles on mass shell.*

n	0	$\langle n \rangle_N$	$2\langle n \rangle_N$
$\Delta\sigma_{tot}$	$\frac{\kappa^2}{2}S$	$-2\kappa^2S$	κ^2S

Therefore we get the AGK cutting rules for the hadron - deuteron interaction, since $\sigma_D^{tot} = 2\sigma_N^{tot}$ corresponds to one Pomeron exchange and the correction to this simple formula just originated from the two Pomeron exchange in our Reggeon approach. However the above discussion, I hope, shows you that the AGK cutting rules have more general background than the Reggeon approach. For example, they hold in QCD providing the so called factorization theorem.

Let me give here the general formula for the AGK cutting rules. If we have the contribution to the total cross section with the exchange of ν Pomerons (σ_{tot}^ν), the cross sections of the process with the multiplicity of produced particles equal μ $\langle n_P \rangle$ which are generated by the same diagram (see Fig.32) are equal[†]:

$$\frac{\sigma^{(\mu)}}{\sigma_{tot}^\nu} |_{\mu \neq 0} = (-1)^{\nu-\mu} \cdot \frac{\nu!}{\mu! (\nu-\mu)!} \cdot 2^\nu \quad (106)$$

while for $\mu = 0$ the ratio is equal

$$\frac{\sigma^{(0)}}{\sigma_{tot}^\nu} = (-1)^\nu \cdot [2^{\nu-1} - 1] \quad (107)$$

For the first 5 exchange you can find these factors in the following table.

$\nu \setminus \mu$	0	1	2	3	4	5
1	0	1	0	0	0	0
2	1	-4	2	0	0	0
3	-3	12	-12	4	0	0
4	7	-32	48	-32	8	0
5	-15	80	-160	160	-80	16

12.4 The Eikonal model.

The simplest way of estimate the value of the SC is so called the Eikonal model. It is easy to explain what is the Eikonal model just from the general solution of the s -channel unitarity (see Eq.(26)):

$$a_{el}(s, b) = i \{ 1 - e^{-\frac{\Omega(s, b)}{2}} \}; \quad (108)$$

$$G_{in}(s, b) = 1 - e^{-\Omega(s, b)}. \quad (109)$$

The weak unitarity constrains are $Im a_{el}(s, b) \leq 1$ and $G_{in}(s, b) \leq 1$ which follow directly from Eq. (108) and Eq. (109).

[†] $\langle n_P \rangle$ is the average multiplicity in one Pomeron exchange

At small values of opacity $\Omega a_{el} = \Omega/1$ and $G_{in} = \Omega$. Since we think that the Pomeron is a good approximation until the SC would be large, we take Ω is equal to the one Pomeron exchange, namely:

$$\Omega(s, b) = \frac{\sigma_0(s = s_0)}{\pi R_{ab}^2(s)} \cdot \left(\frac{s}{s_0} \right)^{\Delta_P} e^{-\frac{b^2}{R_{ab}^2(s)}}, \quad (110)$$

where σ_0 is the total cross section of the $a + b$ scattering at some value of energy ($s = s_0$) where we expect that the SC are small. In exponential parameterization where the t -dependence of Pomeron - hadron vertex $g_a^P(t) m = \exp(-R_{0a}^2|t|)$

$$R_{ab}^2 = 4 \cdot (R_{0a}^2 + R_{0b}^2 + \alpha'_P(0) \ln(s/s_0)).$$

Certainly, this is an assumption which has no theoretical proof. From the point of view of the parton model this assumption looks very unnatural since the Eikonal model describes the SC induced only by “wee” partons originated from the fastest parton (hadron). There is no reason “wee” partons created by decay of each parton, not only the fastest one, cannot interact with the target. Using the s -channel unitarity and our main hypothesis that the Pomeron = “ladder” (the second definition of the Pomeron) one can see that the rich structure of the final state we simplify to two classes of event: (i) the elastic scattering and (ii) the inelastic particle production with uniform rapidity distribution (Feynman gas assumption). In particular, we neglected a rich structure of the diffractive dissociation events as well as all events with sufficiently large rapidity gaps.

In some sense the Eikonal model is the direct generalization of Feynman gas approach, namely, we take into account the Feynman gas model for the typical inelastic even and the elastic scattering since we cannot satisfy an unitarity constrain without the elastic scattering. As I have discussed the G_{in} in Eq.(20) can be treated almost classically and the probabilistic interpretation for this term can be used. However, the first two terms in Eq.(20), namely $2Im a_{el}$ and $|a_{el}|^2$, is our quantum mechanics (optics) and both should be taken into account.

However, such model can be useful in the limited range of energy and the physical parameter which is responsible for the accuracy of calculation in the Eikonal model is the ratio of

$$\gamma = \frac{G_{PPP}(0)}{g_a^P(0)} = \frac{\sigma_{SD}}{2\sigma_{el}}.$$

It is interesting to note that in whole range of accessible energies experimentally $\gamma \leq 1/4$. Therefore, we can use this model for the first estimates of the value of SC, at least to find the qualitative signature of their influence and to select an efficient experimental way to study SC.

First, let us fix our numerical parameters using the Fermilab data at fixed target energy. We take $s_0 = 400 GeV^2$, $\sigma_0 = 40$ mbn, $R_{0p}^2 = 2.6 GeV^{-2}$, $\alpha'_P(0) = 0.25 GeV^{-2}$ and $\Delta = 0.08$. As you can see we take all parameters of D-L Pomeron but we use the simple exponential parameterization for vertices while Donnachie and Landshoff used more advanced t -distribution which follows from the additive quark model. In Fig.33 you can see the result of our calculation for: $\Omega(s, b)$, $Im a_{el}(s, b)$ and $G_{in}(s, b)$ as function of b at two energies $s = s_0$ and at the Tevatron energy.

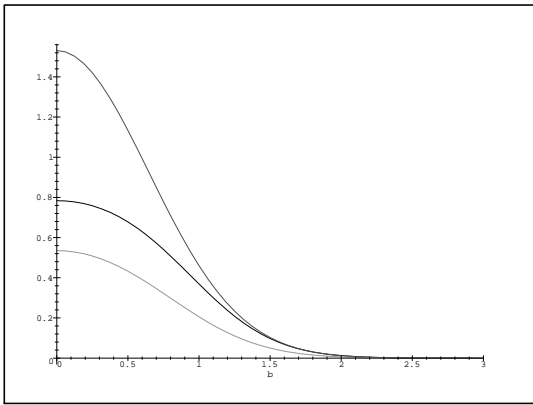


Fig. 33-a

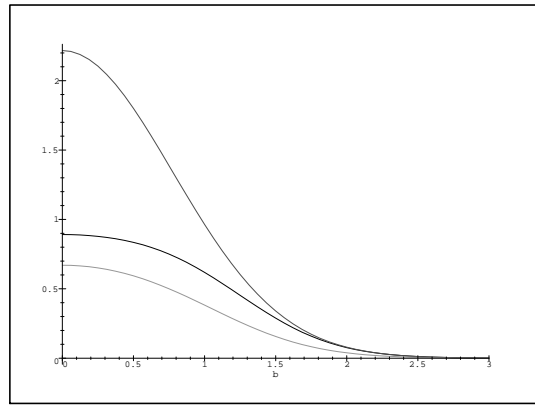


Fig. 33-b

Figure 33: The behaviour of $\Omega(s, b)$ (dashed curve), $Ima_{el}(s, b)$ (dotted curve) and $G_{in}(s, b)$ (solid curve) as function of impact parameter b (in Fm) at $s = 400\text{GeV}^2$ (a) and $s = 410^6\text{GeV}^2$ (b).

Now you can see what a situation with the SC we expect at hadron - hadron collisions. For both energies $\Omega > 1$ and it leads to sufficiently big SC in G_{in} . However, since the SC in the elastic amplitude depends on $\Omega/2$, one can see that they are much smaller. You can see also that G_{in} is close to 1 and in this intermediate energy region the unitarity has a simple solution $a_{el} \approx \frac{1}{2}$ which you can obtain yourselves if you substitute in Eq.(20) $G_{in} = 1$ and consider that $|a_{el}|^2 \ll Ima_{el}$.

The lesson which I want that you will learn with me is very simple: *if we want to measure the SC we have to find a process which depends on G_{in}* . Certainly, this is not the total cross section or elastic one. The second thing which we can see in Fig.33 that we need a process which will be sensitive to sufficiently small impact parameters, namely, $b \leq 1\text{Fm}$.

12.5 Large Rapidity Gap processes and their survival probability.

We call LRG processes any processes in which in sufficiently large rapidity region we have no produced hadrons. Therefore, such good, old processes as single and double diffractive dissociation or central diffraction give examples of such processes (see Fig.24). However, Bjorken suggested to measure LRG processes with an additional signature of “hard” processes. The simplest example of such processes is the production of two large transverse momenta jets with LRG between them ($\Delta y = |y_1 - y_2| \gg 1$) in back - to - back kinematic ($\vec{p}_{t1} \sim -\vec{p}_{t2}$). let us consider this reaction in more details to illustrate how the Pomeron “soft” physics enters the calculation of such typical “hard” process. Of course, I will discuss such processes in more consistent way in the third part of my lectures but, I hope, that brief discussion now will help you to understand how important to get more reliable knowledge on the SC.

The reaction which we consider is (see Figs. 23-d and 24 for notations):

$$p + p \rightarrow \quad (111)$$

$$M_1 \{ \text{hadrons} + \text{jet}_1(x^1, \vec{p}_{t1}) \} + [\text{LRG}(\Delta y = |y_1 - y_2|)] + M_2 \{ \text{hadrons} + \text{jet}_2(x^2, \vec{p}_{t2}) \} ,$$

where

$$\begin{aligned} x^1 &= \frac{2p_{t1}}{\sqrt{s}} e^{y_1} ; \\ x^2 &= \frac{2p_{t2}}{\sqrt{s}} e^{y_2} ; \end{aligned}$$

and

$$\vec{p}_{t1} \approx -\vec{p}_{t2} ; \quad p_{t1} \approx p_{t2} \gg \mu .$$

We denote by μ a typical scale for transverse momentum for “soft” processes.

The cross section of this reaction can be described by simple factorization formula:

$$\begin{aligned} f(\Delta y, y_1 + y_2, p_{t1}, p_{t2}) &= \frac{d\sigma}{d\Delta y, d(y_1 + y_2) dp_{t1}^2 dp_{t2}^2} = \\ &F_p^{(1)}(x^1, p_{t1}^2) \cdot F_p^{(2)}(x^2, p_{t2}^2) \cdot \sigma_{\text{hard}}(p_{t1}^2, x^1 x^2 s) , \end{aligned} \quad (112)$$

where F_p^i is probability to find parton with x^i in the proton (deep inelastic structure function) and σ_{hard} is the cross section of the “hard” parton - parton interaction at sufficiently large energies ($x^1 x^2 s$). We hope, that this “hard” process is due to exchange of a colourless object which we call “hard” Pomeron. This “hard” Pomeron we will discuss in the following parts of my lectures, here we concentrate on the calculation of the probability of such reaction. Indeed, reaction of Eq. (111) can be seen as a statistical fluctuation in the typical inelastic event. The probability is small and it is of the order of $\exp(-\langle n(\Delta y) \rangle)$ where $\langle n(\Delta y) \rangle$ is the average hadron multiplicity of the typical inelastic event in the rapidity region Δy .

Second, we need to multiply Eq. (112) by so called damping factor $\langle D^2 \rangle$. It gives a probability that no partons with $x > x^1$ from one proton and no partons with $x > x^2$ from the other proton will interact with each other inelastically. Indeed, such an interaction produces a lot of hadron in the rapidity gap so they should be taken off in the correct expression for the cross section. Let me point out that Eq. (112) is correct if you believe that the exchange of the single Pomeron describes the “soft” processes, for example, it is true for the D-L Pomeron. Therefore, the experimental deviation from Eq. (112) itself give model independent information that the single Pomeron is not doing its job. Let us remember that actually we have learned what we need to do to calculate $\langle D^2 \rangle$. Indeed, we have discussed that the physical meaning of

$$P(s, b) = e^{-\Omega(s, b)} \quad (113)$$

is the probability that no inelastic interaction between scattered hadron has happened at energy \sqrt{s} and at impact parameter b . Therefore, in the Eikonal model $P(s, b)$ is just the factor that we need to multiply Eq. (112) to get a right answer:

$$f(\Delta y, y_c = y_1 + y_2, p_{t1}, p_{t2}) = \langle D^2 \rangle f(\text{Eq. (112)}) , \quad (114)$$

where

$$\langle D^2 \rangle = \frac{\int d^2b P(s, b) \cdot f(b, \Delta y, y_c, p_{t1}, p_{t2})}{\int d^2b f(b, \Delta y, y_c, p_{t1}, p_{t2})}. \quad (115)$$

Here we introduce $f(b, \Delta y)$ using the following formula:

$$f(b, \Delta y) = \int d^2b' d^2b'' F_p^1(b'; x^1, p_{t1}^2) \cdot \sigma_{hard}(b' - b'', x^1 x^2 s) \cdot F_p^1(b - b'; x^2, p_{t2}^2), \quad (116)$$

where

$$F_p^i(x^i, p_{ti}^2) = \int d^2b' F_p^1(b'; x^i, p_{ti}^2).$$

Actually, for the deep inelastic structure function we can prove that the impact parameter behaviour can be factorized out in the form

$$F_p^1(b'; x^1, p_{t1}^2) = S(b) \cdot F_p^1(x^1, p_{t1}^2),$$

where $\int d^2b S(b) = 1$.

We also can consider that our “hard” process to be located at a very small value of $b' - b''$. Indeed, just from uncertainty principle $b' - b'' \propto 1/p_{t1} \ll$ any impact parameter scale for “soft” processes. Finally, we can put $b' = b''$ in the integral in Eq. (116).

After all these remark, it is easy to see that the damping factor can be calculated as:

$$\langle D^2 \rangle = \int d^2b d^2b' P(s, b) \cdot S(b') \cdot S(b - b'). \quad (117)$$

For $S(b)$ we use the exponential parameterization, namely

$$S(b) = \frac{1}{\pi R_H^2} e^{-\frac{b^2}{R_H^2}}. \quad (118)$$

Taking the integral over b' we get

$$\langle D^2 \rangle = \int db^2 P(s, b) \cdot \frac{1}{2R_H^2} e^{-\frac{b^2}{2R_H^2}}. \quad (119)$$

Fortunately, the value of R_H^2 has been measured at HERA and it is equal to

$$R_H^2 = 8 \text{ GeV}^{-2}.$$

Of course, R_H does not depend on energy. In Fig.34 you can see the impact parameter dependence of

$$\Gamma(s, b) = P(s, b) \cdot e^{-\frac{b^2}{2R_H^2}},$$

or, in other word, of the profile function for the LRG process. From this figure you can conclude that the damping factor should be rather small since Γ turns out to be much smaller than G_{in} . Second, the LRG processes go from larger impact parameters than the

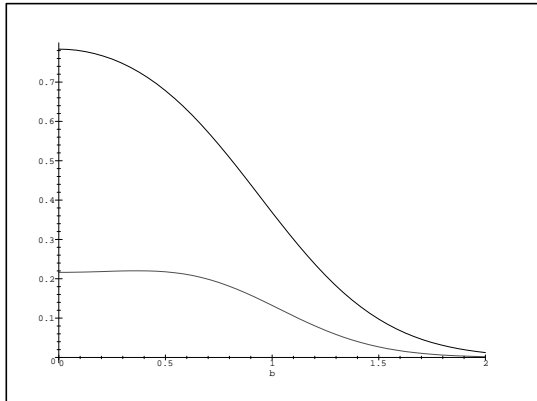


Fig. 34-a

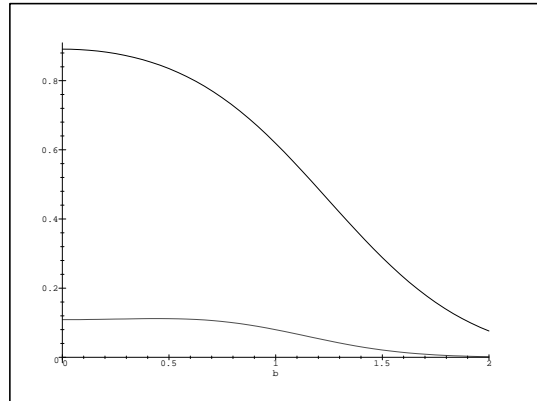


Fig. 34-b

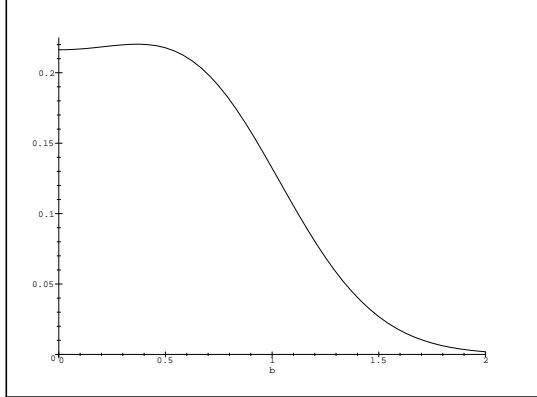


Fig. 34-c

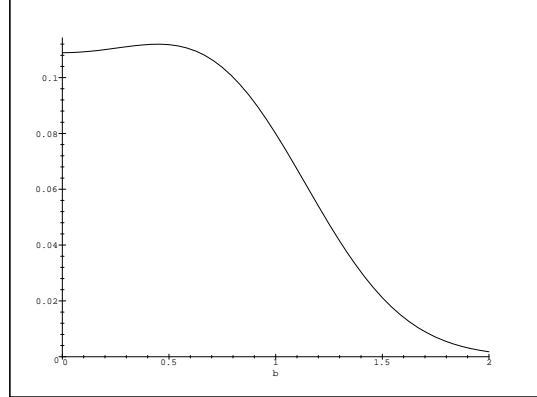


Fig. 34-d

Figure 34: *The impact parameter dependence for $G_{in}(s, b)$ and $\Gamma(s, b)$ at two values of energy $\sqrt{s} = 400 \text{ GeV}$ (Fig.34-a and Fig. 34-c) and $\sqrt{s} = 4 10^6 \text{ GeV}$ (Fig. 34-b and Fig. 34-d).*

average inelastic process since the b - distribution shows a dip in the region of small b and therefore, the LRG processes goes almost entirely from $b \approx 1Fm$.

It is easy to take the integral in Eq. (119) and the answer is:

$$\langle D^2 \rangle = a \cdot \left(\frac{1}{\nu(s)} \right)^a \cdot \gamma(a, \nu(s)) \quad (120)$$

where $\gamma(a, \nu)$ is incomplete Gamma function

$$\gamma(a, \nu) = \int_0^\nu z^{a-1} e^{-z} dz$$

and

$$a = \frac{R^2(s)}{2R_H^2}.$$

The energy behaviour of the damping factor is given in Fig.35a. One can see that in this simple model the damping factor is about 30% and drops in about two times from the Fermilab fixed target experiment energies to the Tevatron one.

It is interesting to notice that the single diffraction process which is also a LRG one has in the Eikonal model a similar damping factor. The difference is only in the definition of parameter a or better to say in the value of R_H which starts to depend on energy. It turns out that for single diffraction

$$a = \frac{2R^2(s)}{(R^2(s) + R^2(M^2) - R^2(s = s_0))}.$$

In Fig.35b we plot the energy behaviour of the single diffraction cross section in the triple Pomeron formula (see Eq.(76)) and taking into account $\langle D^2 \rangle$. One can see that we have a striking difference in energy behaviour. In my opinion this is a direct experimental evidence that we have to take into account the SC in addition to the Pomeron exchange.

12.6 σ_{tot} , σ_{el} and slope B .

Using the general formulae of the Eikonal model(see Eqs.(108) - (110)) one can easily obtain the expression for the total cross section and for elastic one after integration over b . I hope that you will be able to perform this integration with Ω given by Eq.(110) and the result is:

$$\sigma_{tot} = 2\pi R^2(s) \{ \ln(\Omega(s, b=0)/2) + C - Ei(-\Omega(s, b=0)/2) \} \quad (121)$$

and

$$\sigma_{el} = \quad (122)$$

$$\pi R^2(s) \{ \ln(-\Omega(s, b=0)/4) + C + Ei(-\Omega(s, b=0)) - 2Ei(-\Omega(s, b=0)/2) \}.$$

Here, $C=0.5773$ is Euler constant and $Ei(x)$ denotes the integral exponent $Ei(x) = \int_{-\infty}^x \frac{e^{-t}}{t} dt$.

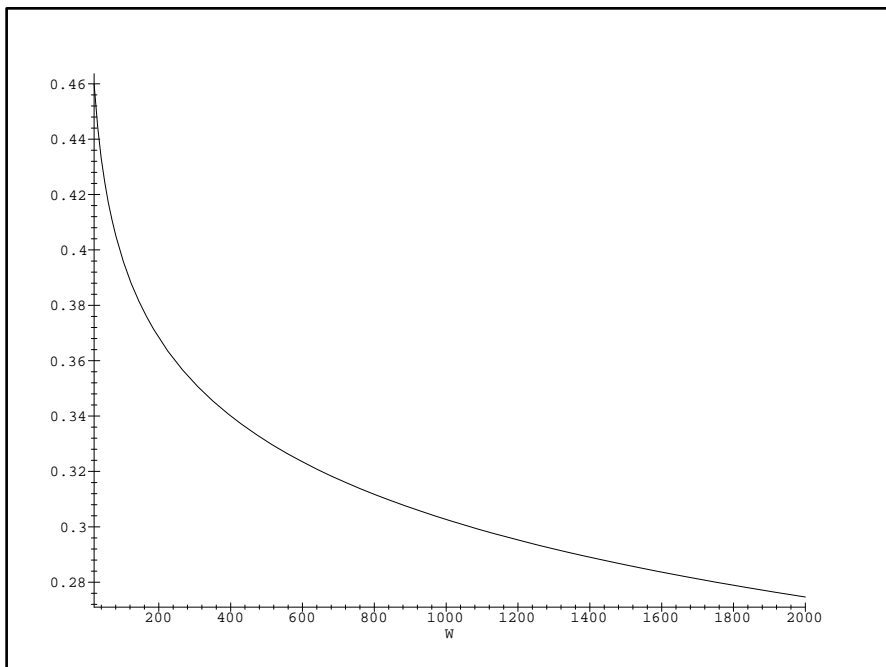


Fig.35-a

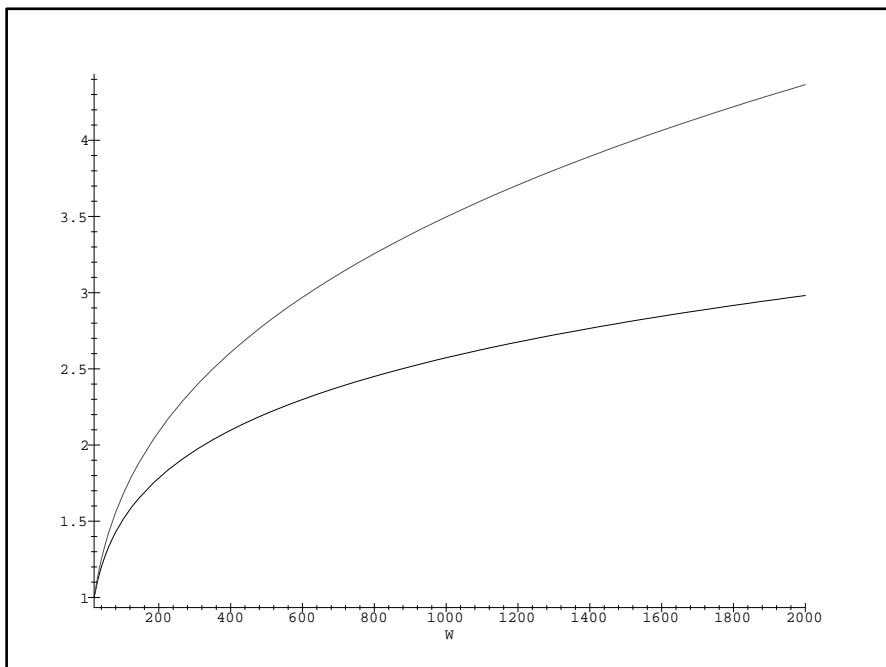


Fig. 35-b

Figure 35: *The energy behaviour of the damping factor for the “hard” processes with LRG (Fig. 35a) and for the cross section of the single diffraction dissociation (Fig.35b): for the triple Pomeron formula (dashed line) and for the triple Pomeron formula multiplied by damping factor(solid line), $W = \sqrt{s}$.*

In Figs.36a and 36.b we plot the energy dependence of the total and elastic cross sections. One can see that in spite of the fact that the influence of the SC can be seen at high energy but it is not so pronounced as in the value of the damping factor and/or in energy dependence of the diffractive dissociation cross section.

For the completeness of presentation let me present here the calculations for the slope B which we can define as

$$B = \frac{\ln \frac{d\sigma}{dt}}{dt} \Big|_{t=0} .$$

Using the impact parameter representation we obtain that

$$B = \frac{\int b^2 \operatorname{Im} a_{el}(s, b) d^2 b}{2 \int \operatorname{Im} a_{el}(s, b) d^2 b} . \quad (123)$$

We can rewrite Eq. (123) as a ratio of two hypergeometrical functions

$$B = \frac{R^2(s)}{2} \cdot \frac{\operatorname{hypergeom}([1, 1, 1], [2, 2, 2], -\Omega(s, b=0)/2)}{\operatorname{hypergeom}([1, 1], [2, 2], -\Omega(s, b=0)/2)} . \quad (124)$$

Here I used the notation of Maple for the hypergeometrical functions to give you a possibility to check all numerics. The calculations plotted in Fig.36c were done with the same values for the parameters of the Eikonal model as have been discussed before in section 12.4. One can see that the SC induce larger shrinkage of the diffraction peak (s -dependence of the slope B) than in the simple one Pomeron exchange approach.

The reason why I discussed these typical “soft” processes observables is the only one: to show you that the SC manifest themselves differently for different processes. I hope, that it is enough to compare Figs.36 with Figs.35 to believe me.

12.7 Inclusive production.

12.7.1 Cross section.

Actually, we have discussed the main result for the inclusive cross section: *due to the AGK cutting rules all SC cancel and only the Pomeron exchange gives the contribution* (see Fig.37a). We want now to stress that only the SC induced by interaction between a parton with rapidity larger than y with a parton with rapidity smaller than y . All interactions between two or more partons with rapidity larger than y are possible as well as the interaction of the produced particle with the parton cloud (see Fig.37a). In the framework of the Eikonal model we neglect such interactions and, therefore, only in the Eikonal model we have the simple one Pomeron exchange diagram for the inclusive cross section.

However, even in general approach the single inclusive cross section has a factorization form and can be written as:

$$\sigma_{inc}(a + b \rightarrow c + X) = a \sigma_{tot}^{(a+c)}(s_1) \cdot \sigma_{tot}^{(b+c)}(s_2) , \quad (125)$$

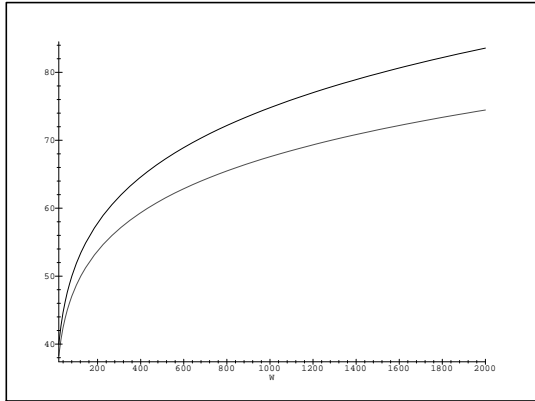


Fig. 36-a

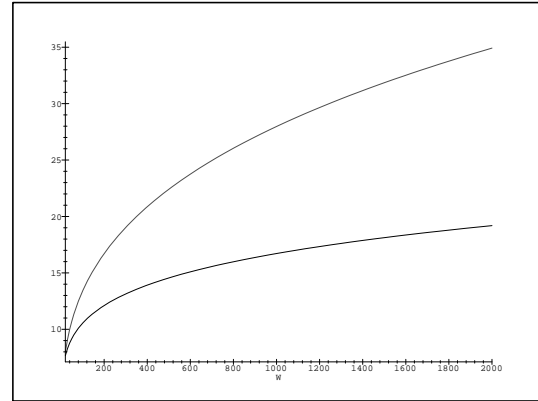


Fig. 36-b

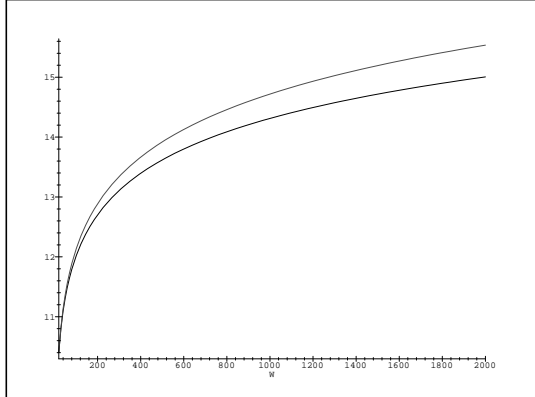


Fig. 36-c

Figure 36: The energy dependence of σ_{tot} , σ_{el} and the slope B for the Eikonal model for the SC (dashed curves) and for the one Pomeron exchange approach (solid curves).

where a is constant and $s_1 = x_1 s$ and $s_2 = x_2 s$ with $x_1 = \frac{m_{tc}}{\sqrt{s}} e^{y_1}$ and $x_2 = \frac{m_{tc}}{\sqrt{s}} e^{-y_1}$ ($m_{tc} = \sqrt{m_c^2 + p_{tc}^2}$).

In the third part of my lectures I will show you that such a factorization leads to the factorization theorem for the “hard” processes.

12.7.2 Correlations.

We have discussed the two particle rapidity correlation for the inclusive reaction in section 9.8 (see Fig. 23f) for the one Pomeron exchange. We found out that in the correlation function R given by Eq.(82) only the contribution of the first diagram in Fig.37b survives which leads to the simple formula of Eq.(83). This equation describes so called short range rapidity correlations which vanishes at large values of $\Delta y = |y_1 - y_2|$ as

$$R \rightarrow |_{\Delta y \gg 1} SR \cdot e^{-\frac{\Delta y}{L_{cor}}}. \quad (126)$$

The new contribution comes from the SC and due to the same AGK cutting rules all diagrams cancels in the correlation function except one, namely, the two Pomeron exchange shown in Fig.37b. Even a slight glance at this diagram shows that it does not depend on the rapidity difference (Δy) and gives a constant contribution to the correlation function R which we call long range rapidity correlations. Therefore, the general form for the rapidity correlation function R (see Eq.(82) for the definition) at large Δy is

$$R = SR \cdot e^{-\frac{\Delta y}{L_{cor}}} + LR \quad (127)$$

The constant term LR we can estimate using the AGK cutting rules. Indeed the cross section of two particle production from different Pomerons (“ladders” in Fig.32) is equal to $\sigma_2^{(2)} = 2 \Delta \sigma_{tot}$ where $\sigma_{tot} = \sigma_{tot}^P - \Delta \sigma_{tot}$, where σ_{tot}^P is the total cross section in one Pomeron exchange model and $\Delta \sigma_{tot}$ is correction to the total cross section due to two Pomeron exchange. Therefore,

$$LR = 2 \frac{\Delta \sigma_{tot}}{\sigma_{tot}}. \quad (128)$$

In the Eikonal model we can find $\Delta \sigma_{tot}$, expanding Eq.(108), namely

$$\Delta \sigma_{tot} = \frac{\pi}{2} \int b^2 \Omega^2(s, b) \quad (129)$$

which gives in the parameterization of Eq.(110) for Ω

$$\Delta \sigma_{tot} = \frac{\sigma_0^2(s = s_0)}{\pi 4 R^2(s)} \cdot \left(\frac{s}{s_0} \right)^{2 \Delta_P}. \quad (130)$$

Using Eq. (130) and Eq. (129), we can obtain to the following estimates for term LR in Eq. (127):

$$RL = \frac{\sigma_0^2(s = s_0)}{\sigma_{tot} \pi 4 R^2(s)} \cdot \left(\frac{s}{s_0} \right)^{2 \Delta_P}. \quad (131)$$

In Fig.37c the value of LR term is plotted as a function of energy. For σ_{tot} we used Eq.(121). One can see that the long range rapidity correlations can be rather essential and give positive correlation of the order of 30% - 50%.

We can also write the two Pomeron contribution to the total double inclusive cross section (σ^{DP}) in the form:

$$\sigma^{DP} = m \frac{\frac{d\sigma}{dy_1} \frac{d\sigma}{dy_2}}{2 \sigma_{eff}} \quad (132)$$

where m is equal 1 for identical particle 1 and 2 while it is equal to 2 if they are different. The Eikonal model gives the value of σ_{eff} which is equal to 25 mbn at $W = \sqrt{s} = 20 \text{ GeV}$ and it rises to 38 mbn at the Tevatron energies ($W = 2000 \text{ GeV}$). we will use the form of Eq. (132) in the next section when we will discuss the data from CDF on the value of σ_{eff} .

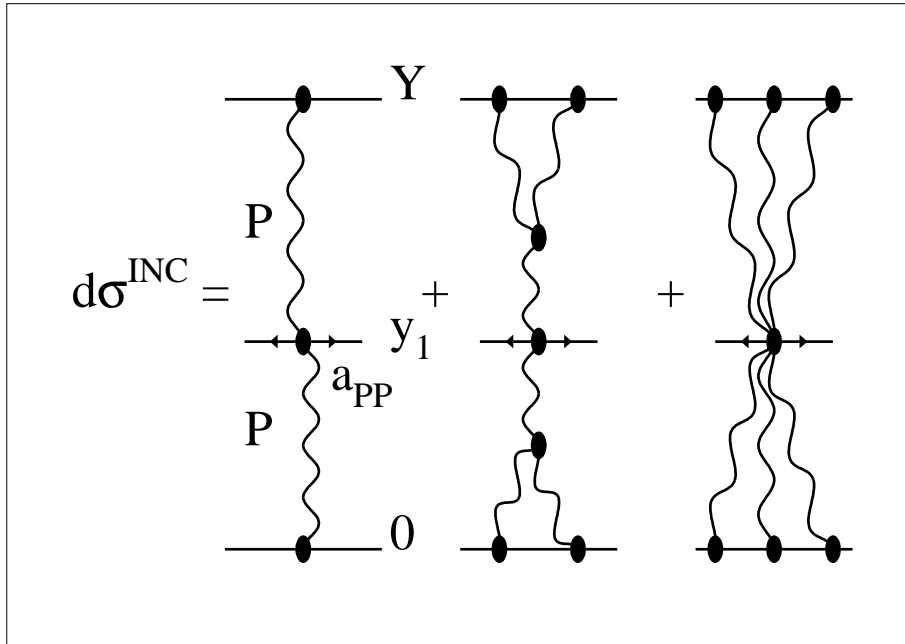


Figure 37-a: *Single inclusive cross section with shadowing corrections.*

13 The Pomeron from HERA and Tevatron experiments.

13.1 Reggeon approach strategy for measuring the Pomeron structure.

Now, let us try to check what have you learned from my lectures. The question which I am asking: **what is a correct strategy to measure the Pomeron structure?** I hope, that you can easily answer this question.

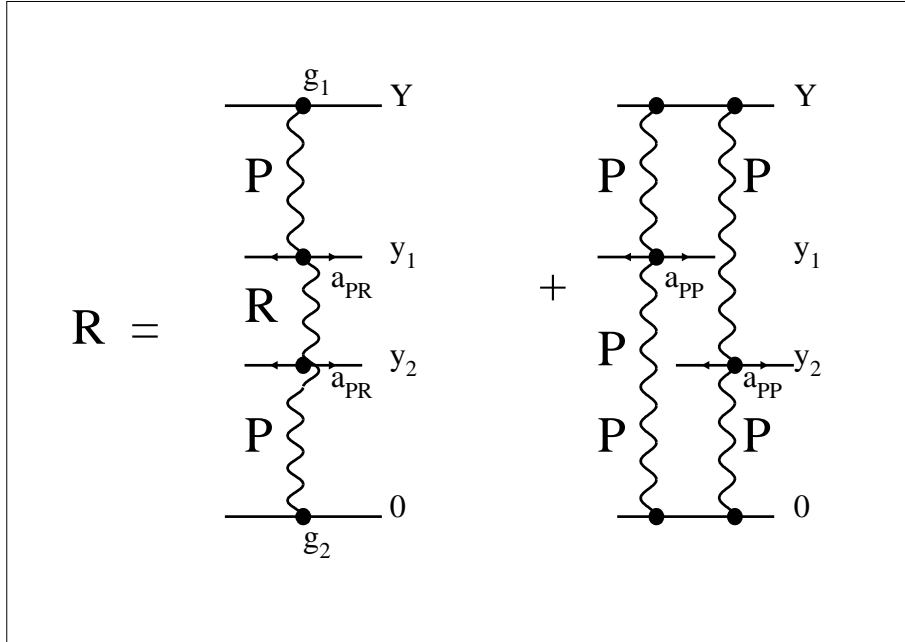


Figure 37-b: *Correlation function R (see Eq.(82)) with shadowing corrections.*

Let me give my answer:

1. The intercept of the Pomeron as well as what kind of the inelastic processes corresponds to the Pomeron exchange we should measure

(i) in the single inclusive processes where the most part of the shadowing corrections cancel

and

(II) in the short range (in rapidity) part of the correlation function.

These are our best signatures for the one Pomeron exchange.

2. The traditional observables like the total cross section, the elastic cross section and the diffractive dissociation cross sections cannot be recommended as the main source of the Pomeron structure since they are suffering with sufficiently large contribution from the shadowing corrections. Among these three the worst is the diffractive dissociation cross section, very bad is the elastic one and bad is the total cross section as far as the value of the SC is concerned.

3. The t - dependence of the Pomeron trajectory and its vertices of interaction with particles and between Pomerons is very interesting since it is closely related to the typical distances involved in the Pomeron problem. unfortunately, I do not know another way of measuring this as to measure the traditional observables like the value and the shrinkage of the t - slope in elastic and diffractive cross sections. We have discussed that these are not the best observables but nobody knows better. To diminish the influence of the SC we have to measure all slopes at very small values of t .

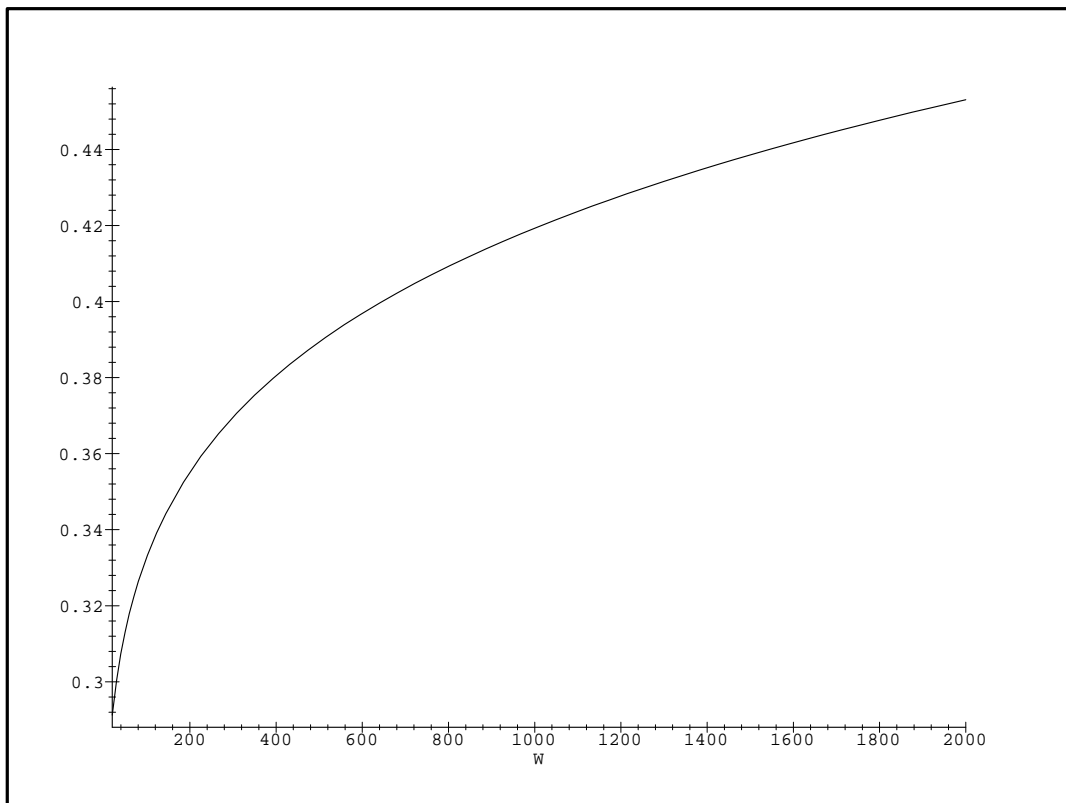


Figure 37-c: *The value of the long range rapidity correlation term (LR)(see Eq. (127)) in the Eikonal model.*

4. The energy behaviour of the diffractive dissociation in DIS. For large value of photon virtuality (Q^2) the SC become to be negligible and only one Pomeron exchange contributes to this process. However, the interpretation of this process in term of the Pomeron exchange at large Q^2 is highly questionable and demands the experimental study on what distances are really essential in the diffractive processes.

However, if I will ask you **what is the best way to measure the shadowing corrections**, the answer will be just opposite:

1. The best way is the diffractive dissociation processes, worse elastic scattering, very bad is the total cross section and extremely bad is the inclusive one. However, here I want to make a remark on diffractive dissociation in the photon - proton interaction. As we have discussed the photon looks as a collection of hadrons with a broad spectrum of masses. It means that measuring the diffractive cross section in photon - hadron interaction we measure mainly the elastic scattering of hadrons with appropriate masses. Therefore, unfortunately, in photon - hadron interaction we have not found yet the best process. The single photon diffraction dissociation certainly is not the best.

2. However, we can improve the situation when we measure the double diffractive dissociation. The hadron vertex looks the same as in hadron - hadron collisions and the double diffractive dissociation provides a tool to measure the SC.

3. I am very certain that the best way of extracting the SC in photon - hadron interaction and one of the best in hadron - hadron collisions is the long range (in rapidity) part of the correlation function. I will show below how such sort of measurement at CDF made a breakthrough the whole issue of the SC.

4. The direct way of measurement of the value of the SC is the LRG processes especially the “hard”. The real measurement of the damping factor which is turns out to be rather big will provide a unique information on the SC.

And let me ask you the third question: **what is the most fundamental problem for the Pomeron?**

Of course as I have discussed the Pomeron hypothesis is outcome mostly from the lack of imagination and we have no real deep arguments that the high energy asymptotic should be a Pomeron like. However, this hypothesis works phenomenologically even now. My answer is that in the framework of the Pomeron hypothesis the fundamental problem is to understand experimentally and theoretically what is going on with the diffractive production of the large mass. As I have discussed the main difficulties of the Pomeron approach are concentrated in this problem. Theoretically, the solution to this problem means that we understood how works the SC between every possible partons.

13.2 The Pomeron before HERA and Tevatron.

Our knowledge about the Pomeron before HERA and Tevatron can be described as Donnachie - Landshoff Pomeron. Actually, it is not correct to call this Pomeron as D-L Pomeron.

Many people introduced such a Pomeron a long before D-L (K.A.Ter-Martirosian, A.Kaidalov et al. in Moscow, A. Capella, Tranh Tran Van et al in Orsay and many others) but we have to give a credit to Donnachie and Landshoff - they were the first who assumed that there is nothing except the D-L Pomeron. We have discussed the certain theoretical difficulties that has the D-L Pomeron, but let us look at D-L Pomeron at different angle, namely, as the shortest way to express the experimental knowledge about the Pomeron. Let us list the parameters of the D-L Pomeron and let us try to extract physics out of them.

$$1. \alpha_P(0) = 0.08.$$

This a small number and let us discuss what this smallness means using the parton model as a guide. First, let me make an essential remark about our partons. In QCD and I hope that everybody knows the main thing about QCD, our partons are gluons (massless particles with spin one) and quarks (antiquarks(massive and have spin 1/2). Going back to Eq.(60) one can see that in the $g\phi^3$ we have extra power of energy s in front of formula for cross section. Actually, in general case the power of s is the following : $(1/s)^{2j-2}$ where j is the spin of partons. It is obvious that in QCD mainly gluons contribute to the expression for cross section because for them the extra power of s just is equal to zero. In this particular case, the intercept of the Pomeron is equal to $\alpha_P(0) = \Sigma(0)$ and closely related to the parton multiplicity (N_G) which is $N_G = \Sigma(0) \ln(s)$.

Therefore, the smallness of the Pomeron intercept means that the main contribution to the Pomeron structure is originated from the first "Born" diagram = the two gluon exchange, but most likely with completely nonperturbative gluons which carry the nonperturbative scale (μ in the parton model). The production of gluons could be considered in the perturbative way with respect to $\alpha_P(0)$.

$$2. \alpha'_P(0) = 0.25 GeV^{-2}.$$

Once more a small value which, at first sight, says that we have sufficiently large typical transverse momentum scale in the Pomeron. Let us estimate this using Eq.(60) and expand $\Sigma(q^2)$ as a function of q^2 at small q^2 .

It gives:

$$\alpha_P(q^2) = \Sigma(0) - q^2 \frac{\Sigma(0)}{6\mu^2}. \quad (133)$$

Comparing Eq. (133) with the value for $\alpha'_P(0)$ we get that $\mu \approx 250 MeV \approx \Lambda$, where Λ is the QCD scale.

3. The experimental slope for the t -dependence of the triple Pomeron vertex (r_0^2) turned out to be smaller than the slope of the Pomeron proton form factor (R_0^2): $r_0^2 \leq 1 GeV^{-2} \ll R_0^2 = 2.6 GeV^{-2}$ in all so called triple Reggeon fits of the diffractive dissociation data. Unfortunately, the accuracy of the data was not so good and the value of r_0^2 could not be defined by the fit. Actually, the fit could be done with $r_0^2 = 0$. This observable is very important since it gives a direct information what transverse momentum scale is responsible for the Pomeron structure. As we have seen the value of $\alpha'_P(0)$ depends on the unknown parton density while r_0^2 does not.

4. The ideas of the additive quark model that a hadron has two scales: the hadron size $R \approx 1Fm$ and the size of the constituent quark $r_Q \approx 0.2 - 0.4Fm$; is still a working hypothesis and it was included in the D-L Pomeron in t - dependence of the Pomeron - hadron vertices.

5. Regge factorization has been checked and it works, but the number of reaction was not too rich.

13.3 Pomeron at the Tevatron.

The Tevatron data, I think, contributed a lot to our understanding of the Pomeron structure. It is a pity that this contribution has not been properly discussed yet. Let me tell you what I learned from the Tevatron.

1. The measurement of the inclusive cross section at Tevatron energy allowed us to extract the intercept of the Pomeron from the energy behaviour of the inclusive spectra in the central rapidity region. The result was surprising: the energy behaviour of the inclusive cross section can be parameterized (Likhoded et al. 1989) as

$$C_0 + C_P(s/s_0)^{\Delta_P(0)}, \quad (134)$$

with $\Delta_P(0) = 0.2$ instead of the D-L value $\Delta = 0.08$!!! Both C_0 and C_P are constant in the above parameterization. In the framework of the Reggeon approach I have to insist that the Pomeron intercept has been measured correctly only in the inclusive cross section and to face a problem that the D-L Pomeron is not a Pomeron at all. Irritating feature of Eq. (134) is the fact that I have to include an additional constant C_0 . Does it mean that I have to deal with two Pomerons: the first with $\Delta_{P_1}(0) = 0$ (term C_0 in Eq. (134)) and the second with $\Delta_{P_2} = 0.2$?!

2. The beautiful data on the diffractive dissociation which shown in Fig.26 changed the whole issue of the SC from theoretical guess to the practical necessity. I have discussed that the Eikonal model for the SC could describe the main feature of the data but I am very certain that data are much richer and have not been absorbed and properly discussed by high energy community, but you can find some discussions in papers and talks of Gotsman et all (1992), Goulianos (1993 - present), Capella et al. (1997) , C-I Tan (1997) and others.

3. The CDF data on so called double parton cross section. The CDF just used the double inclusive cross section to measure the contribution of the SC. Actually, the CDF measured the process of inclusive production of two pairs of “hard” jets with almost compensated transverse momenta in each pair and with almost the same values of their rapidities. The production of two such pairs is highly suppressed in the one Pomeron (one parton cascade) and can be produced only due to double Pomeron interaction (double parton collisions). The Mueller diagram for such process is given in Fig. 38b. We can use formula (132) for this cross section and it turns out that the value of σ_{eff} in Eq.(132) is equal to $14.5 \pm 1.7 \pm 2.3$ mb. This value is approximately in two times smaller than our estimates in the Eikonal model.

Therefore, this data show that the SC exist but even they are bigger than the Eikonal model estimates. Perhaps, the problem is not in the Eikonal model but in our picture for the hadron which was included in the Eikonal model. Namely, if we will try to explore the two radii picture of the proton as it is shown in Fig.38b we will get the average radius in two times smaller than has been used. So for me the CDF data finished with discussion the one Pomeron model, measured the value of the SC and provide a strong argument in favour of the two radii structure of the proton.

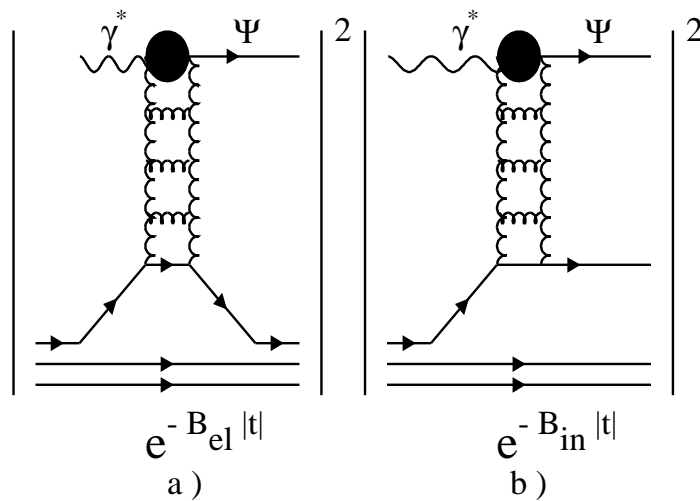


Figure 38-a: *The J/Ψ production without (a) and with (b) proton dissociation.*

13.4 Pomeron at HERA.

1. I think that HERA did a great thing, namely, the HERA data show explicitly that the hadron has two “soft” scale or two radii. Indeed, it comes out from the HERA data on photoproduction of J/Ψ meson. These data show two different slopes in t -dependence for elastic and for inelastic photoproduction in which proton dissociates into a hadron system (see Fig.38a): $B_{el} = 4 \text{ GeV}^{-2}$ and $B_{in} = 1.66 \text{ GeV}^{-2}$, while the cross sections are equal for both processes. Since in a such a process we can neglect the t -dependence of the upper vertex we can interpret these data as

1). that the first measurement of the radius of so called Pomeron - proton vertex (we also called this value as a two gluon form factor in a picture of the “hard” processes). It turns out that this radius is smaller than the radius of electro-magnetic form factor which follows for this vertex from the additive quark model and have been used for the D-L Pomeron.

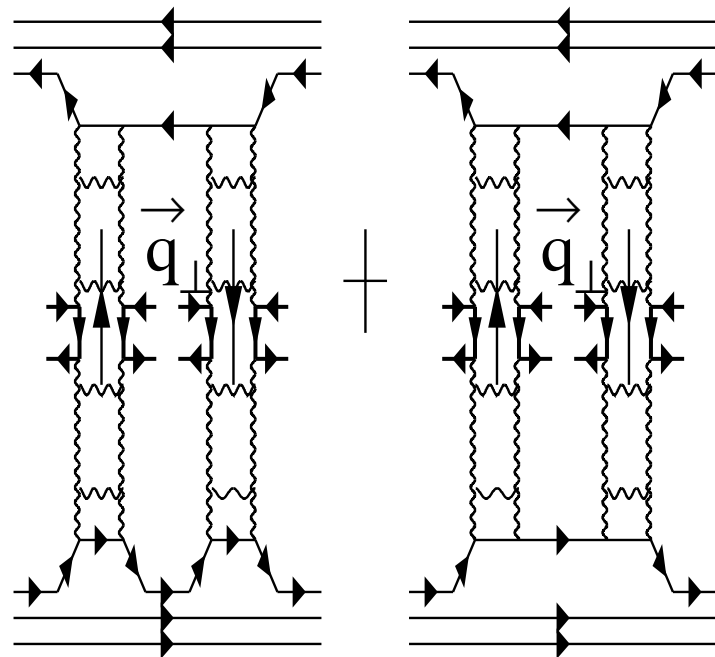


Figure 38-b: *Inclusive production of two pair of “hard” jets in the double parton scattering.*

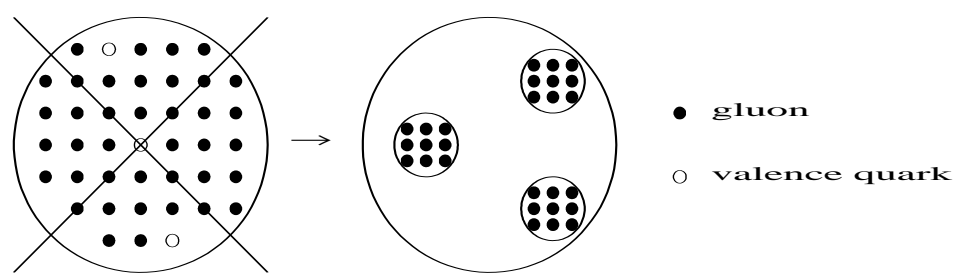


Figure 38-c: *Democratic and two radii picture of proton.*

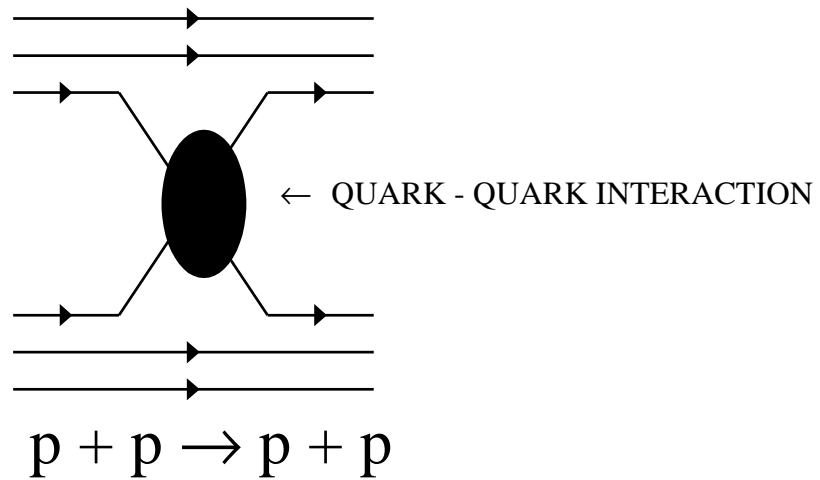


Figure 38-d: *Scattering in the constituent quark model.*

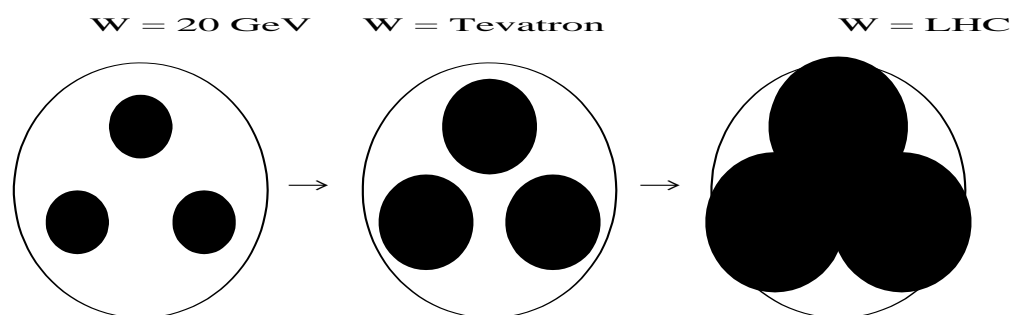


Figure 38-e: *The growth of the interaction radius and the new regime at the LHC energies.*

2). the second radius appears which can be easily interpreted in the picture of the additive quark model (see Fig.38a) as the proper radius of the constituent quark.

Therefore, HERA finished with a democratic picture for gluons and valence quarks and proved the two radii picture of the proton (see Fig. 38c), which could be an additive quark model. The direct observation of the second scale in the “soft” interaction will lead to reconsideration of the simple partonic estimates (see Eq. (133)) of the value of $\alpha'_P(0)$. Our conclusion that the typical scale in the Pomeron problem is about Λ QCD should be revised, but this is a certain problem for the future.

2. The measurement for the energy behaviour of the diffractive dissociation process leads to the intercept of the Pomeron $\Delta_P(0) \approx 0.2$. As I have mention it could be different interpretation of this experimental fact, but in the framework of the Pomeron approach this is the intercept.

3. The HERA data on the deep inelastic structure function can be described by the DGLAP evolution equation if we assume that an initial parton distribution at $Q^2 = Q_0^2 = 3 - 5 \text{GeV}^2$ with energy behaviour $F_2(x, Q_0^2) \propto (1/x)^{0.2}$ which corresponds the Pomeron intercept $\Delta_P(0) = 0.2$.

4. The inclusive production both for photoproduction and DIS can be described assuming the Pomeron with the intercept $\Delta_P(0) = 0.2$.

Therefore, let me conclude this section with the following statement:

In October 1997 after HERA and Tevatron data we have :

- *The Pomeron intercept $\Delta_P(0) = 0.2$;*
- *The SC are large and approximately in two times bigger than the Eikonal model estimates;*
- *The two radii picture of the proton has been proven experimentally and the values of these two radii have been measured.*

14 Instead of conclusions.

14.1 My picture for the high energy interaction.

Let me conclude my lectures sharing with you the truth that starting from year 1977 I do not believe in the Pomeron as a specific Regge pole. In the framework of these lectures I could not show you why and it will be a subject for the second part. Instead of the Pomeron approach Ryskin and me developed a different approach which correspond the following simple picture (see Figs.38c and 38d) with two ingredients: the constituent quark model for hadrons and the “black” disc interaction between two constituent quarks. Now, finally, I got a real pleasure telling you that due to results of HERA we have an experimental confirmation

of this approach. Indeed, let us estimate the value of the total cross section for quark - quark interaction. As we have discussed in section 2.4 the cross section is equal to

$$\sigma_{tot}(q + q) = 2\pi(2 r_Q^2)$$

where r_Q is the quark radius, factor 2 emerges because two quarks collide. Substituting $2r_Q^2 = B_{in}$ (see Fig.38a) we get $\sigma_{tot}(q + q) = 4 - 5mb$ which gives a correct value for the total proton - proton cross section $\sigma_{tot}(p + p) = 9\sigma_{tot}(q + q)$.

In this model the size of the constituent quarks increases with energy (see Fig. 38e) and only at LHC energies the clouds of partons from different constituent quarks will start to overlap. This is the region where we can expect a new physics for the “soft” processes.

The interesting feature of this model that a substantial part of Regge factorization relations holds in it because of the simple fact that only quarks interact.

Since I cannot start new lectures I have to stop, hoping that I have given a lot of ideas to you to think about.

14.2 Apology and Acknowledgements.

Reading back my lectures I found that I have kept my promise and have shared with you all ideas, hopes and difficulties of the Pomeron problem. I hope that after reading these lectures you will know enough about Pomerons to support or to reject this approach.

I thought that I would not give references in this part but one short story changed my mind. Once, when actually I have finished my writing, Aharon Levy called me asking for a help. He tried to find the book of Collins on Regge theory. Indeed, it is the last book on the subject which summarizes our knowledge of Reggeon theory. However, he failed to find it in any library in Hamburg, DESY one including. I also could not find but fortunately, I went to Paris and found one copy in the LPTHE at Orsay. I asked the librarian to check whether the general library has this book. It turns out that no and even more no university libraries in Paris have. So, my usual excuse that you could easily find everything that I have discussed in any book of the sixties being correct is not practical. So, I decided to give a list of references which is far from being full but at least you will be able to read and clarify a subject that you feel to be interesting. By the way, the end of the story with Collins book is happy. In December, Aharon Levy (tel. 2001 at DESY) will be the only one who will have the copy of the book.

I wish to express my deep apology to all my friends whom I did not cite. I hope to prepare the full list of references including Russian physicists to conclude the last part of my lectures.

As I have mentioned I learned everything about the Pomeron from Prof. Gribov and I was actively involved in this problem during the best fifteen years of my life in Leningrad Nuclear Physics Institute under the leadership and strong influence of Prof. Gribov. I cannot

express, at least in english, my deep sorry that we lost him. These lectures was an attempt to look at the problem with his eyes and, unfortunately, this is the only I can do now for him.

I am very grateful to my friends A. Kaidalov, O. Kancheli and M. Ryskin for life long discussions of the Pomeron. I am sure that a lot of ideas, that we discussed, have been shown up in these lectures. I thank E.Gotsman and U.Maor who started with me five years ago an attempt to revise the whole issue of the Pomeron approach. Sections, devoted to the Eikonal model, is written on the basis of our common papers as well as our common understanding that the Donnachie - Landshoff Pomeron is not the right one. E. Gotsman calculated Fig.25 which I used here and I thank him for this. Travelling around the globe I met the Old Reggeon Guard: J. Bartels, K. Boreskov, A. Capella, J.Cohen - Tannoudji, P. Collins, A.Donnachie, A. Krzywicki, S. Matinian, A. Mueller, R. Peschanski, A. Santoro, C-I Tan, K.A. Ter - Martirosian and A. White (more names for search). Most of them, as well as me, are doing a quite different things but all of them still keep alive the interest for the beauty of this difficult problem. My special thanks to them for encouraging optimism.

These lectures would be impossible without help and support of my DESY friends W. Buchmueller, J. Dainton, H. Kowalski and G. Wolf. I am grateful to them as well as to my listerners who asked many good questions which have improved the presentation and contents. Hope for more questions and critism.

15 References.

Books:

1. G.F. Chew: “*S- matrix theory of strong interaction*”, Benjamin, 1962.
2. S.C. Frautschi: “*Regge Poles and S-matrix Theory*”, Benjamin, 1963.
3. R. Omnes and M. Froissart: “*Mandelstam Theory and Regge Poles: An Introduction for Experimentalists*”, Benjamin, 1963.
4. M. Jacob and G.F.Chew: “*Strong interaction physics*”, Frontiers in Physics, 1964.
5. R.J. Eden, P.V. Landshoff, D.I. Olive and J.C. Polkinghorne: “*The analytic S - matrix*”, Cambridge U.P., 1966.
6. R.J. Eden: “*High energy collisions of elementary particles*”, Cambridge U.P. 1967.
7. V. Barger and D. Cline: “*Phenomenological Theories of High Energy Scattering: An Experimental Evaluation*”, Frontiers in Physics, 1967.
8. P.D.B. Collins and E.J. Squires: “*Regge Poles in Particle Physics*”, Springer, 1968.

9. A. Martin: “*Scattering Theory: Unitarity, Analyticity and Crossing*”, Lecture notes in Physics, Springer, 1969.
10. R. Omnes: “*Introduction to particle physics*”, Wiley, 1971.
11. R. Feynman: “*Photon - hadron interaction*”, Benjamin, 1972.
12. D. Horn and F. Zachariasen: “*Hadron Physics at Very High Energies*”, Benjamin, 1973.
13. S.J. Lindenbaum: “*Particle Interaction Physics at High Energy*”, Clarendon Press, 1973.
14. M. Perl: “*High energy hadron physics*”, Wiley, 1974.
15. S. Humble: “*Introduction to particle production in hadron physics*”, Academic Press, 1974.
16. “*Phenomenology of particles at high energy*”, eds. R.L. Crawford and R. Jennings, Academic Press, 1974.
17. P.D.B. Collins: “*An introduction to Regge theory and High energy physics*”, Cambridge U.P., 1977.
18. Yu. P. Nikitin and I.L. Rosenthal: “*Theory of Multiparticle Production Processes*”, Harwood Academic, 1988.
19. “*Hadronic Multiparticle Production*”, ed. P. Carruther, WS, 1988.
20. J.R. Forshaw and D.A. Ross: “*QCD and the Pomeron*”, Cambridge U.P. 1997.
21. **The collection of the best original papers on Reggeon approach:** “*Regge Theory of low p_t Hadronic Interaction*”, ed. L. Caneschi, North - Holland, 1989.

Reviews:

1. P.D.B. Collins: “*Regge theory and particle physics*”, Phys. Rep. **1C** (1970) 105.
2. P. Zachariasen: “*Theoretical models of diffraction scattering*”, Phys. Rep. **2C** (1971) 1.
3. D. Horn: “*Many particle production*”, Phys. Rep. **4C** (1971) 1.
4. F. J. Gilman: “*Photoproduction and electroproduction*”, Phys. Rep. **4C** (1971) 95.

5. P.V. Landshoff and J.C. Polkinghorne: “*Models for hadronic and leptonic processes at high energy*”, Phys. Rep. **5C** (1972) 1.
6. S.M. Roy: “*High energy theorems for strong interactions and their comparison with experimental data*”, Phys. Rep. **5C** (1972) 125.
7. J. Kogut and L. Susskind: “*The parton picture of elementary particles*”, Phys. Rep. **8C** (1973) 75.
8. J. H. Schwarz: “*Dual resonance theory*”, Phys. Rep. **8C** (1973) 269.
9. G. Veneziano: “*An introduction to dual models of strong interaction and their physical motivation*”, Phys. Rep. **9C** (1973) 199.
10. R. Slansky: “*High energy hadron production and inclusive reactions*”, Phys. Rep. **11C** (1974) 99.
11. S. Mandelstam: “*Dual - resonance models*”, Phys. Rep. **13C** (1974) 259.
12. R.C. Brower, C.E. De Tar and J.H. Wers: “*Regge theory for multiparticle amplitude*”, Phys. Rep. **14C** (1974) 257.
13. Ya.I. Azimov, E.M. Levin, M.G. Ryskin and V.A. Khoze: “*What is interesting about the region of small momentum transfers at high energies ?*”, CERN-TRANS 74-8, Dec 1974. 196pp. Translated from the Proceedings of 9th Winter School of Leningrad Nuclear Physics Inst. on Nuclear and Elementary Particle Physics, Feb 15-26, 1974. Leningrad, Akademiya Nauk SSSR, 1974, pp. 5-161(translation).
14. I.M. Dremin and A.N. Dunaevskii: “*The multiperipheral cluster theory and its comparison with experiment*”, Phys. Rep. **18C** (1975) 159.
15. H.D.I. Abarbanel, J.D. Bronzan, R.L. Sugar and A.K. White: “*Reggeon field theory formulation and use*”, Phys. Rep. **21C** (1975) 119.
16. G. Giacomelli: “*Total cross sections and elastic scattering at high energy*”, Phys. Rep. **23C** (1976) 123.
17. M. Baker and K. Ter Martirosyan: “*Gribov’s Reggeon Calculus*”, Phys. Rep. **28C** (1976) 1.
18. A.C. Irving and R.P. Worden: “*Regge phenomenology*”, Phys. Rep. **36C** (1977) 117.
19. M. Moshe: “*Recent developments in Reggeon field theory*”, Phys. Rep. **37C** (1978) 255.
20. A.B. Kaidalov: “*Diffractive production mechanisms*”, Phys. Rep. **50C** (1979) 157.
21. S.N. Ganguli and D.P. Roy: “*Regge phenomenology in inclusive reactions*”, Phys. Rep. **67C** (1980) 257.

22. K. Goulian: “*Diffraction interactions of hadron at high energy*”, Phys. Rep. **101C** (1983) 169.
23. M. Kamran: “*A review of elastic hadronic scattering at high energy and small momentum transfer*”, Phys. Rep. **108C** (1984) 275.
24. E.M. Levin and M.G. Ryskin: “*The increase in the total cross sections for hadronic interactions with increasing energy*” Sov.Phys. Usp. **32** (1989) 479.
25. E.M. Levin and M.G. Ryskin: “*High - energy hadron collisions in QCD*” Phys. Rep. **189C** (1990) 267.
26. A. Capella, U. Sukhatme, C-I Tan and J. Tran Thanh Van: “*Dual parton model*”, Phys. Rep. **236C** (1994) 225.
27. E. Levin: “*The Pomeron: yesterday, today and tomorrow*”, hep-ph/9503399 , Lectures given at 3rd Gleb Wataghin School on High Energy Phenomenology, Campinas, Brazil, 11-16 Jul 1994.
28. J. Stirling: “*The return of the Pomeron*” Phys.World **7** (1994) 30.
29. A.B. Kaidalov: “*Low - x physics*”, Survey in High Energy Physics,**9** (1996) 143.

This figure "gribov2new.jpg" is available in "jpg" format from:

<http://arxiv.org/ps/hep-ph/9710546v1>

This figure "gribov3.jpg" is available in "jpg" format from:

<http://arxiv.org/ps/hep-ph/9710546v1>

